Estimating the impact and economic trade-offs of infectious disease control strategies using metapopulation models

Daniela Olivera Mesa

Department of Infectious Disease Epidemiology
School of Public Health
Imperial College London

Thesis submitted for the degree of Doctor of Philosophy
May 2022

Statement of originality

I declare that all work presented in this thesis is my own, completed under the supervision of Prof Azra Ghani, Prof Katharina Hauck and Dr Peter Winskill. Any ideas or quotations from the work of other people, published or otherwise, or from my own previous work are fully acknowledged in accordance with the standard referencing practices of the discipline.

The work presented in **Chapter 5** has been published in an altered form in:

> **Olivera Mesa, D.,** Hogan, A. B., Watson, O. J., Charles, G. D., Hauck, K., Ghani, A. C., & Winskill, P. (2022). Modelling the impact of vaccine hesitancy in prolonging the need for Non-Pharmaceutical Interventions to control the COVID-19 pandemic. Communications Medicine, 2(1), 14. doi:10.1038/s43856-022-00075-x

Daniela Olivera Mesa

May 2022

Copyright Declaration

Abstract

Infectious diseases remain the main cause of death in low-income countries. Because of this, efforts to control the circulation of infectious agents are a priority for public policy makers. This control is challenged by a combination of complex disease dynamics, funding constraints or lack of political and societal commitment. These challenges are generally heterogeneous between geographical settings making the impact of control strategies hard to assess.

In view of this, the purpose of this research is to integrate economic and epidemiological tools in order to improve support for disease control planning and implementation. To do this, I develop a metapopulation model framework to analyse the impact of control strategies when there are neighbouring populations with different epidemiological conditions. The results from this framework can be incorporated into further economic analysis and optimisations.

The first section of this project aims to understand interventions' effects when transmission intensity varies between populations. As a first approach, I implement the framework to analyse indirect effects of interventions for a transmission-stratified population, using generic models. Then, to contextualise the findings from the generic model, I analyse optimal intervention allocation for malaria control. Results from this section evidenced the importance of aligning local and global control strategies.

The second section of this project focuses on understanding the consequences of disease control when intervention uptake varies between populations. For this, the metapopulation framework is applied to estimate the burden populations undergo due to the presence of an anti-vaccination movement. First, I analyse the burden of an outbreak of a vaccine preventable disease in a population where there are opposing vaccine acceptance views, implementing a measles transmission. Finally, I use the same approach to estimate the likely impact of vaccine hesitancy on the control of the COVID-19 pandemic. Results of this section highlight the importance of addressing vaccine hesitancy as a public health priority.

Acknowledgements

I firstly would like to thank my supervisors, Professor Azra Ghani, Professor Katharina Hauck and Dr Peter Winskill for their guidance and encouragement throughout my PhD. I am deeply grateful for their unconditional support during the last challenging years while they were responding to the COVID-19 pandemic.

I would also like to thank Welcome Trust for funding this work and for all the opportunities they have provided me.

The Department of Infectious Disease Epidemiology has been an amazing place to grow as a scientist. I feel lucky to have the opportunity to study in such a rich and stimulating environment. I am grateful to everyone who has taken time out of their busy schedule to advise me or have small talk in the kitchen. I want to thank my fellow PhD students and friends in the department especially Janetta Skarp and Josh D'Aeth for their friendship, for proofreading all my emails and for making this an unforgettable and enjoyable journey.

Special thanks to my friends across the world especially Sandrina, Gonza, Wen, Sergio and Dianis. Who demonstrated to me that time zones and pandemics are not limitations to feeling loved and motivated.

Lastly, I would like to acknowledge my family. I would like to thank Cora for her company and emotional support during the long hours working from home. I am grateful for my parents who encourage me in all my scientific pursuits. I dedicate this thesis to my mum; without her resilience and unconditional love, I wouldn't be here. *Te amoro*. Finally, I owe my deepest gratitude to Andres, my life partner. I could not have completed this journey without his love, his unfailing support or his magnificent cooking skills, which kept me sane throughout this process.

Table of contents

List of figures

List of tables

List of abbreviations and acronyms

CFR	Case fatality ratio
EIR	Entomological inoculation rate
EMA	European Medicines Agency
FDA	Food and Drug Administration
GTSM	Global Technical Strategy for Malaria
HIC	High income country
ICU	Intensive care unit
IRS	Indoor residual spraying
LLIN	Long-lasting insecticidal nets
LMIC	Low middle income country
MMR	Measles, mumps, and rubella
MPB	Marginal private benefits
MSB	Marginal social benefits
NGM	Next generation matrix
NPI	Non-pharmaceutical interventions
NPV	Net present value
OPV	Oral poliovirus vaccine
QALE	Quality adjusted life expectancy
QALY	Quality adjusted life years
SIR	Susceptible- Infected -Recovered
SIS	Susceptible -Infected – Susceptible
WHO	World health organisation

Chapter 1   Introduction

Despite developed global health care, improved sanitation, and major scientific advances in investigating infectious pathogens, infectious diseases remain a major global health threat. Infectious disease burden is highest in low and middle-income countries (LMIC), being the main cause of death in the former (WHO, 2018, Baker et al., 2022). Furthermore, outbreaks due to emerging diseases are causing significant health burden in both high income countries (HIC) and LMIC (Bloom and Cadarette, 2019).

Infectious diseases do not only affect global health but also pose economic and social risks worldwide. Besides the health care costs of treating an infected individual, there are productivity costs due to missed workdays by those who are ill and their caretakers (Bloom and Cadarette, 2019). In low-income countries where the mortality rate from diseases like tuberculosis and malaria is still high, deaths due to these diseases deplete the country's economic workforce, stalling economic growth. Moreover, emerging disease outbreaks saturate health care facilities, increase morbidity and mortality, and disrupt economic and social activities worldwide (Fonkwo, 2008).

Most infectious diseases can be prevented or treated with available interventions. However, political and societal commitment is needed to finance and uphold intervention control plans (Fonkwo, 2008). Policy makers design interventions aiming to control disease transmission. Yet, disease control is a multidisciplinary challenge which requires the integration of biological, epidemiological, and economical approaches amongst other fields to successfully plan intervention strategies. In view of this, in this thesis, I integrate epidemiological tools and economic analyses to improve support for disease control planning and implementation.

1.1   Epidemiological tools for disease control

Epidemiology studies disease dynamics in order to deepen the understanding of transmission, infer patterns of morbidity and mortality, and find ways of reducing the burden caused by diseases (Rock et al., 2014). Mathematical models have been used as a tool to aid epidemiologists in understanding these dynamics. With these models, the complexity of disease dynamics can be translated into

mathematical language and disease trajectories under different scenarios can be analysed. Moreover, outcomes from mathematical models can be employed to inform economic analyses in order to assess the feasibility and cost-effectiveness of control strategies.

1.1.1   Basic models

Compartmental models are one of the most frequently used mathematical models employed to represent disease dynamics. These models are pathogen centric and divide the population (host) into discrete non-overlapping compartments incorporating a range of epidemiological characteristics, which usually are different infection states (Rock et al., 2014). Susceptible- Infectious – Recovered (SIR) and Susceptible -Infectious- Susceptible (SIS) models are the simplest and most widely used mathematical models. The former are usually implemented to analyse epidemic diseases, whereas the latter are usually implemented to analyse endemic diseases without long-term immunity (Hanski and Gaggiotti, 2004). Simulations with generalised SIS and SIR models provide helpful insights into the effects that alterations in the transmission cycle have on the burden of the disease. These theoretical analyses allow epidemiologists to evaluate intervention and elimination strategies that otherwise would require expensive and sometimes non-ethical trials. An example of this is the study carried out by Fitzpatrick and Bauch (2011), in which they modelled different resource allocations for the eradication of three hypothetical vaccine preventable, paediatric diseases. They found that it is better to allocate the budget for supplementary immunisation activities to one disease at a time rather than evenly distributing resources among 3 diseases (Fitzpatrick and Bauch, 2011).

Basic SIR and SIS models often omit many important aspects of the infection cycle and disease biology. Variations of these models can be used to introduce realism and represent the complex natural history of infection (Rock et al., 2014). These variations may include adding more compartments to represent different stages of the disease or to account for transmission heterogeneity throughout the infection cycle population. For example, analyses of the Global Polio Eradication Initiative are based on a complex compartmental model, which considers the different polio serotypes and includes faecal-oral transmission. Additionally, the model contains different immunity and waning stages representing disease dynamics with different vaccines (Duintjer Tebbens et al., 2015, Duintjer Tebbens et al., 2010).

Another complexity ignored by basic models is population heterogeneity. Simple compartmental models assumed that population is homogenous and parameters of transmission are the same for all

individuals within the same compartment. Population heterogeneity can be included in the model partitioning the population into groups, which may represent age groups, risk stratification, different intervention uptake rates among others. In these models each group would have the same compartments, but parameters may differ (Rock et al., 2014). For instance, some analyses for the control of malaria are based on a mathematical model for the transmission which stratifies humans by age and heterogeneity in heterogenous exposure to mosquito bites (Griffin et al., 2010b). These models with stratified populations have allowed epidemiologists to represent complex population structures and evaluate the outcome of intervention packages and elimination strategies (Duintjer Tebbens et al., 2015, Winskill et al., 2019, Walker et al., 2016).

1.1.2 Metapopulation models

One of the most common population heterogeneities in disease modelling are those associated with spatial aggregations and connections. Simple compartmental models can be modified to represent spatial heterogeneity by using metapopulation models. These models divide the population into independent subpopulations or patches. Each patch has homogenous internal dynamics (e.g., SIR or SIS) and is connected by some degree of migration between the other patches (Keeling and Rohani, 2008, Yan et al., 2018, Colizza and Vespignani, 2008). This metapopulation structure is generalisable to another context to capture different transmission heterogeneity patterns.

Metapopulation models were initially developed for theoretical conservation ecology but are now widely used to represent transmission heterogeneity for infectious diseases. In the epidemiological version of metapopulation models, infection events and susceptible individuals are analogous to colonisation events and patch resources, respectively, from the ecological version of metapopulation models. In 1997, Grenfell and Hardwood developed the first spatial metapopulation model in epidemiology. They modelled measles transmission using the same principles applied in theoretical ecology models (Grenfell and Harwood, 1997). Since then, spatial modelling using metapopulations has been used for the analysis of disease heterogeneity for control and elimination strategies.

To date, the implementation of metapopulation models to analyse disease control strategies has allowed modellers to have a good insight into disease dynamics. Particularly for measles, metapopulation structure and parameterisation has been widely studied (Ball et al., 2015). Furthermore, metapopulation models for measles have been implemented to support research

towards planning of control and elimination plans (Ferrari et al., 2008, Grenfell et al., 2002, Hanski and Gaggiotti, 2004). This can be seen in a study by Lee *et al*. (2019), where they considered whether Kenya should invest in vaccination to geographically hard-to reach population. For this, the authors developed a metapopulation model to estimate the potential benefits of vaccinating the hard-to-reach population over continuing with traditional vaccination campaigns. In their analysis, they conclude that in order to achieve 2020 elimination goals, the efforts of vaccinating hard-to-reach populations are worthy and cost-effective (Lee et al., 2019).

In mathematical terms, in metapopulation models, disease dynamics in each patch are described by a set of differential equations representing homogenous internal dynamics. Connection between patches is represented by a modified force of infection that considers both the infectious population of the patch and the coupling with other patches (Keeling and Rohani, 2008). For a simple compartmental model, the force of infection is represented as $\lambda = \beta \frac{I}{N}$. Here β is the effective contact rate and I/N represents the infectious population. In a metapopulation model the force of infection can be defined as follows.

$$\lambda i = \beta_i \sum_j \rho_{ij} \frac{I_j}{N_i}$$

The subscript *i* refers to a particular patch and ρ_{ij} is the strength of interaction to patch *i* from patch *j* (Keeling and Rohani, 2008). In the absence of interaction $\rho_{ij} = 0$ $(i \neq j)$ and the dynamics of each patch can be defined independently. The interaction coefficients shape the model's mixing matrix (P), where the diagonal values ρ_{ii} represent strength of transmission associated with infectious agents from the same patch and the non-diagonal elements of the mixing matrix ρ_{ij} $(i \neq j)$ represent coupling interactions between patches.

$$P = \begin{bmatrix} \rho_{11} & \cdots & \rho_{1n} \\ \vdots & \ddots & \vdots \\ \rho_{n1} & \cdots & \rho_{nn} \end{bmatrix}$$

There are different types of coupling interactions depending on the nature of hosts and their movement. For instance, plant interactions assume that the hosts do not move, so the coupling transmission is assumed to be wind or vector borne. Animal interactions on the other hand assume that spread of the disease is due to migration and permanent movement between patches. Finally, human interactions assume that the coupling interaction is due to temporal commuters between

patches (Keeling and Rohani, 2008). Throughout this thesis, I will focus on the last type of coupling interaction.

For human coupling interactions, the force of infection in a patch can be expressed as a weighted sum of prevalence in all patches, where the weight is given by the interaction coefficient ρ_{ij}, under these critical assumptions (Keeling et al., 2004, Keeling and Rohani, 2008):

- All patches are the same size.
- Time spent away from the home patch is relatively short compared to the disease dynamics.
- Distribution of commuting individuals is at equilibrium.

1.2 Economic analyses for disease control

The advantages of controlling disease transmission were reaiterated with the eradication of smallpox in 1980. These advantages went beyond the health gain of preventing an infection and include the economic gains of averted morbidity and mortality in addition to the avoidance of the cost of future control measures. When smallpox was declared eradicated, public health organizations were able to stop investing in surveillance, vaccinations and treatment of cases. Economic analyses have demonstrated that smallpox eradication was the best global public investment in history (Barrett, 2013b) and since then, these analyses have been assisting public health and healthcare decision making.

As mentioned above, epidemiological models can be a reliable representation of infection dynamics and the effects of interventions. However, these models ignore aspects which could affect implementation of policies. Including the impact of healthcare on a population, the evaluation of costs, and the analysis of supply and demand of healthcare resources might alter decisions based only on epidemiological model outputs (Klein et al., 2007). Therefore, health economic analyses are key when assessing intervention control policies, particularly in determining the societal value of interventions (Carande-Kulis et al., 2007).

Health economic analyses are challenged by a suboptimal market. The demand and supply of healthcare and health protection goods rely on individual and collective actions which may not be aligned toward allocative efficiency. Individual demand for intervention is usually less than the

economic optimal, given that some indirect effects of prevention and services may be overlooked by individuals. Some of these indirect effects are related to disease prevention interventions which convey benefits to other individuals (not only the one consuming it). Additionally, some public health interventions are public goods (e.g. the infrastructure to respond to disease outbreaks) and people cannot be excluded from benefiting from these (Carande-Kulis et al., 2007).

Given that the private market results in suboptimal outcomes for disease intervention strategies, government interventions are required to achieve socially optimal outcomes. Functioning markets assure allocative and technical efficiency. This assures that the socially optimal quantity of public health goods are produced, and that production uses least amount of resources. In the absence of functioning markets, other tools need to be employed to assure efficiency. One of the most widely used tools are cost-effectiveness and cost-benefit analyses. These analyses are used to estimate the costs and outcomes of alternative health interventions. Cost-effectiveness analysis measures outcomes in natural units or summary measures of health, such as Quality-Adjusted-Life-Years (QALYs), whereas cost-benefit analysis measures both costs and outcomes in monetary terms (Turner et al., 2021). The former is more widely accepted in health policy, as the monetization of health can be challenging (Garber and Sculpher, 2011).

1.2.1 Resource allocation

Both cost-effectiveness and cost-benefit analyses are used to analyse different intervention strategies in order to inform resource allocation decisions. These comparisons are usually made against a counterfactual or baseline scenario that represents the current standard of care (Turner et al., 2021). For both analyses, costs estimation usually includes direct costs such as resources, training, surveillance, and administration logistics in addition to the intervention prices. These costs are then compared to the outcomes of interventions, which can be estimated using transmission modelling projections translated to QALYs or monetary value. Implementing disease transmission models to analyse interventions requires significantly more computation than linear methods applied in other areas of economics. Yet, it is the best approach to capture the non-linear relationship between investment in intervention and health outcomes and most importantly, to estimate the impact of the intervention on both the treated and the untreated individuals, which is a unique challenge for infectious diseases (Brandeau, 2004).

The complexity of cost-effectiveness analyses and disease modelling can be seen in the case of poliovirus control studies. In a comprehensive study of long-term poliovirus risk management policies, Tebbens *et al*. (2015) used a metapopulation model to assess different vaccination strategies towards polio eradication. They evaluated different policies in relation to the cessation of oral poliovirus vaccine (OPV), the current *status quo* vaccination policy in LMIC countries. These policies included different timeframes for the cessation of vaccination and supplementary immunisation activities with an injectable inactivated poliovirus vaccine. They estimate the cost-benefits of these policies over the current policy of administrating OPV and confirmed the cost effectiveness of a coordinated cessation of OPV after eradication is achieved. However, the authors acknowledge the limitations of their analysis, as there is high uncertainty for future costs and transmission parameters, which can alter the results significantly (Duintjer Tebbens et al., 2015).

Comparisons between interventions like the example above can help decide which is the best option available over a finite set of alternatives. Yet, these comparisons do not associate the best option with the funding available (Knerer et al., 2021). The distribution of funds requires optimisation analyses to identify the set of public health interventions that maximise health gain within limited health care resources. In order to do this, the use of constrained optimisation methods integrated with the output of epidemiological models has been proposed (Brandeau et al., 2003). These methods use epidemiological model outputs to assess different intervention packages (i.e. coverages or scheduling) and find the option that maximise the health benefits subject to a funding constraint. This involves complex computational and mathematical calculations. To date, relatively few studies have used constrained optimisation to analyse real-world allocation challenges; some examples can be found for dengue (Knerer et al., 2021), malaria (Walker et al., 2016, Winskill et al., 2019, Scott et al., 2017) and measles (Klepac et al., 2012).

Allocating interventions and funds optimally is not always enough to achieve disease control targets. In order to do so, disease control programs require strong political and societal commitment (Tomori, 2011). This is partly because control interventions not only have effects on the individuals that received them but can have consequences for other people. For example, in vaccination campaigns, when herd immunity is achieved, disease transmission can be stopped without vaccinating everyone. These indirect consequences are known in economics as externalities (Barrett, 2004) and usually are not considered in cost-benefit intervention policy discussions (Boulier Bryan et al., 2007). However, externalities can have a large effect on the costs and benefits of infectious disease control programs.

19

1.2.2 Externalities

In economics, externalities are defined as the effects to uninvolved parties, that arise from an individual's actions. In epidemiology these effects are known as spillover or community-wide effects (Hauck, 2018). Externalities can also be defined as the gap between social and private benefits. Social benefits refer to the overall benefits of an intervention and include both the direct and indirect effects. On the other hand, private benefits refer to the direct benefits derived by the person who received the intervention. Private benefits determine the quantity demanded of products and services, including public health prevention; it is assumed that an individual will purchase based on their estimation of the private benefit which will depend on the expected risk of infection and the cost of the disease (Boulier Bryan et al., 2007, Hauck, 2018).

Externalities may be positive or negative. Preventive interventions (e.g., vaccination) by one individual have positive externalities reducing the risk of infection of others. Most of the time treatments also have a positive effect when they increase the recovery rate of individuals, reducing the infectious population (Hauck, 2018). Negative externalities such as tobacco consumption have indirect health effects on non-consumer due to passive smoking, increasing their healthcare expenses and reducing their quality of life (Carande-Kulis et al., 2007). Moreover, treatments like antibiotics may have both positive and negative externalities, limiting the spreading of a disease but increasing the likelihood of development of resistant bacteria (Klein et al., 2007).

When analysing public health interventions, welfare economics assume humans are altruistic and would base their actions on the social benefits (Hauck, 2018). Yet, when making decisions individuals tend to consider only the effects impacting them directly (Gersovitz, 2011). Thus, positive externalities can generate incentives for individuals, and for countries, to free ride on disease control programs (Barrett, 2004). At the individual level, indirect protection conferred by preventive interventions can encourage individuals to not participate in prevention campaigns and rely on the protection conferred by others. Individual decisions made by free-riders can influence the success of disease control programs. When individuals do not participate in prevention campaigns, the impact can be lower than expected and coverage milestones may be delayed, as has previously been seen for polio (Tomori, 2011) and measles (Larson, 2018) vaccination initiatives. Reluctance to take up interventions is more likely to happen when disease incidence is low, externalities are high, and the perceived risk of vaccination increases (Boulier Bryan et al., 2007). Unfortunately, to date, the impact of individual free-

riding on disease control programs is understudied, particularly when budget allocation for vaccination strategies is evaluated (Deka and Bhattacharyya, 2019).

At the country level, when a country makes the decision to eliminate a disease, this decision will depend on whether all countries in the region eliminate it (Barrett, 2004). This is because countries cannot be excluded from the benefits of disease control in a neighbouring country. These benefits may lead neighbouring countries to free-ride from the countries implementing disease control strategies in the bordering region, as it is the profit maximizing strategy. For example, countries with high malaria transmission usually have little incentive to invest in control on areas bordering low malaria transmission (Khadka et al., 2018). Welfare economics usually addresses these collective decision processes and their outcomes, which are important for disease control success (Sicuri et al., 2015). Retrospective analyses of the smallpox eradication program have used a game theory approach to understand the impact of cooperation on the eradication of the disease (Barrett, 2013b, Barrett, 2006). Still, the effects of neighbouring countries' decisions and cooperation across borders does not receive enough attention when taking public health decisions.

Because of these free-riders, calculating the externality becomes important for the analysis of disease control plans, particularly if there is more than one stakeholder involved. Knowing the effect of externalities allows public policy makers to align private and social benefits when designing disease control programs (Hauck, 2018, Gersovitz, 2011). The most common solution to fill the gap between private and social benefits is to subsidize actions that cause positive externalities, and tax or fine those actions that generate negative externalities (Gersovitz, 2011). Financial incentives (or disincentives) are mechanisms used by governments to correct for market failure in healthcare and increase economic efficiency (Chaudhuri et al., 2017). Known examples of this are high taxes on cigarettes that promote a reduction in tobacco consumption and subsidised cost of vaccines that promote their uptake (Carande-Kulis et al., 2007).

1.3   Diseases of interest

The section below describes three diseases that will be implemented as case studies throughout this thesis. I will analyse challenges faced by public policy makers that are particular for each disease. This case-study approach was chosen to allow a deeper insight into the complexity of planning disease control in real life.

1.3.1   COVID-19

COVID-19 is an infectious disease caused by the severe acute respiratory syndrome coronavirus 2 (SARS-CoV-2). The first human case was identified in Wuhan, China in December 2019. In January 2020 cases were reported outside China and subsequently the virus started spreading worldwide. On March 11, 2020, the WHO declared COVID-19 a pandemic. At the time this thesis is being written the pandemic is still ongoing, the virus is present across the globe, and more than 511 million cases and 6.2 million deaths have been reported worldwide (World Health Organization, 2022b).
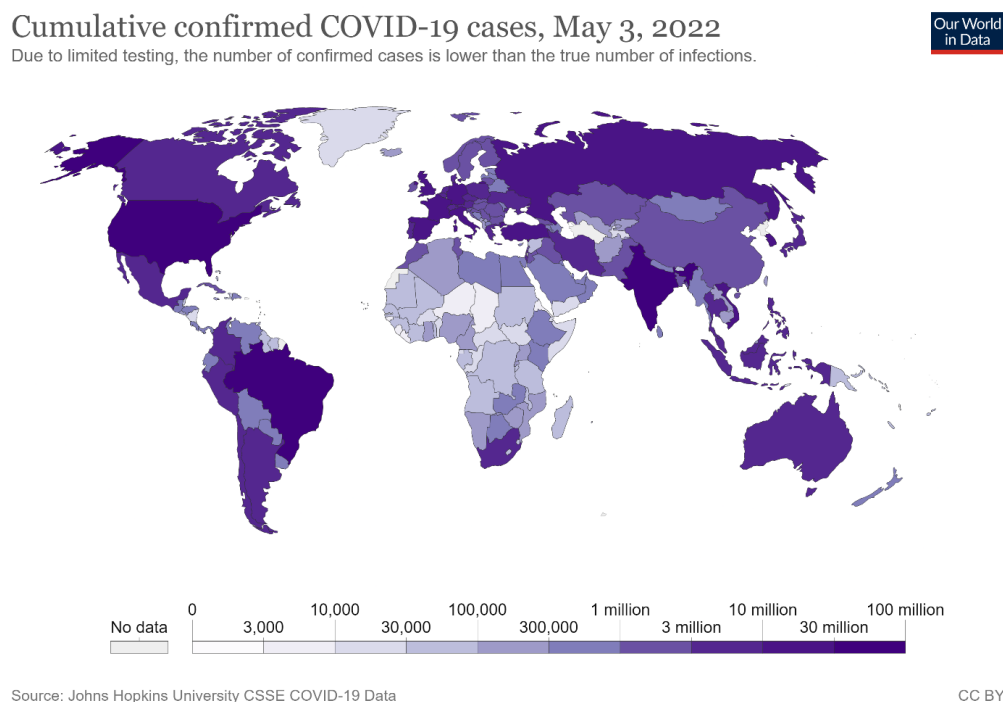
Figure 1. 1 Cumulative reported COVID-19 cases by May 3rd, 2022. Reproduced from (Our World in Data, 2022)

The infection with SARS-CoV-2 causes a mild respiratory illness, which in some cases can become severe and even cause death, particularly in older age groups and those with underlying medical conditions. The virus can be transmitted by respiratory droplets or aerosols from an infectious individual. Once in the host, wild type SARS-CoV-2 has an average incubation period of 5-6 days and can be transmitted from a couple of days before symptoms appear (Anderson et al., 2021, World Health Organization, 2022b). A particular feature of COVID-19 is the high proportion of pre-symptomatic transmission and asymptomatic infectious cases, which make the disease hard to control. Efforts to control the spread of COVID-19 have relied on Non-Pharmaceutical Interventions (NPIs) like social distancing, stay-at-home orders, and venue closures. In the early stages of the pandemic, most countries implemented strict lockdowns, which helped contain the spread of the disease (Banholzer et al., 2021). However, some healthcare systems were saturated and more recent data on excess deaths have shown a high level of mortality (Wang et al., 2022, World Health Organization, 2022a). Now, some pharmaceutical interventions are available, and most countries continue to control the spread of the disease by a combination of these new interventions and NPIs (Anderson et al., 2021).

New coronavirus drugs have been under development since the beginning of the pandemic. To date, 8 have been approved by the European Medicines Agency (EMA) (European Medicines Agency, 2022) and 1 by the Food and Drug Administration (FDA) in the USA (National Institutes of Health, 2022). These treatments reduce the probability of severe COVID-19 and accelerate recovery time. Currently, these drugs are now included in clinical protocols to treat COVID-19. However, treatments are not the key pharmaceutical intervention for the control of COVID-19. Since the licensing and mass production of vaccines, vaccination to build up herd immunity has been the focus for COVID-19 control.

1.3.1.1 Vaccines

During the pandemic, unprecedented speed in scientific research to develop vaccines was witnessed. On December 11, 2020, the first vaccine was approved under emergency use by the FDA and by May 2021, 14 vaccines had been licenced across different countries. These vaccines are based on different underlying technologies, from novel methodologies like mRNA or viral vector vaccines to more traditional methods like inactivated virus vaccines (LSHTM Vaccine Centre, 2021). Ther efficiency against symptomatic disease from wild type SARS-CoV-2 has been reported to vary from 50% to over 95% (Polack et al., 2020, Voysey et al., 2021, Baden et al., 2020, Logunov et al., 2021, Hitchings et al., 2021).

At the beginning of 2021, mass vaccination campaigns started to rollout worldwide and since then a significant reduction in morbidity and mortality has been evidenced (Anderson et al., 2021). To date, 11.5 billion doses have been administered (World Health Organization, 2022b), mainly in high income countries. Unfortunately, only 1.9% of individuals in LMIC have received at least one dose of a COVID-19 vaccine (Batista et al., 2022), whereas in HIC booster dose coverage exceeds 50 doses per 100 individuals (Our World in Data, 2022). This inequity in access has complicated the control of the pandemic, given that until high coverage is achieved worldwide, the risk of new variants emerging is high (Pilkington et al., 2022).

1.3.1.2   SARS-CoV-2 variants

Another feature of SARS-CoV-2 is the continual evolution of the virus, that has led to new and more transmissible variants. Which have established and have dominated transmission in different parts of the world. Each of these variants differs in some way epidemiologically and biologically from the original wild-type virus. Thanks to high throughput sequencing platforms, mutations and phylogenetics of these variants have been identified in record time. However, how these mutations provide an evolutionary advantage and alter the infection process is still under research (Anderson et al., 2021). It has been estimated that for the Delta variant mutations resulted in a 2-3-fold increased infectiousness compared to the original wild type strain (Liu and Rocklöv, 2021). For the Omicron variant, this increase is estimated to be as high as 5 times (Burki, 2022).

Vaccine efficacy and vaccination programmes have also been affected by new SARS-CoV-2 variants. Although vaccines seem to protect against severe disease for most variants, more research is needed to assess the effects on vaccine efficacy and protection durability (Krause et al., 2021). In particular, the Omicron variant has posed a challenge to current vaccination plans as vaccine efficacy against this variant show reduced protection compared with previous variants (Nyberg et al., 2022). This has hastened booster dose programmes in HIC, where both vaccinated and unvaccinated individuals seemed to be similarly infected when Omicron started circulating (Burki, 2022). More research about new variants and vaccine efficacy is needed to estimate how to optimally allocate available vaccines into current vaccination programmes (Krause et al., 2021).

1.3.2 Malaria

Malaria is a vector-borne disease transmitted by the bite of an *Anopheles* mosquito and caused by *Plasmodium* parasites. Currently, there are five species of *Plasmodium* parasites that can cause malaria in humans, with *P. falciparum* and *P. vivax* posing the greatest threat and the former being the deadliest (World Health Organization, 2021c). In 2020 there were 241 million cases and 627 000 deaths reported in the 85 malaria endemic countries. It is estimated that the Africa region accounted for 95% of all malaria cases and 96% of deaths (World Health Organization, 2021d).

Figure 1. 2 Countries with malaria indigenous cases in 2020. *Reproduced from (World Health Organization, 2021d)*

1.3.2.1 Life cycle

Malaria has a complex life cycle that starts when a malaria-infected *Anopheles* mosquito bites a human and inoculates parasites that travel to the liver. In the liver, the parasite remains for 9-16 days, where it reproduces asexually. Afterwards, the parasite leaves the liver to infect erythrocytes. During the blood stages of infection, the parasite undergoes asexual reproduction and the human experiences clinical malaria symptoms. A small proportion of the parasites in the bloodstream differentiate into gametocytes, which are the mosquito's infective stages. This process lasts between 48-72 hours. When a susceptible mosquito bites an infected human, gametocytes are ingested and travel to the mosquito's midgut. The parasite undergoes sexual reproduction and becomes a motile ookinete, that migrates to the midgut wall, grows and matures as an oocyst. The oocyst breaks and releases sporozoites, the infective stage for humans, which travel to the salivary glands to start the life cycle again (Tuteja, 2007).
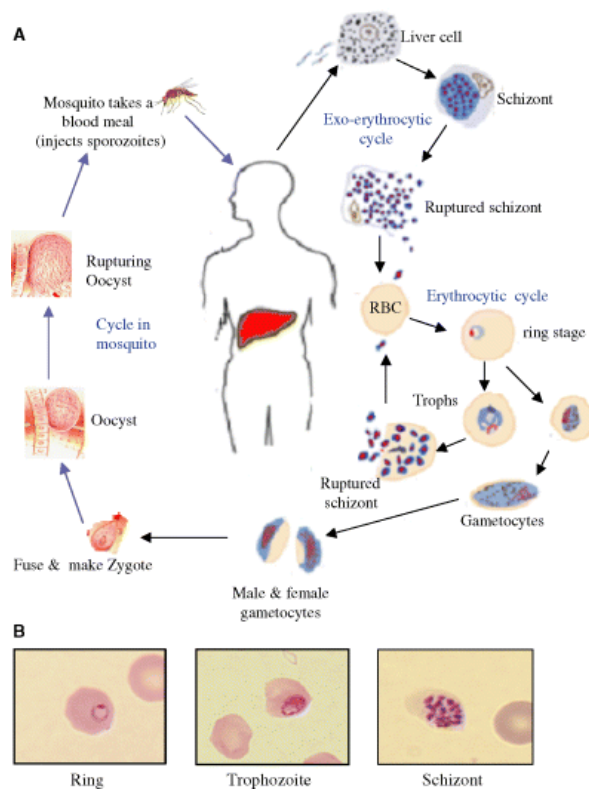
Figure 1. 3 Malaria life cycle. *Reproduced from (Tuteja, 2007)*

1.3.2.2   Malaria control

To date, vector control has been the pillar of malaria prevention. This type of control aims to reduce the vectorial capacity of vector populations and it is tailored to each location based on environmental, epidemiological and entomological characteristics (World Health Organization, 2015, Tizifa et al., 2018). The two main vector control interventions that are broadly implemented are long-lasting insecticidal nets (LLINs) and indoor residual spraying (IRS).

LLINs are nets hung over the bed that protect the sleeper by creating a barrier between vectors and humans. LLINs also act to reduce the vector population size as they are treated with insecticides that can last up to three years. Most national malaria control programs have implemented high coverage LLINs, with 2.3 billion bed nets distributed from 2004-2020, the majority in the African region (World Health Organization, 2021d). Although this has been one of the most successful interventions, in recent years it has been threatened by the resistance to pyrethroid insecticides, which is the most

common insecticide used in LLINs (Tizifa et al., 2018). This resistance is widely spread across the globe, with high levels of resistance reported in at least 27 countries (World Health Organization, 2021d).

IRS aims to kill the vectors by covering indoor surfaces (ceilings and walls) with long lasting insecticides. For the last decades, IRS has been the main strategy for vector control, and it has been responsible for the elimination of malaria in various countries and the reduction of its burden in others (Tizifa et al., 2018). In 2021, it is estimated that 87 million people were protected by this intervention. In the same manner as LLINs, the efficacy of this intervention has been threatened by insecticide resistance (World Health Organization, 2021d).

Besides vector control, seasonal malaria chemoprevention is also employed as a control intervention in countries where malaria is seasonal (World Health Organization, 2021c). This intervention was recommended in 2012 for young children and consists of monthly course of malaria treatment administered during the malaria transmission season (Coldiron et al., 2017). By 2021 at least 33.5 million children had been offered at least one dose in the Sahel region (World Health Organization, 2021d). Unfortunately, due to scale-up, logistic restrictions and drug resistance, this intervention cannot be used in all settings.

All in all, malaria control requires multiple intervention strategies working in conjunction with each other. The distribution of long-lasting insecticidal nets, indoor residual spraying, seasonal chemoprevention and an efficacious treatment have been used as control strategies for malaria and have reduced malaria incidence by 26% between 2000-2013 (Walker et al., 2016). However, new tools will be needed to augment existing control interventions to achieve higher levels of control. New interventions are expected to become available in the next decade to support the fight against malaria. These new tools include new insecticide formulations and methods of application, better rapid diagnostic tests to identify different species and drug resistance and several vaccine candidates, which are in different stages of development (World Health Organization, 2021b).

In 2021 RTS,S, the first vaccine against malaria, was approved to be implemented in children living in regions with moderate to high transmission as a complement to the current package of existing interventions. RTS,S is a pre-erythrocyte vaccine, which targets *Plasmodium falciparum* before it

enters the blood cells. Pilot implementation in three countries showed a favourable safety profile and significant reductions in severe malaria cases, which led to its recent approval (World Health Organization, 2021d).

1.3.2.3   Malaria elimination campaigns

Malaria elimination campaigns have been on the agenda of public health agencies since the 1950s when the potential of reducing transmission levels using insecticides was demonstrated by successful field experiments and mathematical models by Ross and MacDonald (Macdonald, 1956). In 1955 the Global Malaria Eradication Program was launched and by 1978, 68 countries had been declared malaria free (Feachem et al., 2009).

Efforts to eradicate malaria decreased in the late half of the 20th century causing an increase in malaria morbidity and mortality rates. Consequently, early in the 21st century, malaria was recognised again as priority global health issue by the WHO. Since then, unprecedented efforts have been made towards reducing the burden of the disease. In 2015 the Global Technical Strategy for Malaria (GTSM) 2016-2030 was established and new goals towards malaria elimination and control were outlined. These new goals aim to reduce malaria deaths and incidence by 90% and eliminate the disease in at least 35 countries compared with 2015 (World Health Organization, 2015). However, the case incidence 2020 milestone was reported to be off track by 40% and only 3 countries have been certified malaria-free instead of the 10 expected by this date (World Health Organization, 2021d).

1.3.3   Measles

Measles is a highly contagious human viral pathogen. It is caused by a paramyxovirus, and it is air-borne transmitted by respiratory droplets. This virus mainly affects children and can cause a febrile rash illness, which usually starts with general symptoms like fever, conjunctivitis and cough followed by a characteristic maculopapular rash. In some cases, measles can cause life-long complications and even death (Holzmann et al., 2016, Rota et al., 2016).
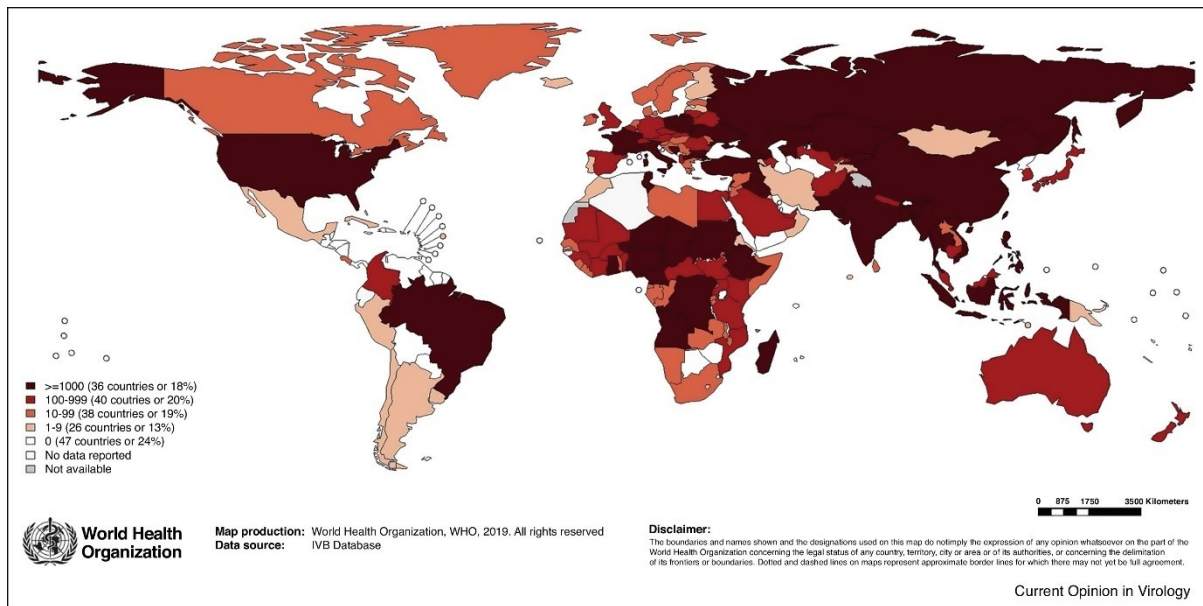
Figure 1. 4 Measles cases reported to WHO in the first half of 2019. Reproduced from (Hotez et al., 2020)

Measles is highly infectious, and a single infected person can infect up to 15-18 people in a fully susceptible population (Anderson et al., 1992). Before the 1960s it was estimated that annual measles incidence was around 30 million cases and 2-3 million deaths globally (Rota et al., 2016). In 1963 an effective and safe vaccine was developed and it was included in the Expanded Immunization Programme of WHO a decade later (Hotez et al., 2020). Since then, measles deaths have decreased 94% with 140 000 deaths reported worldwide in 2018 (World Health Organization, 2019a).

Even though there is no specific anti-viral treatment, measles has all the components of an eradicable disease: a safe and efficient vaccine, no animal reservoirs and adequate infrastructure for global surveillance and control (Paules et al., 2019b). Despite these conditions, the high infectiousness of the disease poses a challenge for elimination plans as vaccine coverages greater than 95% are required to stop the circulation of the virus (WHO, 2012) .

1.3.3.1 Measles elimination strategies

In 2012 the WHO set up a strategic plan to eliminate measles in five of the six WHO regions by 2020. This plan was based on surveillance, routine and supplementary mass vaccination. Before the plan was set, the Americas region had already achieved the goal of elimination in 2002; and the European, Western Pacific, and Eastern Mediterranean Regions were on the path to elimination (WHO, 2012).

By the end of 2020, this strategy aimed to interrupt virus transmission for more than 12 months worldwide and achieve at least 95% coverage for both doses of measles vaccine (WHO, 2012, Paules et al., 2019b).

Unfortunately, despite the elimination efforts in the different WHO regions, measles cases have been increasing since 2017 and now the disease is endemic around the world. In 2019 the number of measles cases reported was the highest of the decade, almost tripling the cases reported in 2018. This set back in the elimination program has been attributed to a decrease in vaccination coverage. Reasons behind lower vaccine uptake include war, and political and socioeconomical conflicts that limit vaccination access to susceptible populations. Additionally, vaccine refusal has been acknowledged as one of the main reasons for the increase in measles cases in countries where vaccines are available and accessible (Hotez et al., 2020). Moreover, the decrease in vaccination coverage has been exacerbated in the last two years by the COVID-19 pandemic. Measles surveillance and vaccination systems weakened during the pandemic response, registering in 2020 the largest increase in unvaccinated children in 20 years (World Health Organization, 2021a).

In 2021 a new measles strategic framework was set up by WHO. This new strategy aims to eliminate measles by 2030, taking into account the rising contextual changes and challenges. In this new strategy weak healthcare systems, increased vaccine refusal and deteriorated surveillance and vaccination programmes are recognised as key challenges.

1.4   Thesis aims and overview

Designing intervention control policies is a multidisciplinary challenge. Epidemiological models can represent pathogen's complex life cycles and help estimate the direct and indirect impact of interventions on disease burden. Economic analyses of these indirect effects or externalities also play an important role in the design of intervention plans with available resources, particularly when multiple stakeholders are involved, and their goals are not aligned. To date, there has been limited connection between epidemiological models and externalities analyses for disease control. Without considering aspects of both the economics and epidemiology, policy makers findings may be biased when assessing disease intervention strategies.

Considering the above, in this thesis I aim to investigate the trade-offs and economic optimisations of infectious disease control strategies in an heterogenous population. I begin the thesis by analysing optimal strategies for the allocation of interventions from different stakeholder perspectives. Then, in the second part of the thesis, I focus on assessing the effect of intervention uptake choices on disease prevention strategies.

The methodology used throughout the thesis is developed in Chapter 2. In this chapter, I establish a metapopulation model framework to analyse impact of control strategies when there are neighbouring populations with different transmission conditions. As a first example, I evaluate vaccination externalities in a heterogenous population for basic SIR and SIS models. Additionally, I compare different vaccine allocation strategies in order to maximise global externalities. In Chapter 3, malaria is used as a case study to compare global and local perspectives on different intervention allocation strategies. For this, I extend the metapopulation model to include malaria transmission dynamics. Using this model, I assess the health impact of different LLIN distribution strategies when sub-populations have different transmission levels. I then compare optimal intervention allocation from different stakeholders' perspectives, minimising health burden for the population and analysing the effects of cooperation between sub-populations to control the disease.

In the second part of the thesis, I evaluate social effects for disease control when intervention uptake varies between populations. In Chapter 4, I adapt the metapopulation framework to model patches with different willingness to adopt optimal vaccination programs instead of modelling different transmission. As a case study, I analyse measles dynamics and assess the societal economic burden of low vaccine uptake due to anti-vaccinators within a population. Using previously reported parameters and costs for measles outbreaks, I estimate the economic impact of an emerging anti-vaccination population in an England-like scenario. In Chapter 5, the methodological approach developed for measles is implemented to understand the likely impact of low vaccine uptake on control of the COVID-19 pandemic. For this, a previously developed mathematical model is implemented and different vaccine uptake scenarios are projected and compared based on survey data on self-reported intention to be vaccinated. Finally, I conclude in Chapter 6 by discussing the key findings of this thesis, their public policy implications, limitations of the methodology implemented and future directions of this work.

Chapter 2 Estimating vaccination externalities in heterogeneous populations

2.1   Introduction

As introduced in Chapter 1, externalities determine the indirect effects of interventions and measure the difference between private and social benefits. Estimating externalities is key when taking public health decisions given that they can help align individual and social goals towards disease control (Gersovitz, 2011). A good illustration of externalities in public health is vaccination programmes. From the social perspective, the ultimate goal of vaccination campaigns is to achieve herd immunity by high vaccine coverage, in order to stop the transmission of the pathogen (Barrett, 2013a). However, this can be challenged by selfish behaviours. Vaccination confers protection not only to vaccinated individuals but to non-vaccinated individuals, by reducing the risk of infection. This incentivises individual behaviour to free ride on the protection conferred by those already vaccinated, particularly, when vaccine coverage levels are close to the herd immunity threshold and consequently the risk of infection is low (Hauck, 2018).

To date, relatively few studies have analysed the role of externalities in vaccination policies. Whilst some theoretical studies had been carried out (Boulier Bryan et al., 2007, Perrings et al., 2014) there have been few empirical investigations into estimating externalities of disease control interventions. Furthermore, these empirical applications fail to include epidemiological frameworks that represent complex infection dynamics (Cook et al., 2009, White, 2021).

In 2007, Boulier et al. implemented a basic SIR model to analyse externalities under different vaccination coverage, disease infectiousness and vaccine efficacy. Their results illustrated that the vaccination externalities behaviour is complex and does not follow a linear relationship with vaccine coverage (Boulier Bryan et al., 2007). This simple approach taken by Boulier et al. (2007) gave important insights about the behaviour of externalities using epidemiological models. Nonetheless, research to date has not yet determined how these externalities vary in more realistic disease models. As described in the previous Chapter, population heterogeneity is omitted in basic SIR models. However, these heterogeneities represent key aspects of disease transmission which may have a

significant effect on intervention externalities. In this Chapter, I assess the effect of population heterogeneity in vaccination externalities, building up on the work developed by Boulier et al.

To evaluate vaccination externalities in a heterogenous population, I develop a generic metapopulation deterministic model. The model represents an infectious disease with three interconnected subpopulations, each with an independent transmission intensity. Using the metapopulation model as a foundation and vaccination as an intervention example, I estimate marginal externalities for different vaccine allocation strategies. These strategies are then compared to find the strategy that maximises health gains under a limited number of vaccine doses.

I evaluate vaccination externalities by adapting the methods proposed by Boulier *et al* (Boulier Bryan et al., 2007). These methods are based on three key concepts:

i. **Marginal Social Benefit**: The marginal social benefit (MSB) of an intervention is the social value of the number of cases averted due to an additional unit of intervention in this application or context. This benefit includes both direct benefits to vaccinated individuals and indirect benefits to the unvaccinated people (Boulier Bryan et al., 2007). When the cost of the disease (*c*) is constant and homogeneous for all individuals in the system, the MSB can be defined as the product of the cost of the disease and the marginal effect of vaccination, where the marginal effect of vaccination is the difference in the number of cases averted due to vaccinating an additional person (Boulier Bryan et al., 2007). Usually, the marginal effect of vaccination is expressed as number of cases prevented, while MSB represent the economic value of these prevented cases.

ii. **Marginal Private Benefit:** Marginal private benefit (MPB) refers to the expected value of illness avoided by an unvaccinated individual due to an additional person in the population being vaccinated. The MPB determines the demand for vaccination considering level of population coverage (and therefore perceived risk of infection). It is assumed that an individual will purchase vaccination based on their estimation of the private benefit, which will depend on the expected risk of infection and the cost of the disease (Boulier Bryan et al., 2007).

iii. **Marginal externalities:** The difference between MPB and MSB refers to the indirect effects on the population due to an additional vaccination. This is known as the marginal externality (Boulier Bryan et al., 2007). This value represents the welfare loss, and it is not constant.

Marginal externalities may rise or fall depending on the infectiousness of the disease, the number of vaccines available and the existing level of vaccination coverage in the population (Boulier Bryan et al., 2007) .

2.2   Methods

2.2.1   The models

I developed two metapopulation models. Each model consisted of three different transmission-stratified interconnected patches, each with a closed population (*i.e.*no births or deaths). In the first model, each patch represented an SIR disease dynamic as shown in **Figure 2. 1A.** In the second model, each patch represented an SIS disease dynamic as shown in below **Figure 2. 1B.** For both models, susceptible individuals can acquire infection from infectious individuals at a transmission rate β. Individuals remain infectious on average a period of time $1/\gamma$, at which point they enter the recovered population (SIR model) or go back to the susceptible population (SIS model). The relative strength of transmission between and within patches is described with the mixing matrix (K), where each entry κ_{ij} represents the strength of transmission to patch *i* from patch *j*. For this matrix, a stronger transmission strength is assumed within patches compared to between patches ($\kappa_{ii} > \kappa_{ij}\ for\ i \neq j$) and the sum of entries of each row is equal to one ($\sum_{j} \kappa_{ij} = 1$) .

Table 2. 1 shows the differential equations describing disease dynamics for each patch i in the models.

Table 2. 1 *Differential equations for the SIR and SIS metapopulation models. Patches are represented by i and j indexes.*

SIR	SIS
$$\frac{dS_i}{dt} = \frac{-\beta_i}{N_i}\left(\sum_{j} \kappa_{ij}I_j\right)S_i$$ $$\frac{dI_i}{dt} = \frac{\beta_i}{N_i}\left(\sum_{j} \kappa_{ij}I_j\right)S_i - \gamma_i I_i$$ $$\frac{dR_i}{dt} = \gamma_i I_i$$	$$\frac{dS_i}{dt} = \frac{-\beta_i}{N_i}\left(\sum_{j} \kappa_{ij}I_j\right)S_i + \gamma_i I_i$$ $$\frac{dI_i}{dt} = \frac{\beta_i}{N_i}\left(\sum_{j} \kappa_{ij}I_j\right)S_i - \gamma_i I_i$$

Figure 2. 1 Metapopulation transmission models. Diagrams show metapopulation structure for the transmission model, where each patch has a different transmission intensity: High ($_H$), medium ($_M$) and low ($_L$). Within each patch, boxes represent infectious states: Susceptible (S), infectious (I) and recovered (R). β_i and γ_i are transmission and recovery rates, respectively; and κ_{ij} represent transmission force between patches. A) Metapopulation model with SIR diseases dynamics. B) Metapopulation model with SIS disease dynamics.

2.2.2 Reproductive number

The basic reproductive number (R$_0$) of an infectious disease is an epidemiological metric, which represents the number of expected secondary infections caused by a single infectious individual in a totally susceptible population. Once there is immunity in the population, this number is referred as the effective reproductive number (R). When this number is greater than 1, the disease can persist within the population. Thus, it is necessary to decrease and maintain R below 1 to successfully achieve disease elimination (Knipl, 2016). Because of this, R$_0$ is an indicator of the effort required to eliminate an infection. For instance, for basic SIR and SIS models, transmission can be interrupted if a proportion of the population greater than $1 - 1/R$ is protected from becoming infected. This value is known as the herd immunity threshold (Roberts and Heesterbeek, 2003).

For metapopulations, the reproductive number can be determined with the spectral radius of the next generation matrix (NGM). In the NGM, each entry η_{ij} represents the number of secondary infections in a fully susceptible population *i* that are expected to arise from an infectious individual from

population *j* (Knipl, 2016). In 2010, Diekmann et al proposed a step-by-step method for the construction of the NGM. This method is based on the differential equations of the infectiousness states and it follows the steps outlined below (Diekmann et al., 2010).

Step 1: *Linearisation of the infectious subsystem*

First, the equations that describe the changes and production of infected individuals are selected as the infectious subsystem (Diekmann et al., 2010). For the models presented here, the equations for the infectious states are equal for both the SIR and SIS metapopulation models. Therefore, the infectious subsystems and the NGM are the same.

Once the infectious subsystem is identified, the linearisation is done for the infection-free steady state. At this state the susceptible population (S) is almost the same as the total population (N). In which case, the linearised equations for the subsystem are described by the following equation:

$$\frac{dI_i}{dt} = \beta_i \left(\sum_j \kappa_{ij} I_j \right) - \gamma_i I_i$$

Step 2: *The transmission matrix (T)*

The transmission matrix describes the production of new infections. Each entry of this matrix t_{ij} represents the rate at which an individual from population *j* generates a new infected individual in population *i* (Diekmann et al., 2010). Regarding the linearised subsystem, the transmission matrix for the metapopulation model is:

$$T = \begin{bmatrix} \beta_L \kappa_{LL} & \beta_L \kappa_{LM} & \beta_L \kappa_{LH} \\ \beta_M \kappa_{ML} & \beta_M \kappa_{MM} & \beta_M \kappa_{MH} \\ \beta_H \kappa_{HL} & \beta_H \kappa_{HM} & \beta_H \kappa_{HH} \end{bmatrix}$$

Step 3: *The transition matrix (Σ)*

The transition matrix represents changes in the infectious states, such as death or immunity acquisition. The negative inverse of this matrix $-(\Sigma^{-1})$ describes the average time an individual from population *j* spends in population *i* (Diekmann et al., 2010). For the metapopulation model, this transition matrix is:

$$-\Sigma^{-1} = \begin{bmatrix} 1/\Upsilon_L & 0 & 0 \\ 0 & 1/\Upsilon_M & 0 \\ 0 & 0 & 1/\Upsilon_H \end{bmatrix}$$

Step 4: *The next generation matrix*

The NGM of the infectious subsystem is the product of the transmission matrix and the inverse of the transmission matrix (Diekmann et al., 2010).

$$NGM = -T\Sigma^{-1} = \begin{bmatrix} \dfrac{\beta_L \kappa_{LL}}{\gamma_L} & \dfrac{\beta_L \kappa_{LM}}{\gamma_M} & \dfrac{\beta_L \kappa_{LH}}{\gamma_H} \\ \dfrac{\beta_M \kappa_{ML}}{\gamma_L} & \dfrac{\beta_M \kappa_{MM}}{\gamma_M} & \dfrac{\beta_M \kappa_{MH}}{\gamma_H} \\ \dfrac{\beta_H \kappa_{HL}}{\gamma_L} & \dfrac{\beta_H \kappa_{HM}}{\gamma_M} & \dfrac{\beta_H \kappa_{HH}}{\gamma_H} \end{bmatrix}$$

Using the NGM, the basic reproductive number is the dominant eigenvalue of this matrix. However, for the metapopulation models presented here, the NGM eigenvalues cannot be estimated analytically, thus R_0 does not have an explicit expression.

2.2.3 Interventions: Vaccination

As an intervention strategy, vaccination was included into the metapopulation models. Infection dynamics with vaccination are described by the equations in **Table 2. 2.** For both models, it is assumed that the vaccine has 100% efficiency (to simplify the model structure) and confers life-long immunity, the coverage level is σ_i in each patch and susceptible individuals are vaccinated at a rate δ_i. In the SIR model, when individuals are vaccinated, they enter the recovered population. Conversely, in the SIS model, vaccinated individuals enter a new compartment V, reducing the fraction of the population susceptible to the diseases.

Table 2. 2 Differential equations for the SIR and SIS metapopulation models with vaccination

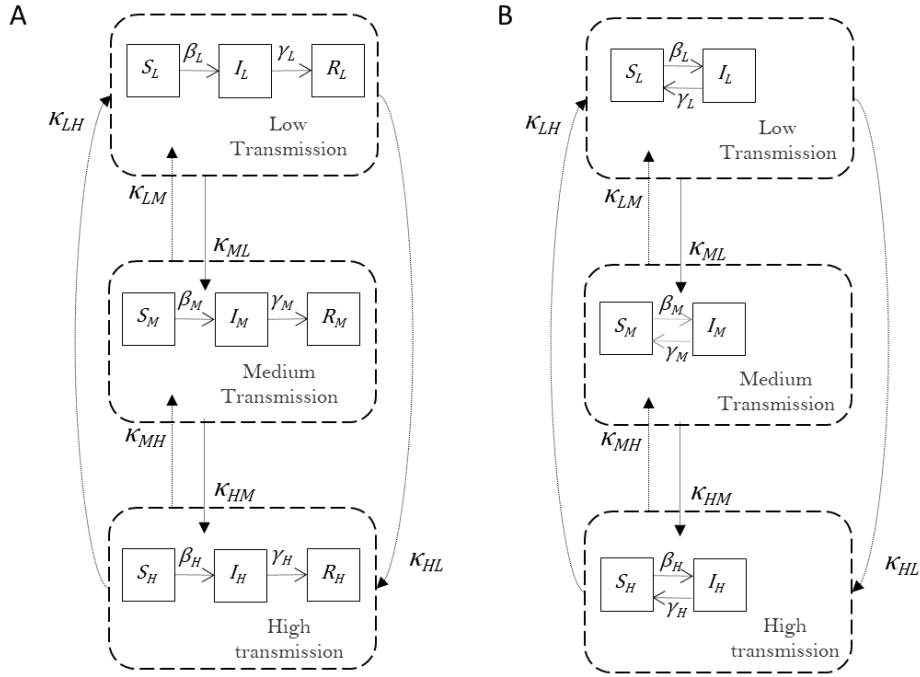| SIR	SIS
$\dfrac{dS_i}{dt} = \dfrac{-\beta_i}{N_i}\left(\sum_j \kappa_{ij} I_j\right) S_i - \delta_i S_i$	$\dfrac{dS_i}{dt} = \dfrac{-\beta_i}{N_i}\left(\sum_j \kappa_{ij} I_j\right) S_i + \gamma_i I_i - \delta_i S_i$
$\dfrac{dI_i}{dt} = \dfrac{\beta_i}{N_i}\left(\sum_j \kappa_{ij} I_j\right) S_i - \gamma_i I_i$	$\dfrac{dI_i}{dt} = \dfrac{\beta_i}{N_i}\left(\sum_j \kappa_{ij} I_j\right) S_i - \gamma_i I_i$
$\dfrac{dR_i}{dt} = \gamma_i I_i + \delta_i S_i$	$\dfrac{dV_i}{dt} = \delta_i S_i$

In order to evaluate the impact of vaccination as an intervention, R was estimated using the NGM of the model with vaccination. To construct the NGM, the method outlined above was implemented. The linearised infectious subsystem for the model including vaccination is given by,

$$\frac{dI_i}{dt} = \beta_i \left(\sum_j \kappa_{ij} I_j \right) (1 - \sigma_i) - \gamma_i I_i$$

And the NGM is as follows:

$$NGM = -T\Sigma^{-1} = \begin{bmatrix} \dfrac{\beta_L \kappa_{LL}(1-\sigma_L)}{\gamma_L} & \dfrac{\beta_L \kappa_{LM}(1-\sigma_L)}{\gamma_M} & \dfrac{\beta_L \kappa_{LH}(1-\sigma_L)}{\gamma_H} \\ \dfrac{\beta_M \kappa_{ML}(1-\sigma_M)}{\gamma_L} & \dfrac{\beta_M \kappa_{MM}(1-\sigma_M)}{\gamma_M} & \dfrac{\beta_M \kappa_{MH}(1-\sigma_M)}{\gamma_H} \\ \dfrac{\beta_H \kappa_{HL}(1-\sigma_H)}{\gamma_L} & \dfrac{\beta_H \kappa_{HM}(1-\sigma_H)}{\gamma_M} & \dfrac{\beta_H \kappa_{HH}(1-\sigma_H)}{\gamma_H} \end{bmatrix}$$

Infection trajectories with vaccination were evaluated for different model scenarios for both the SIR and SIS metapopulation models. These scenarios evaluated the effect of mixing between populations and the effect of limited vaccine availability. The scenarios analysed were as follow:

i. *Isolated model:* For the first scenario, there is no transmission between patches in the model. Additionally, it is assumed that the vaccine is available for the whole population in each patch.

ii. *Interconnected patches:* In this scenario, there is transmission between patches and, as in the previous scenario, the vaccine is available for the whole population in each patch.

iii. *Limited vaccines available*: For the final scenario, it is assumed there is transmission between patches and there is a limited number of available vaccines (*Vmax*). Different vaccine allocation strategies are evaluated to understand the effects of resource allocation on externalities.

For all scenarios, the model parameters are listed in **Table 2. 3**. The parameter values are for a plausible hypothetical disease and are based on values for common diseases (Anderson et al., 1992). Transmission rates for each patch (β_i) were estimated based on the local reproductive number and the recovery rate. Each simulation was initiated as a fully susceptible population with one infectious individual per patch and projected for 80 weeks.

For the SIR model, it was assumed that all vaccines were administrated before the onset of the outbreak. As a simulation output, the total number of infected individuals during the outbreak

(outbreak size) was estimated. The number of cases averted by vaccination was determined by comparing the outbreak sizes of the vaccination model to the outbreak size without intervention. On the other hand, for the SIS model, it was assumed that all vaccines were administered before the simulation started. As an output, prevalence of infection was estimated at the steady state. The number of cases averted was calculated as the difference in infectious individuals at the endemic state between the model with vaccination and the model without vaccination.

Table 2. 3 *Parameters used in the model. Values are for a hypothetical disease, with assumed reproductive numbers and interaction matrices which produce a realistic disease dynamics.*

Parameter	Symbol	Value	Reference
Total population per patch	N_i	1,000,000	Assumed
Recovery rate	γ_i	0.5 weeks^{-1}	(Verguet et al., 2015)
Reproductive number for low transmission intensity patch	R_{0L}	1.5	(Anderson et al., 1992)
Reproductive number for the medium transmission intensity patch	R_{0M}	3	(Anderson et al., 1992)
Reproductive number for the high transmission intensity patch	R_{0H}	9	(Anderson et al., 1992)
Interaction matrix for simulations for isolated scenarios.	α	$\begin{pmatrix} 1 & 0 & 0 \\ 0 & 1 & 0 \\ 0 & 0 & 1 \end{pmatrix}$	Assumed
Interaction matrix for simulations with interconnected patches.	α	$\begin{pmatrix} 0.95 & 0.02 & 0.03 \\ 0.02 & 0.96 & 0.02 \\ 0.03 & 0.02 & 0.95 \end{pmatrix}$	Assumed
Expected cost of the disease per case	c	US$ 1	Assumed

2.2.4 Vaccination externalities

For each scenario, marginal externalities were estimated following the methods presented by Boulier et al. In their study, marginal externalities are defined as the difference between marginal social and private benefits (Boulier Bryan et al., 2007). As described in the introduction, the term marginal refers to the change in the quantity of benefits or costs per one additional unit produced, in this case, when an additional vaccination is administered. **Table 2. 4** summarises the most important concepts required for the analysis of vaccination externalities.

Table 2. 4 *Summary of important marginal benefit terms used for the estimation of externalities.*

Expression	Acronym	Definition	Equation
Marginal effect of vaccination	MEV	Additional number of cases averted per additional person vaccinated.	$MEV = \dfrac{\partial(Averted\ cases)}{\partial(Vaccinations)}$
Marginal social benefit	MSB	Social value of the change in the number of cases averted per additional person vaccinated.	MSB = MEV* c
Marginal private benefit	MPB	Change in the expected risk of infection per additional person vaccinated	MPB = p(V) *c
Marginal externalities	ME	Change in indirect effects of vaccination per additional person vaccinated	ME= MSB- MPB

The risk of infection $(p(V))$ is the probability of being infected given that V individuals are vaccinated, and it is estimated as follows

$$p(V) = \frac{I_T - I_o}{N - V - I_o}$$

where I_o is the initial infectious population and I_T represents the overall infectious individuals at the end of the simulation. For the SIR model, I_T refers to the outbreak size and for the SIS, I_T refers to the prevalence at the steady state.

To understand the effect of vaccine allocation on externalities, three different allocation schemes were evaluated (**Table 2. 5**). With 80% global vaccine coverage, vaccination externalities were evaluated for a scenario where vaccines were distributed equally; a scenario where vaccine distribution was prioritised to high and medium transmission patches; and a scenario where vaccine distribution was prioritised to low and medium transmission patches.

Table 2. 5 *Number of vaccines allocated in each patch under different schemes. The total number of vaccines available was 2,400,000 which covered 80% of total population.*

Allocation Scheme	Low transmission	Medium transmission	High Transmission
Equal	800 000	800 000	800 000
Scheme 1	400 000	1 000 000	1 000 000
Scheme 2	1 000 000	1 000 000	400 000

2.3 Results

2.3.1 Isolated dynamics

The marginal benefits for the SIR isolated metapopulation model are shown in **Figure 2. 2**. For all panels the x-axes represent vaccination coverage, and the y-axes represent the monetary value for each marginal benefit assuming an expected cost of the disease *(c)* of US$1 per case.

Marginal externalities are initially small and start to rise as the number of vaccinations increases until they reached a peak, and then decrease sharply. After the herd immunity threshold for each patch is reached, marginal benefits become negligible given that transmission has been interrupted. Additionally, as can be seen from the three panels in **Figure 2. 2**, the magnitude of marginal benefits depends strongly on the transmission intensity of the disease. In low transmission intensity settings, vaccination has a MSB effect greater than 1.5 from the first vaccination. The magnitude of this benefit is related to a low demand for a vaccine; therefore, MBP are relatively low and never exceed 0.58 (**Figure 2. 2B**). For this patch, after 19.6% of the population is vaccinated, the magnitude of MSB peaks and drops below 1. Conversely, in higher transmission intensity settings, vaccination coverage needs to be higher than 82.1% in order to have a MSB greater than 1.5 (**Figure 2. 2A**). This relates to a high MPB that only decreases steeply once the patch herd immunity threshold (88.9% coverage) is achieved.
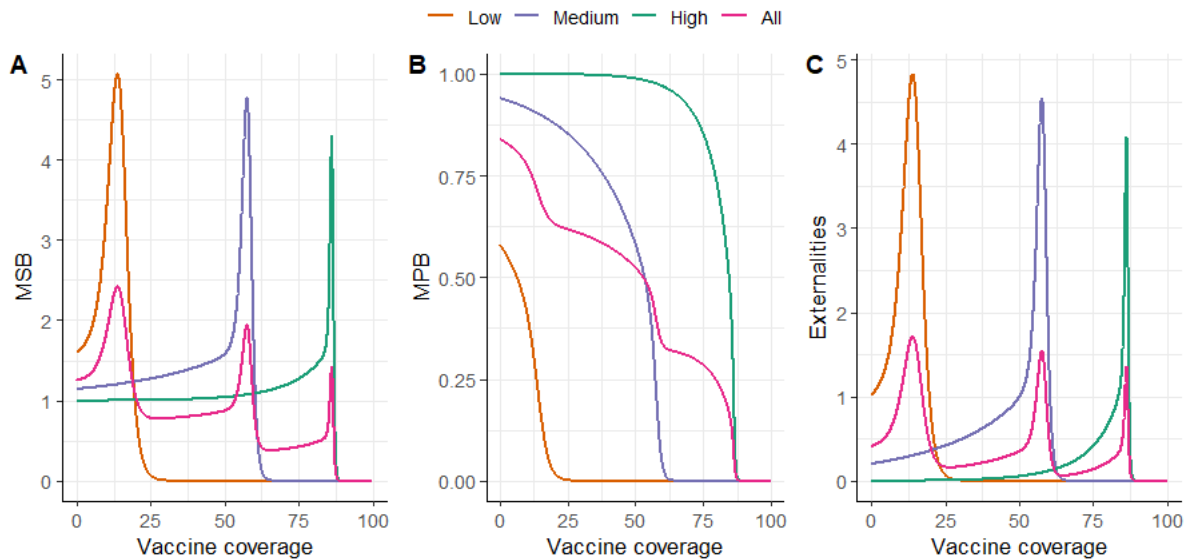
Figure 2. 2. *Marginal benefits of vaccination for an SIR disease dynamic. Simulations are run for three isolated patches with differing transmission intensity: high transmission intensity (green), medium transmission intensity (purple), low transmission intensity (orange) and global results (Pink). Y- axes show monetary value of each marginal benefit assuming an expected cost of the disease of US$1. A) Marginal social benefits (MSB) of vaccination. B) Marginal private benefits or demand curve. C) Marginal Externalities. These are the differences between marginal social and private benefits. Simulations are run with a vaccine coverage of 100% with even distribution among patches.*

When modelling the metapopulation for a disease with SIS dynamics, marginal benefits showed a similar behaviour to those for the SIR dynamics (**Figure 2. 3**). Nonetheless marginal benefit values are significantly lower than those from the SIR simulations. This difference is associated with individuals who were infected and entered the recovered population contributing to herd immunity in the SIR model. Whereas, for the SIS model, vaccination is the only contributor to herd immunity. **Figure 2. 3A** shows that MSB are significantly large for coverages close to the herd immunity threshold. However, the range of coverages where MSB are greater than one is small and varies between transmission intensity settings. When transmission intensity increases, this range decreases. 1
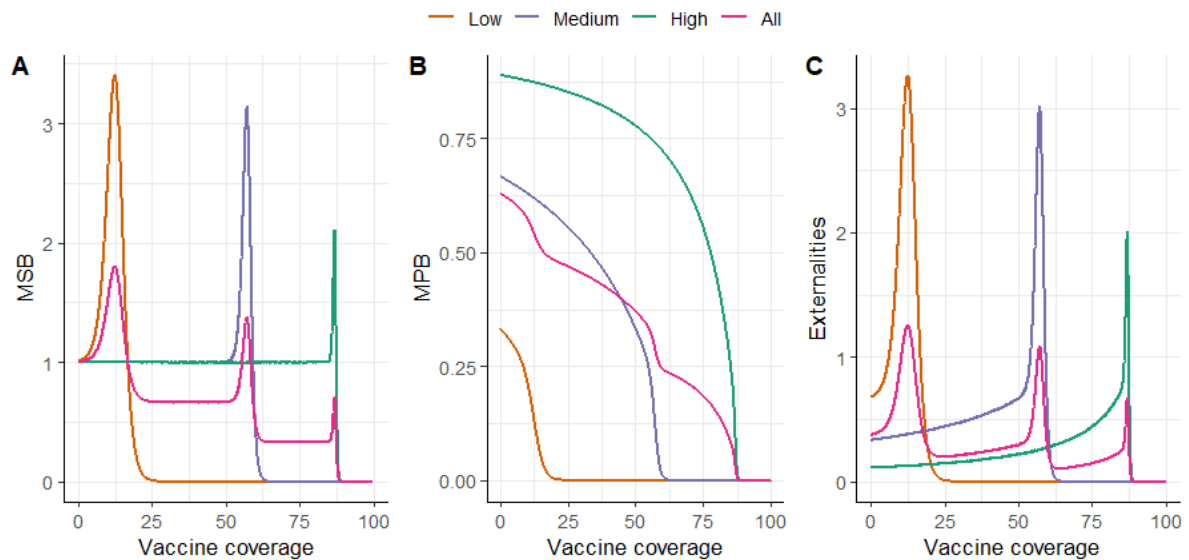
Figure 2. 3 Marginal benefits of vaccination for an SIS disease dynamic*. Simulations are run for three isolated patches with differing transmission intensity: high transmission intensity (green), medium transmission intensity (purple), low transmission intensity (orange) and global results (Pink). Y- axes show monetary value of each marginal benefit assuming an expected cost of the disease of US$1. **A)** Marginal social benefits (MSB) of vaccination. **B)** Marginal private benefits or demand curve. **C)** Marginal Externalities. These are the differences between marginal social and private benefits. Simulations are run with a vaccine coverage of 100% with even distribution among patches.*

2.3.2   Metapopulation dynamics

When transmission between patches is included in the model, the dynamics of social benefits and externalities change. In the low and medium transmission patches, dynamics are strongly influenced by the dynamics of the high transmission intensity patch (**Figure 2. 4**). Given that transmission cannot be interrupted in the high transmission setting with a low number of vaccines, importation of cases reduces the MSB in the low and medium transmission patches. The most striking reduction can be seen in **Figure 2. 4D**, where MSB never exceeds one. This means that in these patches, vaccination can only protect the vaccinated individuals as it generates only benefits for the vaccinated individual herself

On the other hand, MBP do not change drastically with the introduction of transmission between patches (**Figure 2. 4B, E**). MPB are initially the same for both the interconnected and isolated metapopulation model. As vaccination increases, the demand for a vaccine decreases along with the expected risk of infection. However, when there is transmission between patches, MPB do not decrease as steeply after the herd immunity threshold is reached. Given the importation of cases, the

demand for the vaccine only reaches zero, in all the patches, when there is no risk of infection in the high transmission intensity patch.
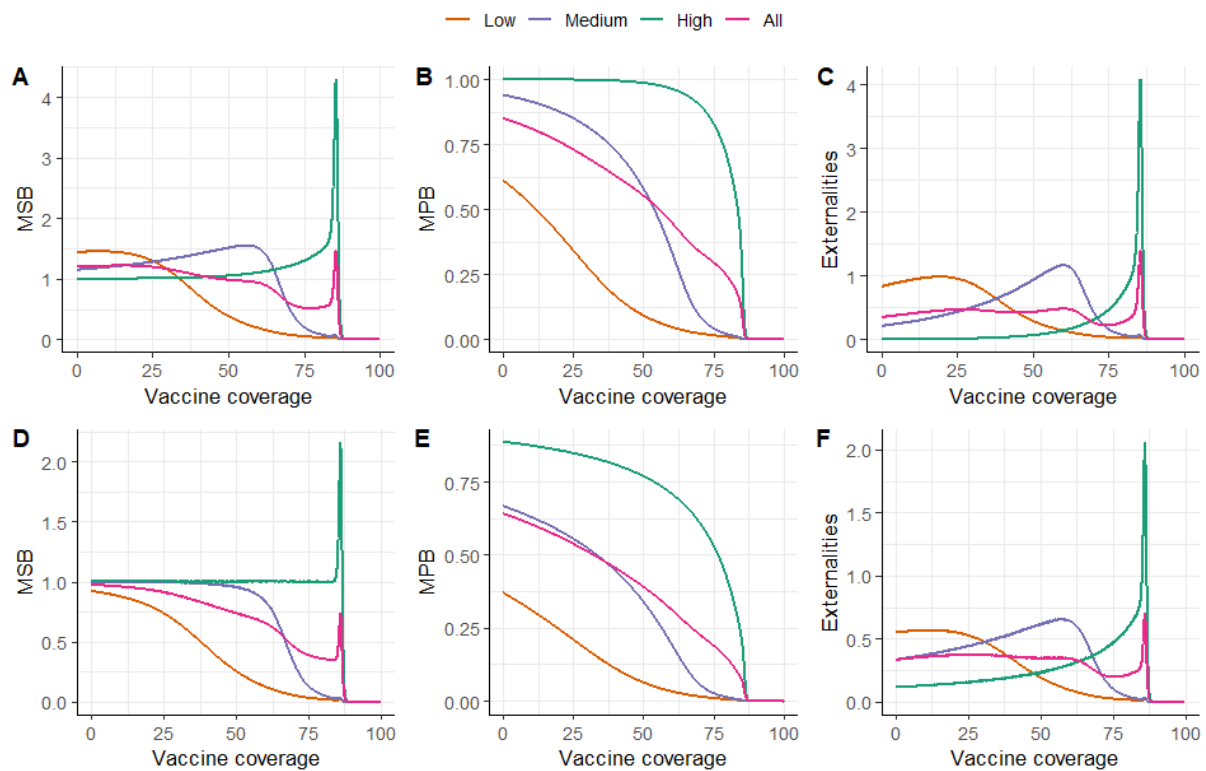
Figure 2. 4 Marginal benefits of vaccination for a metapopulation model with three interconnected patches with differing transmission intensity: High transmission intensity (green), medium transmission intensity (purple), low transmission intensity (orange) and global results (pink). Upper row shows marginal benefits for SIR disease dynamics. Bottom row shows marginal benefits for SIS disease dynamics. A, D) Marginal social benefits of vaccination. B, E) Marginal private benefits or demand curve. C, F) Marginal externalities for each patch. These are the difference between marginal social and private benefits. Simulations are run with a vaccine coverage of 100% with even distribution among patches. Y-axis represent the monetary value of each marginal benefit assuming an expected cost of the disease of US$1.

Marginal externalities represent the benefit to the unvaccinated individuals. Values greater than one imply that more than two cases are averted per vaccination. **Figure 2. 4** shows that in the high transmission patch (green line), marginal externalities can be remarkably large and vaccinating an individual can fully protect up to 4 unvaccinated individuals in the SIR model (**Figure 2. 4C**) and up to 2 unvaccinated individuals in the SIS model (**Figure 2. 4F**). Marginal externalities for the overall population are determined by a weighted average of marginal externalities in each patch, based on the population size of each patch. Given the large discrepancy in externalities between high and low transmission patches, marginal externalities for the whole population (pink line), rarely exceed a value

of one. This difference between local and global marginal benefits demonstrates how local benefits of an intervention may not align with global benefits when there is transmission heterogeneity.

2.3.3   Vaccine allocation
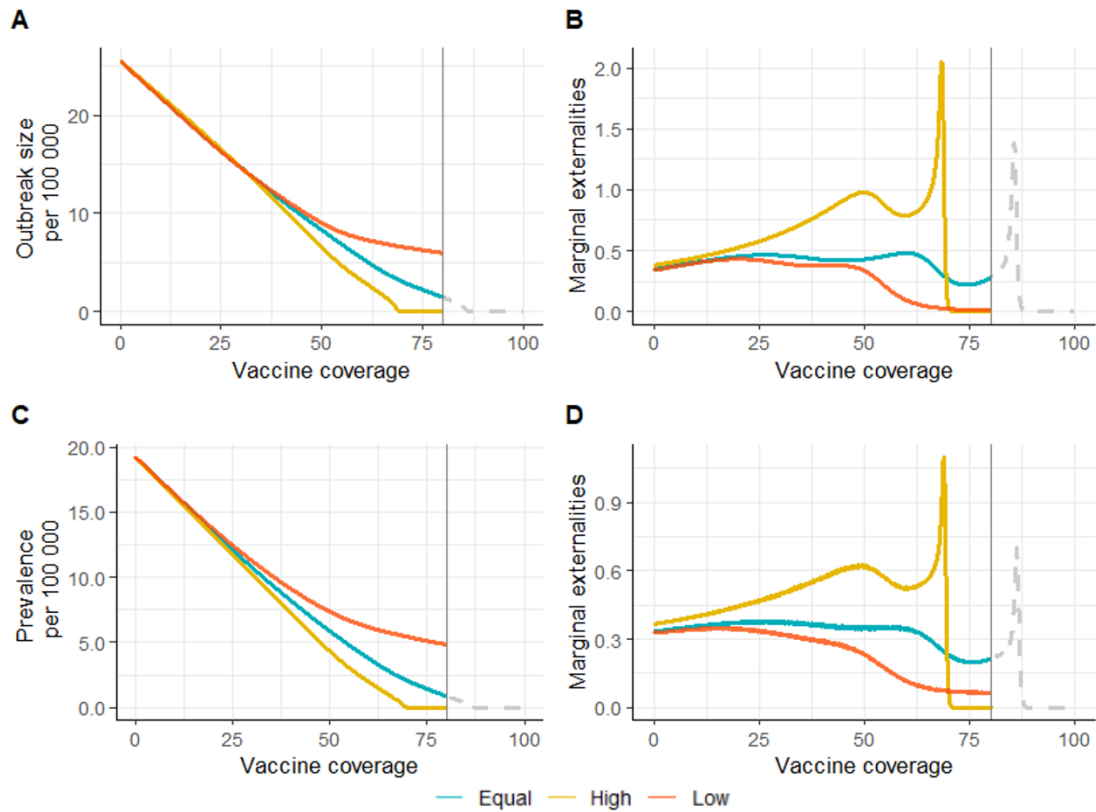
Figure 2. 5 Marginal global benefits and effects of vaccination for the metapopulation model with limited number of vaccines*. Maximum number of vaccine available: 80% global coverage. Colours show different resource allocation strategies: Equal distribution among parches(green), prioritisation to high transmission patch (yellow), prioritisation to low transmission patch (red). For the purpose of comparison with vaccination available for everyone, dashed grey line shows global marginal benefits when vaccines are allocated equitably. Upper row shows vaccination effects for an SIR disease dynamic. Bottom row shows vaccination effects for an SIS disease dynamic. **A)** Outbreak size under different allocation schemes. **C)** Endemic prevalence for the different allocation schemes **B, D)**   Global marginal externalities for SIR and SIS models respectively. Y-axis shows the monetary value of each marginal benefit assuming an expected cost of the disease of US$1 per case.*

Simulations under different vaccine allocation schemes suggest that prioritising high transmission settings has the greatest effect on increasing the marginal global benefits of vaccination (**Figure 2. 5**). When there is a limited number of vaccines, equal distribution of resources cannot guarantee a peak for the overall benefits. However, when prioritising high transmission intensity settings, the maximum global externalities peak is reached approximately with 20% fewer vaccinations and is 47.5% and

56.1% higher for the SIR and SIS metapopulation model respectively, compared to an equal distribution of resources. Additionally, model simulations showed that changing vaccine allocation strategies can significantly impact the number of vaccinations required to interrupt the transmission of the disease ($R < 0$). When high transmission intensity settings are prioritised, transmission can be stopped with 17% less vaccine coverage compared to equal allocation for both the SIS and the SIR disease dynamics (**Figure 2. 6).**
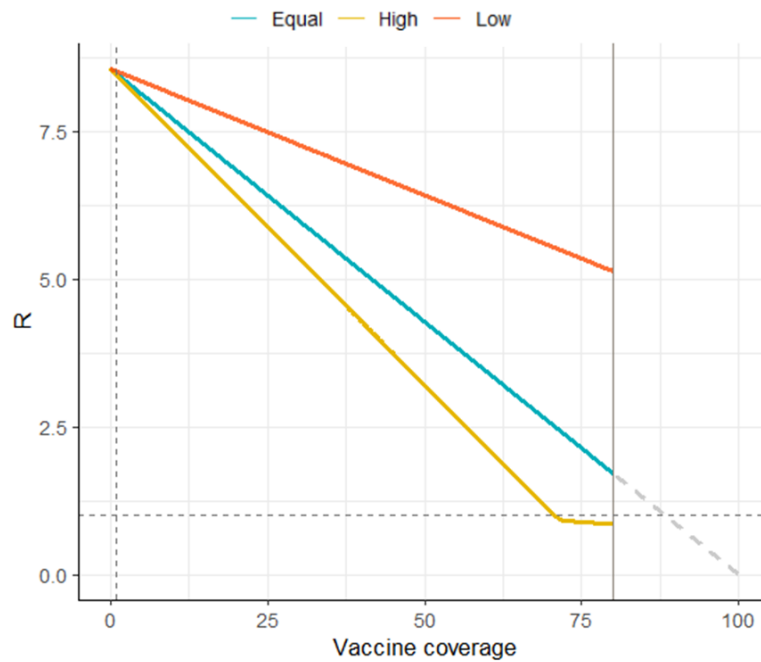
Figure 2. 6 Global reproductive number for each vaccine allocation scheme. Colours show different resource allocation strategies: Equal distribution among parches(green), prioritisation to high transmission patch (yellow), prioritisation to low transmission patch (red). For the purpose of comparison with vaccination available for everyone, dashed grey line shows global marginal benefits when vaccines are allocated equitably. Horizontal dotted line denotes elimination threshold (R=1) and vertical dotted line denotes herd immunity threshold for the system without interventions. Maximum number of vaccine available: 80% global coverage.

2.4   Discussion

In this chapter a framework is developed for modelling a metapopulation model in order to analyse the impact of control strategies. The framework proposed here is flexible enough to incorporate different infection dynamic structures and its outputs can be integrated into any economic analyses. Here, I use the framework to analyse vaccination externalities under different vaccine allocation schemes for two simple disease dynamics models.

As a first analysis, I compared marginal benefits between the SIR and SIS dynamics. For both models, transmission intensity has a strong effect on the magnitude of marginal benefits as reported by Boulier et al. (Boulier Bryan et al., 2007). In higher transmission intensity settings vaccination would generate higher marginal benefits but in order to do so, higher vaccination coverage is required. Additionally, my results illustrated how model structure has an important effect on the marginal benefits for the individual populations as well as for the overall population. Model projections estimated substantially higher benefits for the SIR model structure compared with the SIS model. Nevertheless, when mixing between populations was included in the simulations, this discrepancy was less prominent given that importation of cases from higher transmission patches influenced transmission in lower transmission intensity patches. These results further support the idea that including importation of cases in disease dynamics has a strong effect on infection trajectories (Hickson and Roberts, 2014) and therefore has significant impact on marginal economic benefits (Klepac et al., 2011).

As a second analysis, I evaluated different vaccine allocation strategies. Funding allocation for control strategies aims to distribute interventions as efficiently as possible to maximise welfare. Results presented here showed that when vaccines are allocated equally between patches, the indirect effect of an additional vaccination is fairly low and marginal externalities rarely exceed 1. However, when vaccines are allocated proportional to transmission intensity, marginal externalities can be as high as four cases averted among the nonvaccinated for the high transmission patch. These results reflect those by Ndeffo Mbah et al. (Ndeffo Mbah and Gilligan, 2011), who also found that the most efficient and simple strategy to allocate resources in a metapopulation with different rates of transmission is to give preference to the sub-population with the greatest disease burden, protecting the other subpopulations through herd immunity (Ndeffo Mbah and Gilligan, 2011). Additionally, results from vaccine allocation evaluation also evidenced the importance of aligning local and global goals. Intervention schemes that improve welfare in one patch, eliminating transmission locally, may not generate benefits for the overall population and would slow down disease control processes globally. As discussed in Chapter 1, international cooperation is important for disease control success (Barrett, 2004). Including global externalities in analyses can help determine the optimal allocation of interventions that maximises the well-being from both social and local perspectives, encouraging cooperation from all parties (Gersovitz, 2011).

Overall, the results in this chapter illustrate that in order to formulate correct social policies, externalities cannot be ignored from policy analyses. High externalities were found, particularly when

coverages levels are closer to the herd immunity threshold and the disease is just transmissible enough to survive, as has been reported previously (Goodkin-Gold et al., 2020, Boulier Bryan et al., 2007). These results further support the idea that overlooking vaccination indirect effects may underestimate the real social benefits of intervention programs, leading to biased public policy decisions, which would result in an underprovision of vaccinations (Hauck, 2018, Gersovitz, 2011, Perrings et al., 2014).

The integration of economic and epidemiological models like the one presented in this Chapter, allows public policy makers to identify and quantify the gap between social and private benefits. Economic incentives such as subsidies are common economic instruments implemented to fill this gap (Perrings et al., 2014, Klein et al., 2007, Althouse et al., 2010). However, to date, there is little guidance on how to estimate the magnitude of these incentives (Goodkin-Gold et al., 2020). The methods developed in this chapter provide a robust framework for estimating externalities and guide public health planners to efficiently control infectious diseases.

The scope of this study was limited to the development of a general framework that integrated metapopulation modelling and economic analysis. I have described simple SIR and SIS dynamics that do not represent a particular disease but instead give insights into how disease projections can be used to analyse marginal benefits of interventions. More complex transmission models may be required to better capture the effect of interventions for a specific disease. Additionally, all results presented in this chapter are based on one metapopulation structure with a single mixing matrix analysed. The number of subpopulations and the strength of coupling between populations have been recognised to be important factors in metapopulation dynamics (Klepac et al., 2011, Ndeffo Mbah and Gilligan, 2011). As an extension to this work, a sensitivity analysis to assess the effect of metapopulation structure (i.e. number of patches and interconnectivity strength) and vaccine allocation strategies would help to identify relationships between the structure of the population and the most efficient way for allocating interventions. As discussed above, externalities evaluation can help policy makers improve disease control planning. Therefore, results from the sensitivity analysis would provide general guidance to policy makers on how interventions can be allocated efficiently for a specific scenario. Another complexity not explicitly included here is human behaviour. Uptake of an intervention depends on individual behaviour which may change over time (Klein et al., 2007). I have assumed individual's demand for vaccination depends only on MPB, yet it has been demonstrated that risk perception and group pressure have a direct effect on vaccination uptake and may slow down

vaccination programmes (Oraby and Bauch, 2015). Combining behavioural economics and epidemiological externalities is an important topic for future work.

In spite of its limitations, this Chapter adds to the understanding of the dynamics of externalities for infectious disease interventions. I have demonstrated that intervention externalities strongly depend on disease structure and population heterogeneity. This chapter has described the methods used in this thesis and it has emphasised the great need for further research in the integration of economic and epidemiological analyses to aid public policy makers to maximise global and local welfare. Using this framework as a starting point, in the chapters that follow I consider more complex transmission models in order to address real-world disease challenges such as optimal resource allocation and low intervention uptake.

Chapter 3 Evaluating trade-offs between local and global priorities for the control of malaria

3.1 Introduction

As described in Chapter 1, the Global Technical Strategy for Malaria (GTSM) sets out global goals to eliminate the disease in 35 countries and reduce the burden by 90% by 2030 (World Health Organization, 2015). One of the main challenges faced in achieving this ambitious goal is the heterogeneous geographical distribution of malaria. Of the 86 countries where malaria is endemic, 29 carry 96% of the disease burden, whereas almost 20 have low transmission rates and are on the path to elimination (World Health Organization, 2021d). Even within countries, the incidence of malaria varies significantly based on seasonality profiles, urbanization, vegetation, nearest mosquito breeding site, among other factors (World Health Organization, 2015, Bousema et al., 2016). This varied epidemiology between geographical regions makes the planning of malaria control strategies a difficult task.

Another challenge faced by the GTSM is insufficient resources to achieve the stated objectives. In order to achieve 2030 milestones, it is estimated that malaria investment would need to increase substantially from the current annual spending of US$ 3.0 billion to US$10.5 billion (World Health Organization, 2021d). Therefore, the optimal allocation of available resources is crucial to get closer to achieving GTSM goals. Currently, allocation of interventions is based on stratification by malaria burden, defined by the annual number of reported cases and deaths (World Health Organization, 2021b). In 2018 the WHO launched the "High burden to high impact" strategy in order to support the 11 highest burden countries (World Health Organization, 2021d). This strategy focuses on allocating more resources to high-burden settings where interventions can have the greatest impact. However, this approach may not be fitting for countries at near elimination stages where disease burden is low but still require significant investment for surveillance and prevention (Newby et al., 2016).

Malaria epidemiology in near elimination settings is different from high transmission settings. This poses distinct challenges towards the control of the disease. In near elimination settings, the

population at risk usually shifts towards working adults, particularly men, and hard to reach populations such as nomadic communities (Cotter et al., 2013). Additionally, as local transmission declines, attention shifts to importation of cases as these become an important source of infection (Cotter et al., 2013, Walker et al., 2016). The introduction of parasites from linked areas with ongoing transmission may cause the resurgence of local transmission, hindering efforts to eliminate malaria. This importation is normally linked to travellers from countries with economic, cultural and geographical ties (Lai et al., 2019). In order to reduce the risk of importation of cases, cross-border control initiatives are important to support individual control efforts. These initiatives are based on sharing resources between neighbouring countries to control the disease in the bordering region.

Cross-border control initiatives are not novel and have been implemented in the last decades as part of malaria control (Lover et al., 2017). This type of cooperation between countries supports elimination plans when low transmission countries are epidemiologically linked with high transmission countries (Moonasar et al., 2016). Sharing resources with neighbouring countries has been proven to be successful for China, which was certified malaria free in 2021. Elimination was possible due to a strong surveillance and response program as well as the cooperation with Myanmar to control malaria transmission in the bordering province of Yunnan, where the highest number of imported malaria cases during the elimination stage were reported (Huang et al., 2021, Lai et al., 2019). In the 8 southernmost countries of Africa, efforts to accelerate malaria control and achieve 2030 goals have been facilitated by the E8 cross-border initiative (Maharaj et al., 2019). A successful example of this initiative is the MOSAWA region. Since 1999, Swaziland (now Eswatini) and South Africa, two malaria eliminating countries, have been collaborating with Mozambique, a neighbouring country with high transmission. South Africa and Eswatini have been extending their malaria interventions, particularly IRS, to the southern region of Mozambique in order to reduce the risk of importation. This strategy has reduced substantially malaria burden in the bordering regions (Moonasar et al., 2016).

Cross-border initiatives, like in the MOSAWA region, rely on cooperation between countries, more than relying on equal (i.e. all parties received the same resources) or equitable (i.e. resource allocation according to health need) allocation in each country individually. Cooperation in disease control is based on sharing resources and coordinating activities to ensure the optimal use of funding towards a common end. However, there is currently limited evidence on the quantifiable impact of such cooperative strategies and whilst global donors like the Global Fund support some regional initiatives like the E8, most of their resources are still focused on supporting countries individually, allocating

funds equitably and prioritising those with a high burden of malaria (Gueye et al., 2012, Khadka et al., 2018). Cooperative interventions still rely on national funding and the willingness for cooperation from neighbouring countries.

In this chapter, I aim to provide quantitative evidence of the impact of cooperative strategies in the malaria context. In the previous chapter, I highlighted the importance of aligning local and global strategies toward disease control. In the case of malaria, aligning strategies at the local, regional, and global level is a hard task due to the extreme geographical heterogeneity in disease burden and complex funding landscape. Modelling studies have been useful to understand how to prioritise the use of current malaria interventions with the available funding. Non-linear constrained optimisation methods have been developed (Drake et al., 2017) to find the optimal combination of malaria interventions. In these studies, health gain is maximised using a set budget (Scott et al., 2017, Winskill et al., 2019, Drake et al., 2017) or an epidemiological target as a constraint (Walker et al., 2016). Nonetheless, given the complexity of the disease epidemiology, substantial computation time is required to run these optimisations. Therefore, sometimes the complexity of models has been reduced, assuming homogeneous conditions within countries (Scott et al., 2017). In this chapter, I extend the metapopulation framework developed in Chapter 2 to compare global and local perspectives on different resource allocation strategies incorporating malaria disease dynamics and transmission heterogeneity.

3.2   Methods

In order to capture the complex disease dynamics as well as transmission heterogeneity, I modified the metapopulation model from Chapter 2 such that in each patch malaria transmission was represented by a previously published age-structured mathematical model for *P.falciparum*. This deterministic compartmental model captures mosquito biology as well as disease dynamics among six different infection states in humans (Griffin et al., 2010a). The model is coded in R, and it is available as the ICDMM package (Hellewell et al., 2022). The package allows users to create new versions of the original model. Using this package, I extended the original model code to create a metapopulation model, where in each patch the original model was represented. Mathematical details on the model and how it was modified to represent a metapopulation model are explained below.

3.2.1 Human model

In each patch, *i,* susceptible individuals (S_i) become infected at a rate determined by a force of infection Λ_i. This force of infection depends on mixing coefficients between patches and the proportion of infectious mosquitoes per patch as described in section 3.1.1.1. A delay (d_E) in the force of infection is included to represent the latent liver stage of infection. Infected people can develop clinical disease with a probability ϕ and be treated (T_i) at a fixed probability f_T. These treated individuals will clear the infection at a rate r_T and enter a prophylactic protection state (P_i) before becoming susceptible again at a rate r_P. Untreated individuals (D_i), start clearing the infection at a rate r_D and become patently asymptomatic (A_i). Asymptomatic individuals will move to a sup-patent stage (U_i) (asymptomatic infection undetectable by microscopy) at a rate r_A. Sub-patent individuals will clear the infection at a rate r_U and become susceptible again (Griffin et al., 2010a).
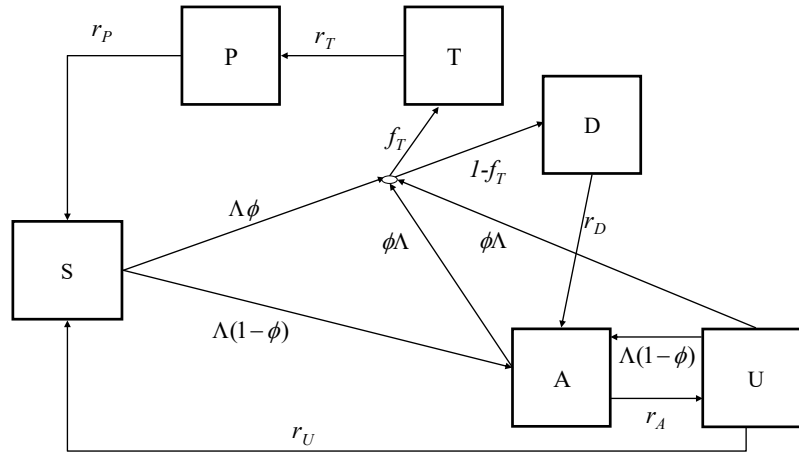
Figure 3. 1 Schematic representation of malaria transmission in humans. Reproduced from (Griffin et al., 2010a)

The model partial differential equations for the human dynamics are as follows, with *t* representing time, *a* age and *i* patch.

$$\frac{\partial S_i}{\partial t} + \frac{\partial S_i}{\partial a} = -\Lambda_i(t - d_E)S_i(t) + r_P P_i(t) + r_U U_i(t)$$

$$\frac{\partial T_i}{\partial t} + \frac{\partial T_i}{\partial a} = \phi f_T \Lambda_i(t - d_E)[S_i(t) + A_i(t) + U_i(t)] - r_T T_i(t)$$

$$\frac{\partial D_i}{\partial t} + \frac{\partial D_i}{\partial a} = \phi(1 - f_T)\,\Lambda_i(t - d_E)[S_i(t) + A_i(t) + U_i(t)] - r_D D_i(t)$$

$$\frac{\partial A_i}{\partial t} + \frac{\partial A_i}{\partial a} = (1 - \phi)\Lambda_i(t - d_E)[S_i(t) + U_i(t)] + r_D D_i(t) - \phi\Lambda(t - d_E)\,A_i(t) - r_A A_i(t)$$

$$\frac{\partial U_i}{\partial t} + \frac{\partial U_i}{\partial a} = r_A A_i(t) - r_U U_i(t) - \Lambda_i(t - d_E)\, U_i(t)$$

$$\frac{\partial P_i}{\partial t} + \frac{\partial P_i}{\partial a} = r_T T_i(t) - r_P P_i(t)$$

The probability of developing clinical disease(f_T) as well as all transition rates (r_x) are assumed constant and equal for all patches.

3.1.1.1 Force of Infection

The force of infection in the original model was defined by:

$$\Lambda = \varepsilon\, b = I_M \frac{\alpha}{\omega} \zeta \left(1 - \rho e^{-\frac{a}{a_0}}\right) b,$$

where I_M is the proportion of infectious mosquitoes, α is the biting rate on humans, ω a constant to normalise the biting rate over ages, 1-ρ is the relative biting rate at birth compared to adults, a_0 determines the timescale of the increase in biting rate with age and b is the probability of infection if bitten by an infectious mosquito. The model assumes each person has a relative biting rate ζ. This relative rate has a log-normal distribution between people with a mean of 1.

$$\log(\zeta) \sim N(-\frac{\sigma^2}{2}, \sigma^2)$$

For the metapopulation model, the force of infection also depends on the mixing between patches and the proportion of infectious mosquitoes in other populations. The new force of infection in each patch is described by:

$$\Lambda_i = \frac{\alpha}{\omega} \zeta \left(1 - \rho e^{-\frac{a}{a_0}}\right) b \sum_j \kappa_{ij} I_{Mj}$$

As explained in Chapter 1, in a metapopulation mixing between patches is described by the mixing matrix. In this matrix, diagonal values (κ_{ii}) represent the transmission within the patch. This transmission is associated with infectious agents from the same patch. Non-diagonal elements of the mixing matrix ($\kappa_{ij\,(i \neq j)}$) represent transmission between patches. This transmission is associated with infectious individuals from patch j transmitting to susceptible individuals in patch i. The mixing matrix is symmetrical, and row and column values always sum to 1.

$$Mixing\ matrix = \begin{pmatrix} \kappa_{11} & \cdots & \kappa_{1n} \\ \vdots & \ddots & \vdots \\ \kappa_{n1} & \cdots & \kappa_{nn} \end{pmatrix}$$

For the force of infection in this metapopulation model I assume that

- the biting rate is the same in all patches;
- the age distribution is the same in all patches; and
- the probability of infection if bitten is the same in all patches.

3.1.1.2 Human Immunity Functions

The model incorporates three different points at which immunity may act in the transmission of malaria. First is the pre-erythrocytic immunity, (I_B) which reduces the probability of infection establishment after an infectious bite. Then, clinical immunity (I_C), which reduces the probability of clinical disease after infection. Finally, blood-stage immunity (I_D), which reduces the duration of patent parasitaemia. Each of these points is considered as separate functional forms that depend on age and exposure (Griffin et al., 2014).

Immunity to infection (I_{Bi}) reduces the probability of symptomatic or asymptomatic infection. For a population in patch *i*, exposed to an entomological inoculation rate (EIR) ε and a mean duration of immunity d_B is defined by the equation:

$$\frac{\partial I_{Bi}}{\partial t} + \frac{\partial I_{Bi}}{\partial a} = \frac{\varepsilon_i}{\varepsilon_i\, u_B + 1} - \frac{I_{Bi}}{d_B} \qquad I_{Bi}(0,t) = 0$$

Clinical immunity reduces the probability of symptomatic infection in favour of asymptomatic infection. It is driven by the combined impact of acquired immunity (I_{CAi}) and maternal immunity (I_{CMi}):

$$I_{Ci} = I_{CAi} + I_{CMi}$$

Clinical acquired immunity depends on the force of infection Λ_i , described above, the mean duration of immunity d_C and the time between immunity boosting of u_C.

$$\frac{\partial I_{CAi}}{\partial t} + \frac{\partial I_{CAi}}{\partial a} = \frac{\Lambda_i}{\Lambda_i\, u_C + 1} - \frac{I_{CAi}}{d_C} \qquad I_{CAi}(0,t) = 0$$

Clinical maternal immunity at birth $(I_{CMi}(0,t))$ is assumed to be a proportion (P_{CM}) of the level of immunity present in a 20-year-old woman living in the same location and which decays at a constant rate $\frac{1}{d_M}$.

$$\frac{\partial I_{CMi}}{\partial t} + \frac{\partial I_{CMi}}{\partial a} = -\frac{I_{CMi}}{d_M} \qquad I_{CMi}(0,t) = P_{CM}\, I_C(20,t)$$

Blood-stage immunity (I_{Di}) immunity reduces the detectability and infectiousness of asymptomatic infections. This immunity depends on the force of infection Λ_i, the duration of immunity d_D and the time between immunity boosting u_D. This immunity is given by the equation:

$$\frac{\partial I_{Di}}{\partial t} + \frac{\partial I_{Di}}{\partial a} = \frac{\Lambda_i}{\Lambda_i\, u_D + 1} - \frac{I_{Di}}{d_D} \qquad I_{Di}(0,t) = 0$$

3.1.1.3 Immunity dependent parameters

The probabilities of infection *(b)* and clinical disease *(ϕ)* are given by Hill functions that depend on immunity to infection and clinical immunity respectively:

$$b(a) = b_0\left(b_1 + \frac{1 - b_1}{1 + \left(\frac{I_B}{I_{B0}}\right)^{\kappa_B}}\right) \qquad \phi(a) = \phi_0\left(\phi_1 + \frac{1 - \phi_1}{1 + \left(\frac{I_C}{I_{C0}}\right)^{\kappa_C}}\right)$$

where b_0 and ϕ_0 are the probability with no immunity. $b_0\, b_1$ and $\phi_0\phi_1$ are the minimum probability. I_{B0}, I_{C0}, κ_B and κ_C are scale and shape parameters. These parameters are set and assumed to be constant for all patches.

The probability that an asymptomatic infection (A) will be detected by microscopy is given by,

$$q = d_1 + \frac{1 - d_1}{1 + f_D\left(\frac{I_D}{I_{D0}}\right)^{\kappa_D}}$$

where d_1 is the minimum probability, I_{D0} and κ_D are scale and shape parameters. f_D is and age-dependent function, described by $f_D = 1 - \frac{1 - f_{D0}}{1 + \left(\frac{a}{a_D}\right)^{\gamma_D}}$

3.2.2 Mosquito model

In each patch *i*, susceptible mosquitoes (S_{Mi}) get infected after biting an infected human (T, D, A, U). Infected mosquitoes first are latently infected (E_{Mi}) before becoming infectious (I_{Mi}). A delay in this last transition is included to represent the extrinsic incubation period (τ_M). The transmission dynamics in mosquitoes can be represented by the equivalent set of differential equations for a deterministic model (though the code implements this stochastically):

$$\frac{dS_{Mi}}{dt} = \frac{P_{Li}}{2d_{PL}} - S_{Mi}\left(\sum_j \Lambda_{Mj}\kappa_{ij}\right) - \mu_M S_{Mi}$$

$$\frac{dE_{Mi}}{dt} = \left(\sum_j \Lambda_{Mj}\kappa_{ij}\right)S_{Mi} - \left(\sum_j \Lambda_{Mj}(t-\tau_M)\,\kappa_{ij}\right)S_{Mi}\,(t-\tau_M)P_M - \mu_M E_{Mi}$$

$$\frac{dI_{Mi}}{dt} = \left(\sum_j \Lambda_{Mj}(t-\tau_M)\,\kappa_{ij}\right)S_{Mi}\,(t-\tau_M)P_{Mi} - \mu_M I_{Mi}$$

It is assumed that half of emerging adult mosquitoes from the pupal stage (P_{Li}) are female (noting that only female mosquitoes are involved in transmission). The probability that a mosquito survives the latency period is defined by $P_{Mi} = \exp(-\mu_M \tau_M)$ and μ_M is the mosquito mortality rate which is constant and independent of infection status. κ_{ij} represents the mixing coefficient between patches and it is assumed to be the same for humans and mosquitoes.

The force of infection acting on a mosquito in patch *j* (Λ_{Mj}) is defined by,

$$\Lambda_{Mj} = \frac{\alpha_M}{\omega}\iint \zeta(1-\rho e^{-\frac{a}{a_0}})(c_D D_j + c_T T_j + c_A A_j + c_U U_j)da\,d\zeta$$

where α_M is the rate at which mosquito takes human blood, and c_D, c_T, c_A and c_U are the onward infectivity to mosquitoes of the different infectious human states, which are assumed constant for all patches.

3.1.1.1 Mosquito population dynamics

Mosquito population dynamics are taken from White et al. (2011). In the model, the vector's lifecycle is simplified into three main stages: Early larval instar stage (E_{Li}), which groups the eggs and the first larval instars (i.e. the first and second larval stages); late larval stages (L_{Li}), which groups the third

and fourth larval stages; and the pupal stage (P_{Li}). The equations that describe these dynamics are as follows:

$$\frac{dE_{Li}}{dt} = \beta M_i - \mu_E^0 \left(1 + \frac{E_{Li} + L_{Li}}{K_i}\right) E_{Li} - \frac{E_{Li}}{d_{E_L}}$$

$$\frac{dL_{Li}}{dt} = \frac{E_{Li}}{d_{E_L}} - \mu_L^0 \left(1 + \gamma_L \frac{E_{Li} + L_{Li}}{K_i}\right) L_{Li} - \frac{L_{Li}}{d_{LL}}$$

$$\frac{dP_{Li}}{dt} = \frac{L_{Li}}{d_{LL}} - \mu_{PL} P_{Li} - \frac{P_{Li}}{d_{PL}}$$

The average number of eggs laid per day by a female mosquito is defined by β. The developmental time periods are defined by d_{E_L}, d_{LL}, d_{PL} for each stage. The overall vector population is given by $M_i = S_{Mi} + E_{Mi} + I_{Mi}$. The larvae experience density dependent daily mortality where μ_E^0 and μ_L^0 are the death rates at very low densities and K_i is the environmental carrying capacity of the patch (White et al., 2011).

3.2.3   Model validation

The dynamic metapopulation model presented above was coded in R v4.1.2 as an extension of the ICDMM package. To check the metapopulation version of the model code, I simulated disease dynamics for 3 isolated patches with equal population sizes and compared model outputs with individual simulation results for each patch. Individual simulations were run implementing the original model within the ICDMM package. Each patch was modelled to have a different transmission intensity: low, medium, and high. Transmission intensity in the model is expressed as the entomological inoculation rate (EIR), which refers to the number of infective bites per person per year. The model was run for 21 years with the parameters specified in **Table 3.1**. Initial conditions for all simulations were set as the algebraic solution for the equilibrium of the original model, which is estimated by the ICDMM package.

In order to assess the effect of including population mixing in malaria dynamics, I carried out a sensitivity analysis for 3 different mixing matrices. In these matrices, diagonal values were varied between isolated populations ($k_{ii} = 1$) and totally mixed populations ($k_{ii} = 0.33$). For each simulation, diagonal values were set the same for all three patches and non-diagonal values were set such that the matrix was symmetrical, and columns and rows values added to 1. As an output, parasite prevalence in children between 2- and 10-years old at the steady state was analysed.

Table 3.1 *Model parameters for a three patched metapopulation analysis*

Parameter		Value
EIR	Low transmission intensity	1
	Medium transmission intensity	10
	High transmission intensity	100
Mixing matrix (Three patches)	Isolated populations	$\begin{pmatrix} 1 & 0 & 0 \\ 0 & 1 & 0 \\ 0 & 0 & 1 \end{pmatrix}$
	Mixed population	$\begin{pmatrix} 0.63 & 0.18 & 0.18 \\ 0.18 & 0.63 & 0.18 \\ 0.18 & 0.18 & 0.63 \end{pmatrix}$
	Perfectly mixed populations	$\begin{pmatrix} 0.33 & 0.33 & 0.33 \\ 0.33 & 0.33 & 0.33 \\ 0.33 & 0.33 & 0.33 \end{pmatrix}$

3.2.4   Malaria interventions

The ICDMM package in R also allows the user to analyse the effects of long-lasting insecticide treated bed nets (LLINs) and indoor residual spraying (IRS) on malaria transmission. In this chapter, I will focus on the effects of LLINs as an illustration of implementing an intervention in the metapopulation model. LLINs have four different effects on the mosquitoes dynamics: killing directly the mosquito that lands on the net; repelling the mosquito, which leads the mosquito to other blood sources; reducing transmission from an infectious human sleeping under the net to a susceptible mosquito; and directly protecting susceptible humans sleeping under the net from an infectious bite (Griffin et al., 2010a). These effects are incorporated into the equations impacting the mortality rate of the vector (μ_M) and the probability of a mosquito biting a host, which further affects the biting rates α and α_M.

3.2.5   LLIN allocation strategies

I used the extended metapopulation model to evaluate and compare different LLIN allocation strategies. For a fixed number of LLINs, I sought to find the allocation strategy for the LLINs between the patches that maximised health. I estimated the LLIN coverage in each patch for each LLIN availability scenario that resulted in the maximum achievable reduction in the health metric using a constrained optimisation by linear optimisations algorithm (COBYLA) (Powell, 1994). This optimisation algorithm was implemented as part of the R package *nlopt* (Johnson, 2022). Due to limited computational capacity for the optimisations, the model was reduced to a two-patch population for all the allocation scenarios analysed.

In the first analysis, to understand the effect of mixing and transmission intensity disparity between patches on the optimal LLIN allocation, I used the overall parasite prevalence in 2–10-year-olds at steady state as a measure of health impact. I undertook the optimisation across different combinations of EIRs and 3 mixing matrices (**Table 3. 2**). For each optimisation, the model was run for 40 years, with LLINs implemented at the beginning of the 21st year (to ensure equilibrium had been reached) and renewed every three years. I assumed that the maximum global LLIN coverage was 50% across all patches and that the population size and demographic structure were the same for all patches.

Table 3. 2 Mixing matrices used for the optimisation analysis for a metapopulation with two patches

Mixing matrix	Value
Isolated populations	$\begin{pmatrix} 1 & 0 \\ 0 & 1 \end{pmatrix}$
Mixed populations	$\begin{pmatrix} 0.75 & 0.25 \\ 0.25 & 0.75 \end{pmatrix}$
Perfectly mixed population	$\begin{pmatrix} 0.5 & 0.5 \\ 0.5 & 0.5 \end{pmatrix}$

Next, to analyse the effect of different allocation strategies on local and global control objectives, I implemented a scenario representing two neighbouring populations with different transmission intensities (EIRs: 5 and 50), again with a maximum LLIN coverage across all patches of 50%. For this scenario 4 LLIN allocation strategies were evaluated under different mixing patterns. The allocation strategies assessed were as follows:

1. **Equal allocation:** 50% LLIN coverage in each patch.
2. **Health equity allocation:** In this scenario, LLNIs are distributed proportionally to the transmission intensity in each patch, based on the following equation:

$$Coverage\ in\ patch\ i = \frac{EIR_i}{EIR_1 + EIR_2}$$

   For the scenario modelled, this corresponded to 9% coverage for the low transmission patch and 91% coverage for the high transmission patch.
3. **Donor's optimal allocation:** Optimal LLINs coverage per patch was estimated minimising average global parasite prevalence in 2-10 year olds at steady state. The optimisation was constrained by a maximum overall LLIN coverage of 50%.

4. **Individual optimal allocation**: Optimal LLIN coverage was estimated minimising average prevalence in 2-10 year olds at steady state in the patch with low transmission intensity. As before, the optimisation was constrained by a maximum LLIN coverage of 50% for the overall population and the low transmission patch, so that LLIN sharing only occurs from the low transmission patch to the high transmission patch.

For each allocation strategy, the average parasite prevalence in 2-10 year olds and yearly clinical incidence in 0-5-year-olds at steady state were analysed as outputs. Additionally, I defined the level of cooperation as the deviation in LLIN coverage from the equal allocation scenario.

3.3   Results
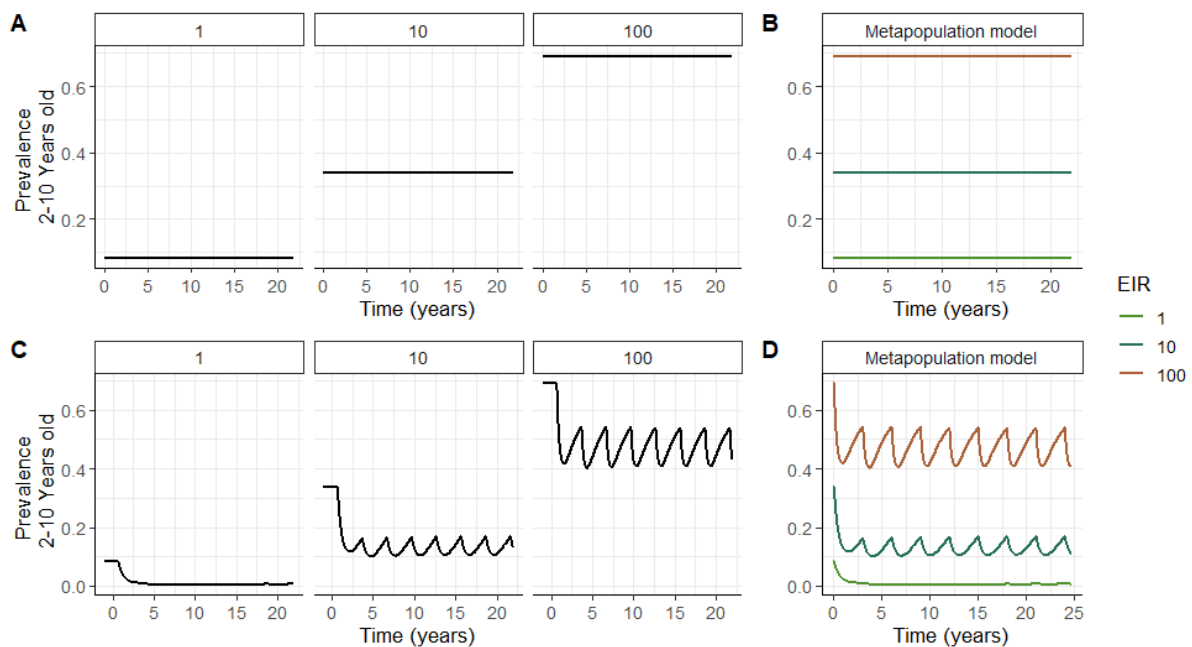
Figure 3. 2 Projected malaria dynamics from the original model *described by (Griffin et al., 2010a) and the metapopulation framework described in this chapter.* ***A*** *and* ***C*** *Simulations run independently using the original model.* ***B*** *and* ***D*** *projected malaria dynamics for a metapopulation with three isolated patches* ***A-B)*** *Dynamics without any intervention, initial conditions are set as the equilibrium point.* ***C-D)*** *Dynamics when population has 50% LLINs coverage, renewed every 3 years. Transmission intensities evaluated: Low (EIR=1), Medium (EIR=10) and High (EIR=100).*

3.3.1   Metapopulation model validation

To validate the extension of the ICDMM package to model metapopulation dynamics, I compared the outcomes from the original malaria model and the extended metapopulation model. **Figure 3. 2 A** and **C** show how malaria trajectories from independent simulations implementing the original model are the same as the simulations from the metapopulation extension (**Figure 3. 2 B** and **D**). However, when populations are mixed, infection trajectories diverge from the isolated patches trajectory (**Figure 3. 3** mid and right panel) towards a new equilibrium. **Figure 3.4** illustrates how this new equilibrium state varies in relation to the level of mixing between populations. When populations are isolated, the equilibrium is the same as when patches are modelled individually, whereas when patches are perfectly mixed the equilibrium converges to a single value for the overall population.
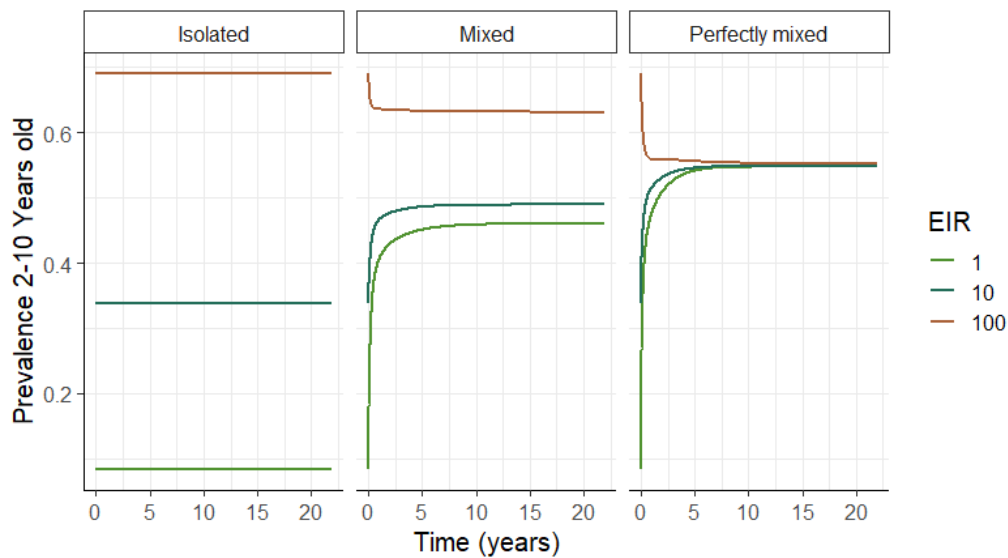
Figure 3. 3 Projected malaria dynamics under different mixing matrices: *Isolated populations (left), mixed populations (middle) and perfectly mixed populations (right). Dynamics are shown for a metapopulation with three patches with different transmission intensities: EIR 1(Green), EIR 10(Blue) and EIR 100 (Red).*
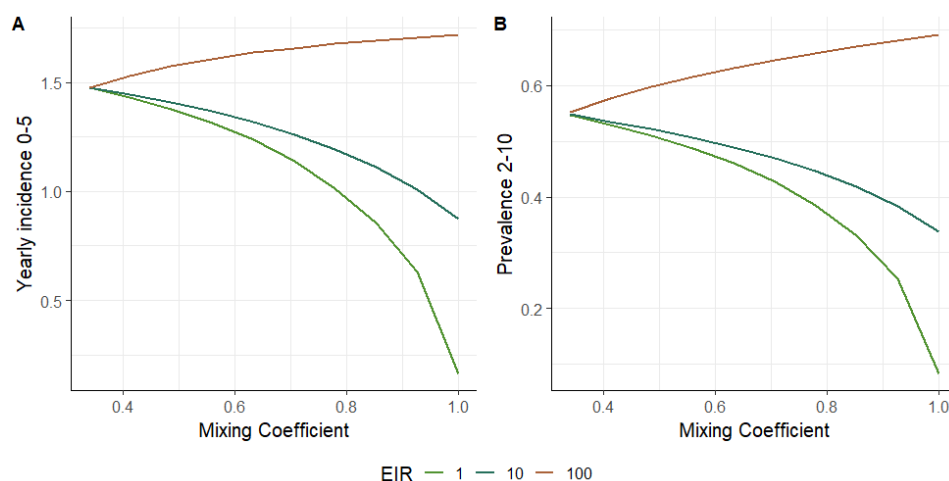
Figure 3.4 The modelled impact of population mixing on malaria burden. *Yearly incidence in 0–5 years-old individuals (left) and prevalence in 2-10 years old individuals (right) in an endemic state are shown for a metapopulation with three patches with different transmission intensities: EIR 1(Green), EIR 10(Blue) and EIR 100 (Red). Mixing coefficient refers to the diagonal of the mixing matrix where 0.33 is perfectly mixed and 1 is perfectly isolated.*

The relationship between population mixing and malaria burden at equilibrium is non-linear and varies between patches. The low transmission intensity patch experiences the greatest impact from mixing, increasing yearly incidence by 806% at equilibrium (**Figure 3.4A**). In contrast, the highest transmission intensity patch benefits from mixing, decreasing yearly incidence at equilibrium by 14.2% when patches are perfectly mixed compared to a scenario where patches are totally isolated (**Figure 3.4A**).

3.3.2   LLIN allocation

To explore the impact of LLINs in the metapopulation dynamics, I first ran the model implementing LLINs for all patches with 50% coverage in each and replacement every three years. When LLINs are implemented, malaria trajectories display an oscillatory behaviour given by the LLIN renewal schedule. In the same way as projections with no intervention (**Figure 3. 3**), higher mixing between populations leads to malaria trajectories converging to the same equilibrium point in all patches (**Figure 3. 5**), benefiting higher transmission intensity patches by reducing the burden of the disease at equilibrium.
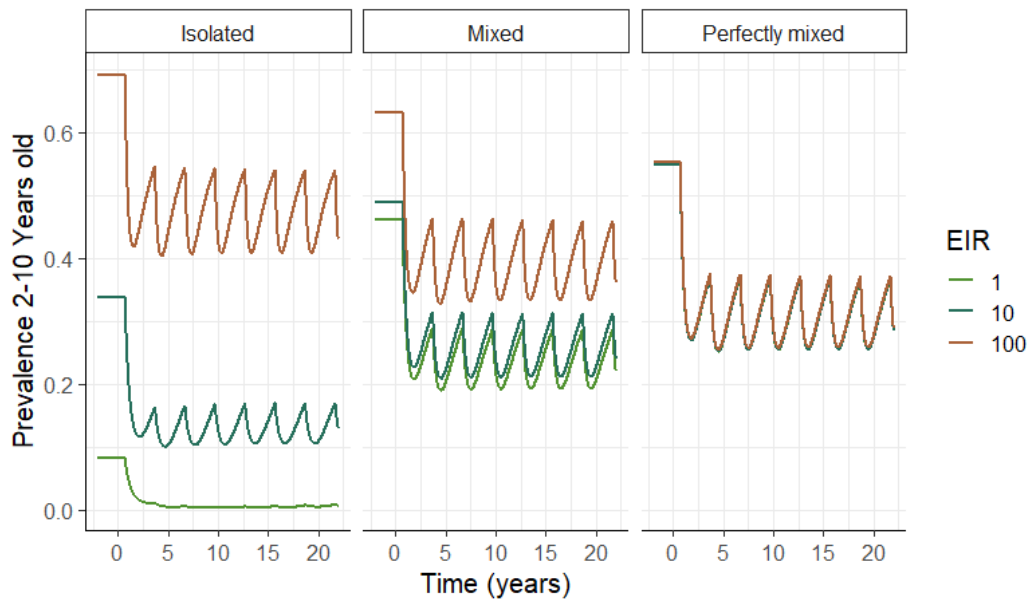
Figure 3. 5 Projected malaria dynamics when LLINs are implemented as intervention for different mixing matrices: Isolated populations (left), mixed populations (middle) and perfectly mixed populations (right). It is assumed a 50% coverage of LLINs in each patch with renewal every three years. Dynamics are shown for a metapopulation with three patches with different transmission intensities: EIR 1 (Green), EIR 10 (Blue) and EIR 100 (Red).

In order to determine the LLIN coverage that would benefit the overall population when there is heterogeneity in transmission, I performed an optimisation minimising average population prevalence in 2–10-year-olds at steady state. This optimisation was constrained by 50% total coverage of LLINs in the overall population. From **Table 3. 3** it can be seen that the optimal allocation is aligned with the GTSM "high burden to high impact" allocation strategy with LLINs prioritised to the highest transmission settings, leaving low transmission settings with low or no coverage.

Mixing between populations does not change the optimal LLIN allocation. This could be attributed to the large transmission disparity between patches in the metapopulation analysed. To confirm this, I explored the extent to which optimal LLIN allocation would change when transmission intensities between patches varied, screening different transmission intensity combinations and three mixing scenarios. Due to limited computational capacity, the metapopulation model was reduced to two patches for this analysis.

Table 3. 3 Optimal LLIN coverage for a three-patch metapopulation under different mixing scenarios

Mixing	Low transmission EIR=1	Medium transmission EIR=10	High transmission EIR =100
Isolated	*0%*	*50%*	*100%*
Mixed	*0%*	*50%*	*100%*
Perfectly mixed	*0%*	*50%*	*100%*

Figure 3. 6A shows the optimal allocation for different transmission intensity combinations in a two-patch metapopulation model. When transmission disparity between patches is high, the most efficient allocation is to distribute all available LLINs to the high transmission patch, leaving the low transmission patch without any intervention. By contrast, when transmission disparity between patches is low, the most efficient allocation suggests distributing resources between the two patches. This disparity can be measured as the ratio of transmission intensities between patches $\left(EIR_{high}/EIR_{low}\right)$, which is shown in more detail in **Figure 3. 6B**.

The white border in **Figure 3. 6A**, delimits the disparity threshold from which one deviates from giving all resources to the highest transmission population alone and starts distributing LLINs in both patches; this area is amplified in **Figure 3. 6B**. As mixing between populations increases, the area within the white border narrows, and the disparity threshold decreases. This threshold is not constant across all EIR combinations, for the mixed population this threshold can be as high as 30, whereas for a perfectly mixed population the maximum threshold is 7. For a scenario with isolated populations, LLIN distribution between two patches only occurs when both have low transmission levels (EIR <10).
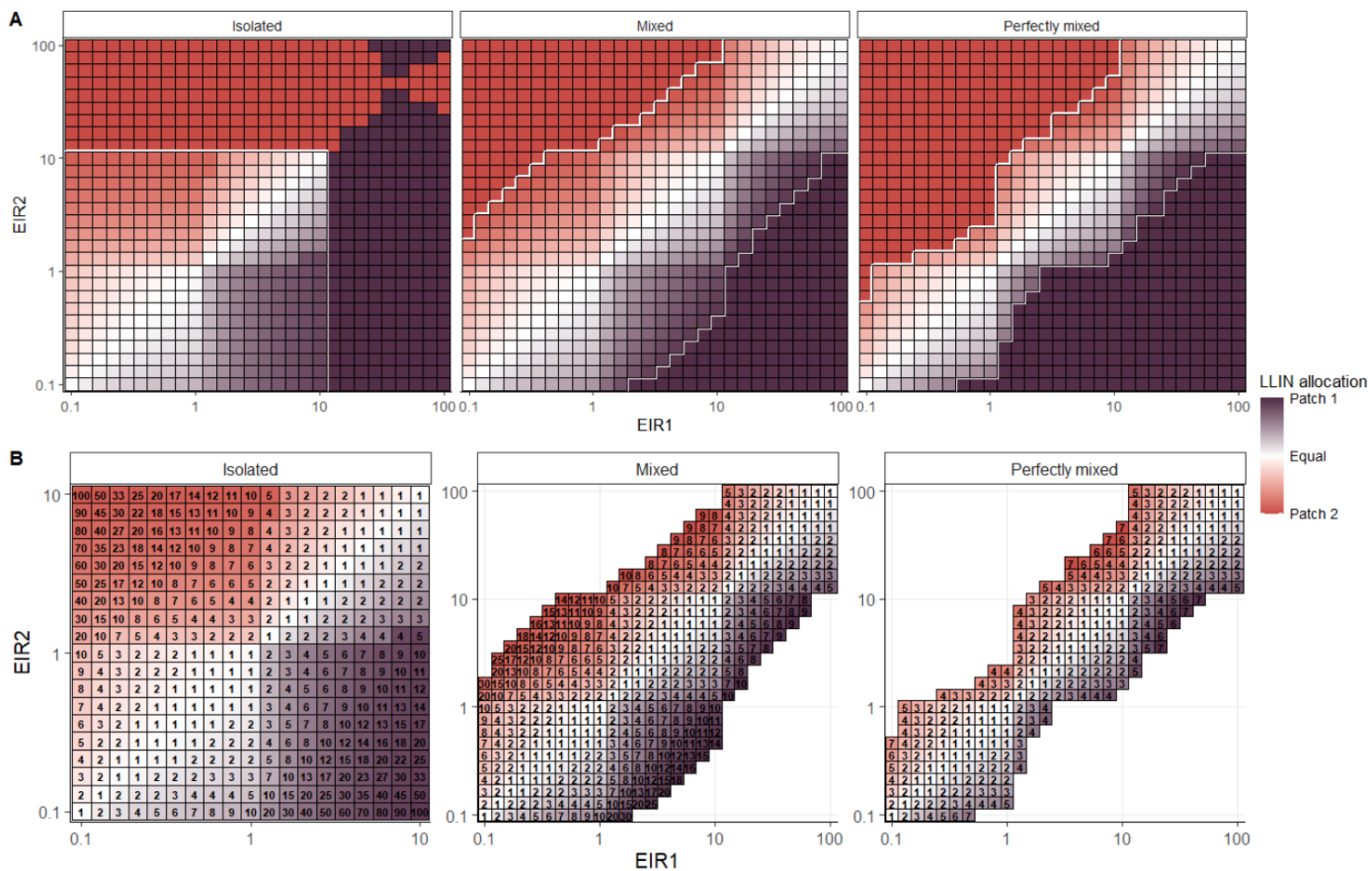
***Figure 3. 6 Optimal LLIN distribution for a two patched metapopulation under different mixing matrices. A)** Allocation for all EIR combinations evaluated. **(B)** Allocation and transmission ratio for EIR combination where LLINs are distributed between both patches. Isolated populations (left), mixed populations (centre) and perfectly mixed populations (right). Colours show If LLIN are all allocated to patch 1 (purple), patch 2 (red) or equally distributed between patches (white). It was assumed a total LLIN coverage of 50% for the overall population.*

In **Figure 3. 6**, when patches are isolated (left panel), the optimal LLIN allocation for high transmission intensity patches (EIR >10) displays different trends compared to the other scenarios evaluated. This can be explained by the non-linear relationship between transmission intensity (EIR) and prevalence at the steady state (**Figure 3. 7A).** Small changes in transmission (EIR) have a higher impact on infection prevalence at lower transmission intensities than in high transmission settings. Consequently, reducing the prevalence of infection in high transmission settings requires greater effort. This is evidenced in **Figure 3. 7B,** where the reduction in malaria prevalence when increasing LLIN coverage displays a convex decay for low EIRs compared to a concave decay for high transmission settings. As a result of this, LLINs are most likely to display an "all or nothing" impact in high transmission settings. This is illustrated in **Figure 3. 7C** when the objective function in high

transmission patches is lower when all LLINs are distributed to one of the patches instead of sharing resources between the two patches.
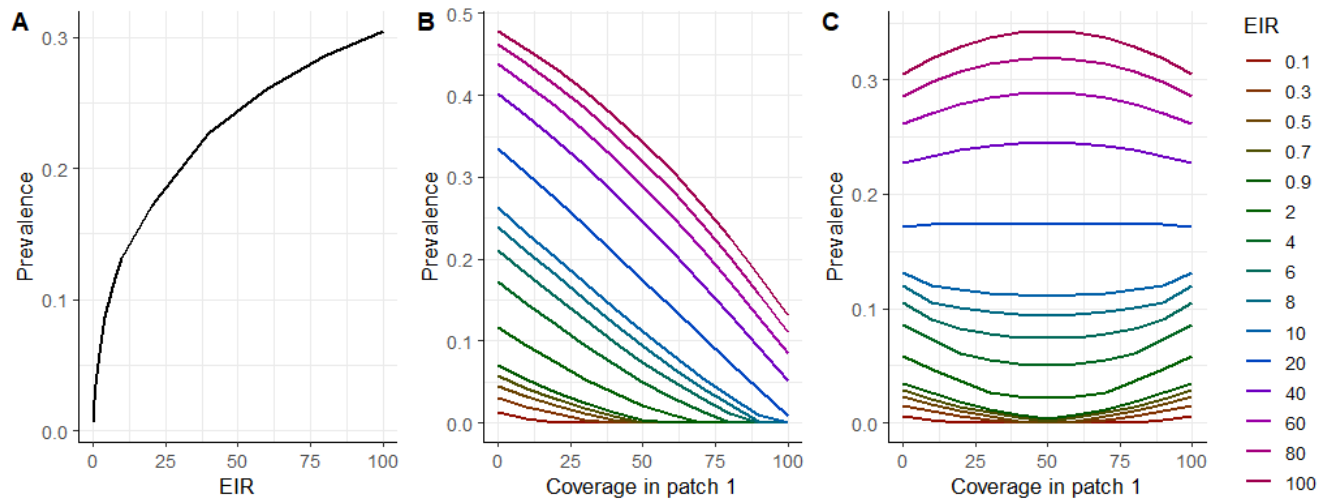
Figure 3. 7 Impact of LLINs coverage and EIR for a metapopulation of two isolated patches with the same transmission intensity. **A)** Relationship between metapopulation prevalence and EIR when there are no interventions in place. **B)** Average prevalence at steady state in one patch for different LLINs coverages metapopulation. **C)** Overall average prevalence at steady state in the overall population.

3.3.3 Cooperation effects

As shown in **Figure 3. 6**, it is more efficient to give most resources to the high transmission intensity population to reduce overall infection prevalence in a population, which is usually the donor's objective when allocating resources. However, this may not be the optimal allocation strategy for a patch with low transmission intensity, which may be also aiming to reduce or eliminate local infection. Here I compare the perspective of the low transmission patch in determining whether there is value in sharing some of their LLINs with the high intensity patch in order to reduce their own transmission. I contrast this with the perspective that the global actor would have in determining the optimal allocation across the two patches. I defined the degree of sharing as the proportion of LLINs given to the other patch, assuming an equal allocation as a baseline scenario.

Figure 3. 8 illustrates these different perspectives for four resource allocation strategies. From the individual (low transmission patch) point of view, this patch would only start sharing LLINs with their high transmission neighbour if there are at least moderate levels of mixing between the populations (> 16%) (**Figure 3. 8A**.). From this level upwards, there is a linear relationship between the level of mixing and the proportion of the low transmission patch LLINs that would be shared with the high transmission patch in order to minimise infection prevalence in the low transmission patch. **Figure 3.**

8B compares the effect of allocation strategies on the low transmission patch. With low levels of mixing, equal distribution of LLINs is predicted to have similar results to the optimal allocation from an individual point of view, given that low levels of sharing are expected. On the other hand, strategies focusing on health equity and minimising optimal allocation from the donor's point of view increase the prevalence of infection in the low transmission patch at low levels of mixing. However, as mixing and sharing increase, optimal allocation from the individual point of view converges to the optimal allocation from the donor's perspective.
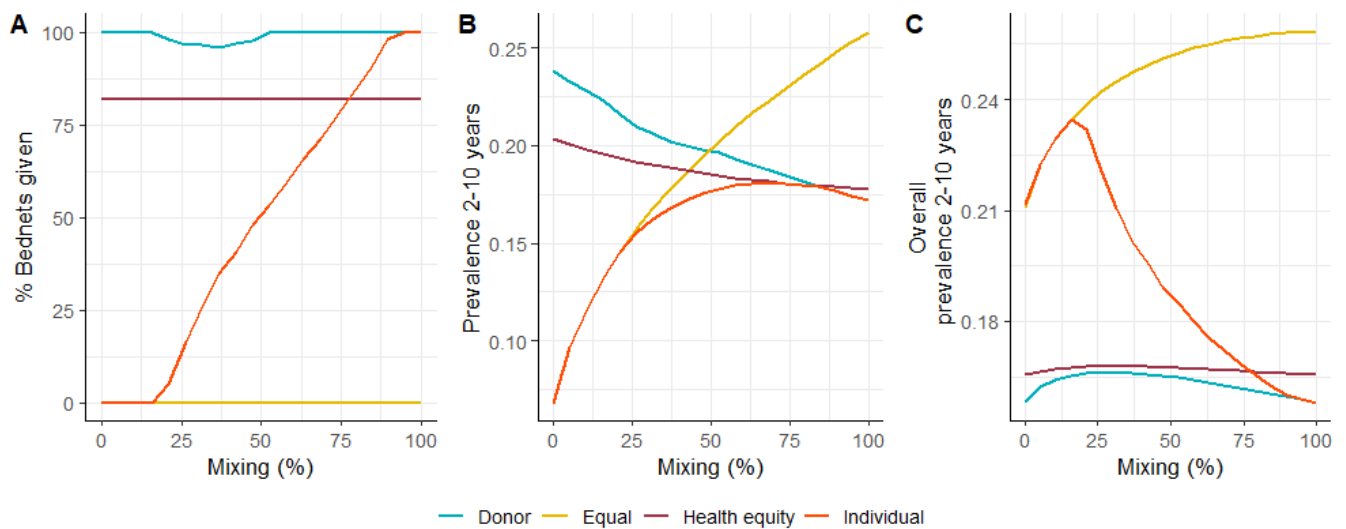
Figure 3. 8 Cooperation under different LLINs distribution scenarios. *Assuming a total bed net coverage of 50% for the overall population with an equal distribution between two patches, the low transmission intensity patch (EIR=5) can share LLINs to high-intensity transmission patch (EIR=50).* ***(A)*** *Percentage of LLINs shared by low transmission intensity patch compared to a base scenario of equal distribution* ***(B)*** *Prevalence at steady state in low transmission intensity patch.* ***(C)*** *Overall metapopulation prevalence at steady state. Yellow line shows equal distribution between the two patches. Blue line shows optimal distribution from the donor's point of view. Orange line shows optimal distribution from the low transmission intensity patch point of view. Red shows distribution based on health equity allocation.*

Health equity strategy allocation results are similar to those from the optimal allocation from the donor's point of view. Both strategies are in line with current allocation guidelines, distributing most LLIN to the high transmission patch. From the donor's point of view, in order to minimise infection prevalence in the overall population, the low transmission patch would need to share all LLINs with the high transmission patch (**Figure 3. 8A**). Optimisation results from the donor's point of view (blue line **Figure 3. 8A**) show a dip between 13-53% mixing, where some LLINs are allocated to the low transmission patch, which can be attributed to artefacts of the optimisation algorithm chosen. As

COBYLA is a local derivative-free optimization (Powell, 1994), it is plausible that during the optimisation process the algorithm got stuck in a local optima value close to the global optima.

In order to measure the value of each strategy, I compared all allocation strategies against an equal distribution baseline and estimated the annual number of cases averted in the low transmission patch and globally (**Figure 3. 9**). Findings from this comparison emphasise that for low levels of mixing, sharing resources to the high transmission patch has a negative effect increasing the number of cases in the low transmission patch (**Figure 3. 9**A). For this patch, optimal allocation from the donor's perspective is sub-optimal across almost all mixing levels. However, when analysing the value of allocation strategies as cases averted in the overall population, all allocation strategies at moderate and high levels of mixing propose sharing LLINs with the high transmission patch (**Figure 3. 8A**) and could generate additional value, averting up to 2795 cases per 10,000 individuals annually when populations are perfectly mixed (**Figure 3. 9B**). When comparing the health equity allocation and donor's perspective optimisation, there is a slight increase in benefits of the latter, regardless of the mixing conditions, at the expense of leaving the low prevalence patch without any intervention.
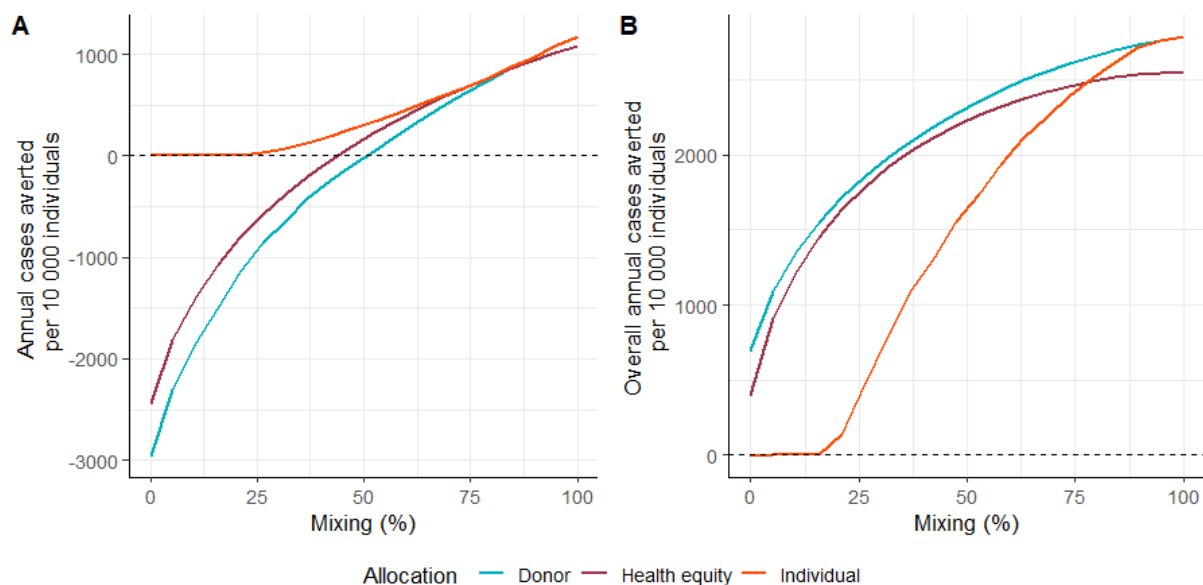
Figure 3. 9. *Annual cases averted at steady state compared with an equal allocation policy. A)* *Annual cases averted in the low transmission patch. B)* *Annual cases averted in the overall population. Assuming a total bed net coverage of 50% for the overall population, low transmission intensity patch with EIR=5 and high-intensity transmission patch with EIR=50. LLIN coverage per patch is defined as explained in the main text for three scenarios: health equity (red), individual' optimal allocation (orange) and donor's optimal allocation (blue)*

3.4   Discussion

In this chapter, the metapopulation framework developed in Chapter 2 was modified to include a malaria transmission model. With this model, I evaluated optimal LLIN allocation strategies under different assumptions for the level of transmission in the patches and the degree of mixing between patches. These optimal allocation strategies were then used to estimate the trade-off between local and global priorities to control malaria.

First, I have shown that including malaria connectivity between populations has a major effect on disease dynamics projections. As mixing between populations increases, so does the infection prevalence in low transmission patches. In accordance with these results, previous studies have demonstrated the effect of including interaction with neighbouring populations on infection trajectories and the impact of interventions (Citron et al., 2021, Silal et al., 2015). Whilst the work presented here simulated a theoretical scenario, these results reflect those of real-life scenarios, like the ones found by Silal et al., who also implemented a metapopulation model and demonstrated that controlling importation of cases was crucial to achieve elimination in the MOSAWA region, endorsing the need for regional support to achieve elimination goals (Silal et al., 2015).

Sensitivity analysis showed that levels of mixing between populations affect optimal allocation strategies. When populations are isolated, interventions only have a local effect. However, as the level of mixing between populations increases, there is an indirect effect of local interventions in other patches. This indirect effect is clearly evident when populations are perfectly mixed. In this scenario, the single optimal allocation strategy for all parties is to distribute all resources to the high transmission patch, where higher coverage will reduce malaria burden for all settings (i.e., individual patches and overall population). Consequently, when planning resource allocation for malaria interventions it is important to consider transmission connectivity between populations. In real-life scenarios, this linkage is not the same for all settings and varies between populations and in time. Recent studies have indicated that when planning intervention strategies, some populations may be considered as isolated (Chang et al., 2021), whereas in other settings high levels of mixing between populations cannot be ignored (Silal et al., 2015).

In the second part of this Chapter, I sought to determine optimal allocation strategies from different perspectives. Results showed that the current allocation strategy based on health equity is in line with optimal resource allocation strategy from the donor's point of view. There are minor differences between both allocation strategies, given that optimisation results allow patches to go without any intervention. In contrast, global donors like the Global Fund ensure funding is not overly concentrated in a few countries by constraining shares distributed to a country between a minimum (US$500,000 per disease) and a maximum value (10% funding available for the disease) (The Global Fund, 2019). Both strategies prioritise high burden locations to minimise global burden, which is disadvantageous for the low transmission locations when populations are poorly mixed or isolated.

The high burden to high impact strategy is not the only strategy towards malaria elimination. In 2007, the Roll Back Malaria Global Malaria Action Plan included shrinking the malaria map as a dimension of moving towards eradication. In this action plan, this strategy was viewed to be as important as reducing burden in high transmission settings. The shrinking the map strategy focuses first on eliminating malaria where feasible to concentrate resources to high burden locations later (Feachem et al., 2009). From the individual perspective of a near-eliminating country, keeping LLINs in the low transmission patch is the optimal allocation strategy and averts more cases than current allocation strategies, particularly if populations are not well connected. However, my results have shown that when mixing levels are high, sharing resources may be better for the low transmission setting as it prevents importation and benefits from the indirect protection of reducing transmission in the high transmission patch.

The mathematical model implemented in this work is a simplification of complex malaria dynamics and the scenarios simulated are representative examples to provide intuitive insight into the malaria dynamics between different populations. I have assumed that the parameters of transmission between patches are the same for human and vector populations. However, mosquitoes cannot travel long distances and humans are usually thought to be responsible for moving infections between populations (Midega et al., 2007). Additionally, I have also assumed vector-human interactions are equal in all patches. However, ecological conditions in each patch may vary and change vector biting behaviours such as the level of anthropophagy. A deeper insight into human-mosquito dynamics heterogeneity would help to provide more accurate predictions of the effect of mixing populations.

As an illustrative example, this analysis was constrained to use LLINs as the only resource to be distributed. This intervention reduces both malaria burden and transmission significantly when implemented. It is plausible that optimisation results with other preventive interventions like seasonal chemoprevention, would not strongly support cooperation with neighbouring populations as these are unlike to provide indirect protection and reduce transmission significantly (Walker et al., 2016). However, malaria interventions are usually deployed as packages of multiple interventions to ensure the reduction of disease burden (Winskill et al., 2019). It is, therefore, possible that results presented here may have underestimated the effect of interventions in each patch. Furthermore, funding for disease control comprises more than the cost of buying intervention commodities (e.g., LLINs, treatment etc.). In low transmission settings, surveillance and response account for the major costs instead of intervention commodities (Feachem et al., 2009). Hence, resources needed by low transmission settings may be underestimated by results presented in this work. While optimal allocation strategies suggest low transmission settings may benefit from sharing LLIN, these settings may need higher funding to support surveillance plans.

Despite its exploratory nature, this study offers some insight into how transmission heterogeneity and mixing between populations is a challenge that needs to be considered when allocating malaria interventions. I have shown that there is not a "one size fits all" optimal allocation strategy and that linkage between populations is a key factor when deciding how to share resources. Cross-border funding is necessary to encourage cooperation between countries in order to align individual and global goals. Due to computational limitations, optimisation analyses were restricted to a two patched metapopulation and a generic scenario. Thus, further work is required to analyse allocation strategies with more patches and realistic mixing parameters.

Chapter 4 Estimating the cost of vaccine hesitancy for measles

4.1 Introduction

4.1.1 Vaccine Hesitance

Since the introduction of the smallpox vaccine in 1853, vaccines have had a significant impact on the global burden of disease and were responsible for successfully eradicating smallpox in 1980. However, despite the evident benefit of this intervention, vaccinations have not always had full public acceptance. Vaccination campaigns have faced scepticism throughout history due to concerns about vaccine safety and efficacy (Simas and Larson, 2021). In the 1970s, a significant drop in Pertussis vaccination uptake was seen in the U.K, after a link between the vaccine and brain damage was suggested by some medical doctors. Two decades later, another vaccination crisis arose. After unfortunate publicity around erroneous research findings of the MMR (Measles, Mumps and Rubella) vaccine in 1998, vaccine coverage fell from 91.8% in 1996 to 79.7% in 2004 in England (Millward, 2019).

Vaccine hesitancy is defined as a "delay in acceptance or refusal of vaccination despite availability of vaccination services" (MacDonald, 2015). It is a spectrum that ranges from complete vaccine refusal (in this thesis referred as anti-vaccination) to acceptance and eventually active demand for vaccination. Within those who accept vaccines (from now on referred as pro-vaccination), vaccination uptake can still be less than ideal due to system failures such as limited vaccination services (MacDonald, 2015) or medical exemptions. Vaccine hesitancy leads to lower vaccination uptake, which has caused the resurgence of diseases that had previously been eliminated as a public health concern, such as measles (Paules et al., 2019a). Because of this concern, in 2019, the WHO declared vaccine hesitancy a threat to global health (de Figueiredo et al., 2020).

Underlying reasons for vaccine hesitancy are a complex interaction between trust in government and health authorities (Lazarus et al., 2021) coupled with misinformation on vaccine safety and risk

perception of the disease (Larson and Broniatowski, 2021). Previous studies have found that vaccine hesitancy is heterogeneous among individuals and can be found in various socioeconomic, ethnic and cultural settings (Simas and Larson, 2021) (Dubé et al., 2018). Yet, most determinants of vaccine refusal can be related to mistrust in pharmaceutical companies, healthcare providers and the government (Larson, 2018). Additionally, contextual factors such as social norms are also associated with vaccine uptake decisions. A systematic literature review assessing the determinants of vaccine acceptance shows that in societies where vaccination is the "normal thing to do", most individuals accept vaccination without second thoughts (Dubé et al., 2018). Political and historical experiences also contribute to strengthening or weakening trust and communal vaccine perceptions. For instance, in Nigeria, the controversial Pfizer drug trial in 1996 where many children died and developed disabilities, resulted in community mistrust towards the company and contributed to the boycott of the Polio vaccination campaigns in 2003 and also possibly the low vaccine acceptance reported during the COVID-19 pandemic (Pertwee et al., 2022).

4.1.2   Negative Externalities

As mentioned above, low vaccine uptake leads to increased transmission of preventable diseases and a higher risk of infection for those that are unvaccinated. Additionally, as most vaccines are imperfect (i.e., not 100% effective), vaccinated individuals can still get the disease, especially when community transmission rates are high (Chen and Fu, 2019). Because of suboptimal vaccination coverages and imperfect vaccines, pro-vaccination individuals cannot be excluded from the health and economic burden caused by anti-vaccination individuals due to a decrease in vaccination coverage and the associated increase in infection risk. In the same manner, anti-vaccination individuals cannot be excluded from the population-level benefits of vaccination.

Anti-vaccination individuals can be considered to be "free riders" that are protected from the disease because of the indirect effects of vaccination, particularly at high population coverage levels and once herd immunity is reached (Bauch et al., 2010). In addition to the immediate public health impact of sub-optimal vaccine coverage, anti-vaccination individuals may also be delaying disease elimination plans as resources need to be allocated to control the outbreaks (Deka and Bhattacharyya, 2019). Anti-vaccination individuals impose negative externalities onto pro-vaccination individuals by increasing transmission of the disease. This spillover effect can be compared to the consumption of goods with adverse impacts that impose a cost on a third party such as tobacco. The costs that society has to bear due to the consumption of these goods may be offset by prohibition mandates or higher taxation to

compensate for early deaths and indirect health effects (e.g., passive smoking for tobacco consumers) (Hoffer et al., 2014, Yurekli and Beyer, 2001).

The analysis of negative externalities from consumption of specific goods has been examined since the 1990s. However, negative externalities caused by the decision of not consuming a good such as vaccination have received scant attention in the research literature. As evidenced in previous Chapters, externalities and social benefits of vaccination have been previously studied (Boulier Bryan et al., 2007, Perrings et al., 2014, Gersovitz and Hammer, 2003). Yet, the aggregate societal burden of deciding not to take vaccinations has rarely been determined. Some researchers have estimated the costs of reported outbreaks of previously eliminated diseases (Pike et al., 2020, Ghebrehewet et al., 2016, Njau et al., 2019). Recently, a study evaluated the increase in annual costs due to increased measles vaccine hesitancy in the United States, from the perspective of the public sector (Lo and Hotez, 2017). However, the dynamics and societal economic burden of anti-vaccinators within a population have not yet been studied.

4.1.3   The case of measles

As was indicated in Chapter 1, the remarkable progress in reducing measles burden, and the global efforts towards disease elimination, has slowed over the last couple of years resulting in an increase in measles cases worldwide (World Health Organization, 2019b). Since the vaccine crisis in early 2000s, multiple measles outbreaks across England have been reported (Millward, 2019). In 2019, this increase in local cases led the U.K. to lose its measles-free status. Similarly, in the United States, after being eliminated in 2000, measles incidence has been increasing. In 2019, more than 1200 cases were reported in this country, threatening its measles elimination status (Larson, 2018, Hotez et al., 2020, CDC, 2020) .

One of the key determinants that has been attributed to the increase in measles incidence is vaccine hesitancy (Hotez et al., 2020). Hesitancy for measles vaccination is a growing public health concern worldwide and has been acknowledged as a key challenge in the new Measles and Rubella Strategic Plan (World Health Organization, 2020). Given the high reproductive number of measles, small reduction in measles vaccine uptake can have a big impact and precipitate the risk of measles outbreaks (Kirby, 2022). This risk has been aggravated in the last two years as measles vaccination

rates have dropped dramatically below critical thresholds as a consequence of the COVID-19 pandemic (Kirby, 2022, Dubé and MacDonald, 2020, Dixon et al., 2021).

In this Chapter, I use measles as a case study to examine the societal burden of an outbreak due to a growing anti-vaccination population. For this, the metapopulation framework developed in Chapter 2 is adapted to represent measles dynamics. I use simulation outputs to estimate the economic burden of additional measles cases based on previously reported costs and to evaluate how the health and economic costs increase when the anti-vaccination population increases within the overall population.

4.2   Methods

4.2.1   Mathematical model

I adapted the SIR metapopulation framework developed in Chapter 2 to represent measles dynamics based on the compartmental model developed by Verguet et al. (Verguet et al., 2015). Unlike the metapopulation models described in Chapters 2 and 3, this metapopulation model consists of two patches with the same transmission intensity but opposing vaccine acceptance views. Vaccinations are given to newborns with a coverage δ_i and a vaccine efficacy τ. Successfully vaccinated and protected individuals are assumed to have lifetime protection against infection, along with recovered individuals (R). Susceptible individuals (S) get infected at a rate that is proportional to the existing proportion of infectious individuals (I), as well as the strength of transmission between patches (κ_{xy}), which represents the rate of coupling between patches between the two populations.
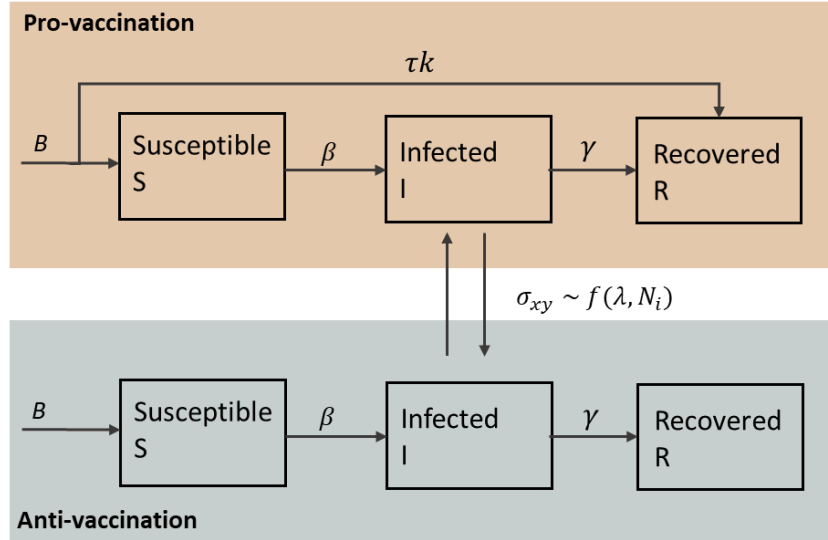
Figure 4. 1 Measles metapopulation model *Each patch represents a population with different vaccine acceptance views. Boxes represent infectious states S, susceptible; I, infected; R, recovered.*

The rate of coupling between patches (κ_{xy}), was modelled as proposed by Keeling et al (Keeling and Rohani, 2008). This rate depends on short duration movements from individuals from patch *i* to patch *j*. The expected fraction of time an individual from patch *i* spends away from home is defined as λ. In the absence of mixing ($\lambda = 0$), patches are isolated and the dynamics in each patch are independent. As the mixing increases, so does the correlation between patches. When patches are perfectly mixed ($\lambda = 0.5$) the dynamics in both patches are the same. It was assumed that time away from home is short compared to the disease dynamics.

Measles dynamics is described in each patch *i* by the following set of equations:

$$\frac{dS_i}{dt} = B(1 - \tau\delta_i)\, N_i - \beta_i S_i\big(\kappa_{ij} I_j + \kappa_{ii}\, I_i\big) - \mu S_i$$

$$\frac{dI_i}{dt} = \beta_i S_i\big(\kappa_{ij} I_j + \kappa_{ii}\, I_i\big) - \mu I_i - \gamma_i I_i$$

$$\frac{dR_i}{dt} = B\, \tau\delta_i\, N_i + \gamma_i I_i - \mu R_i$$

where *B* is the birth rate for the population and μ the mortality rate, which are assumed to be the same to maintain a constant population. β is the transmission coefficient and γ is the recovery rate. κ_{ij} are the conventional rate of coupling between populations and these are given by the equations described by (Keeling et al., 2004):

$$\kappa_{ii} = \frac{(1 - \lambda)^2}{(1 - \lambda)N_i + \lambda N_j} + \frac{\lambda^2}{\lambda N_i + (1 - \lambda)N_j}$$

$$\kappa_{ij} = \frac{(1 - \lambda)\lambda}{(1 - \lambda)N_i + \lambda N_j} + \frac{(1 - \lambda)\lambda}{\lambda N_i + (1 - \lambda)N_j}$$

N_i and N_j are each sub-population size. While these may vary in the scenarios modelled, the overall population remains constant for all simulations ($N_i + N_j = N$).

4.2.2 Model analysis

The dynamic compartmental model presented above was run for 200 years to find a post-vaccination equilibrium as a baseline scenario. In this scenario, both populations were assumed pro-vaccination and were perfectly mixed with a vaccine coverage of 90%. This coverage represents the reported value for a high-income country like England (NHS, 2019) and considers the proportion of the population that cannot get vaccinated due to medical conditions or accessibility difficulties. Vaccine efficacy and model parameters are specified in **Table 4. 1**. The endemic equilibrium of this baseline scenario was used as the counterfactual scenario and as initial conditions for the different scenarios modelled.

Table 4. 1 Measles metapopulation model parameters

	Parameter	Value	Reference
B	Birth rate	$2 \, x \, 10^{-4} \, week$	(ONS, 2019, Love-Koh et al., 2015)
μ	Death rate	B	-
γ	Recovery rate	$1/14 \, days^{-1}$	(Verguet et al., 2015)
β	Force of infection	$R_0 \, (\mu + \gamma)$	-
R_0	Basic reproductive number	15	(Anderson et al., 1992)
δ_i	Vaccine coverage	90%	(NHS, 2019)
τ	Vaccine efficiency	95%	(Verguet et al., 2015)
λ	Interaction parameter	$0 - 0.5$	Assumed
A_p	Proportion of anti-vaccination population	0-100%	Assumed

To understand the effect of anti-vaccination population size and mixing between sub-populations (λ) in disease dynamics, I carried out a sensitivity analysis for different combinations of these parameters. For this, the anti-vaccination population size was represented as a fraction of the overall population (Ap) (**Figure 4. 2**). For all simulations, the initial conditions and overall population were kept the same. Vaccine coverage was maintained at 90% for the pro-vaccination population and was set to 0% for the anti-vaccination population.
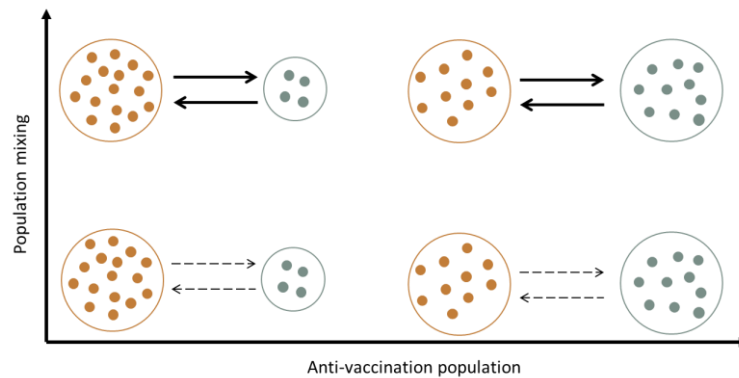
Figure 4. 2 A schematic illustrating anti-vaccination population and population mixing scenarios considered in the sensitivity analysis. The mixing coefficient was varied between 0-0.5 and anti-vaccination population size was varied as a proportion of the overall population.

For the analysis, dynamics for the first outbreak were extracted and compared to the baseline scenario. All simulations were run in R 4.1.2, the model equations were solved using the *odin* package (FitzJohn and Fischer, 2022).

4.2.3 Case study parameters

To estimate disease costs due to an anti-vaccination population, I selected a case scenario representing a developed country like England, with a population of 60 million individuals. Vaccine refusal in Europe has been reported to vary between 0.7% (Giambi et al., 2018) and 20% (Rey et al., 2018). For this case scenario, the antivaccination population was set at 3%, which is the reported percentage of parents refusing to vaccinate children in the United Kingdom (Bamber et al., 2019).

The mixing coefficient (λ) between sub-populations was estimated based on the anti-vaccination interaction network described by Johnson et al (Johnson et al., 2020). In their work, the authors analysed data from Facebook groups related to vaccine acceptance. Using groups posts and

connections with other Facebook groups, Johnson et al. generated an interaction network between anti-vaccination, pro-vaccination, and neutral groups. The latter ones are groups without a set stance but linked to the vaccine uptake debate (e.g., school parents associations). Using their network matrix, I estimated the network assortative mixing coefficient (r) using the *assornet* package in R (Farine, 2016). The assortative coefficient describes the tendency of nodes with the same characteristics to link to each other. A fully assortative network ($r = 1$) will have separate communities that do not mix (Newman, 2003). This coefficient relates to the mixing parameter (λ) in the model as follows.

$$\lambda = \frac{1 - r}{2}$$

Given that the measles metapopulation model only considered two populations, I assumed neutral groups behave like pro-vaccinators and determined the level of assortative mixing of the network based on vaccine uptake behaviour. After doing this, the mixing parameter λ was set to 0.292.

4.2.4 Economic impact

To estimate the societal costs of vaccine refusal for measles, economic impact was classified into two categories: costs and disease burden. The former considers direct healthcare costs due to the disease as well as costs associated with productivity loss. Direct medical costs include GP consultation time, additional staff hours and hospitalisation related costs. Productivity losses are costs associated with absenteeism of adult patients and carers of child patients due to measles related issues (Ghebrehewet et al., 2016). While there is no agreed definition on what constitutes productivity costs (Drummond et al., 2015), in this Chapter, these costs are defined as those borne by the employers due to absenteeism of measles non-fatal cases.

For the case scenario simulations, I used the direct and productivity costs from the 2012 measles outbreak in northwest England. These values were estimated by Ghebrehewet et al. based on literature reviews and interviews with key stakeholders in the outbreak (Ghebrehewet et al., 2016). Costs per case were converted to present value (i.e., GBP in 2020) using the *quantmod* package in R (Ryan et al., 2020) and the "Consumer Price Index of All Items in the United Kingdom" database from the Organization for Economic Co-operation and Development (OECD, 2022).

Table 4. 2 Economic parameters of measles. Prices are shown in 2020 GBP

Parameter	Value	Reference
Health care cost per case	GBP 312.13	(Ghebrehewet et al., 2016)
Productivity cost per case(non-fatal)	GBP 898.56	(Ghebrehewet et al., 2016)
Disease burden per case	0.019 QALY	(Thorrington et al., 2014)
QALY value	GBP 30 000/GBP 13 000	(Claxton et al., 2015, McCabe et al., 2008)
Health related quality of life (Qt)	0.86	(Love-Koh et al., 2015)
Life expectancy	82 years	(Love-Koh et al., 2015, ONS, 2019)

The second category, disease burden, refers to the impact of the disease due to direct health problems caused by morbidity and mortality. Morbidity is associated with the loss of health-related quality of life while sick and due to the disease's long-term consequences. Disease burden due to mortality refers to the years lost due to an earlier death caused by the disease. For both cases, disease burden is measured in Quality-adjusted life years (QALY). In the case of measles, short term morbidity has been previously estimated for an England-like context by Thorrington et al (2014). In their study, the authors measure the short-term impact of measles, through standardised health impact questionnaires from individuals with measles from the 2012 outbreak in England (Thorrington et al., 2014). Long-term morbidity was not considered for the case scenario analysis given that measles long-term effects are very rare in HIC like England (Edmunds and Van Hoek, 2009).
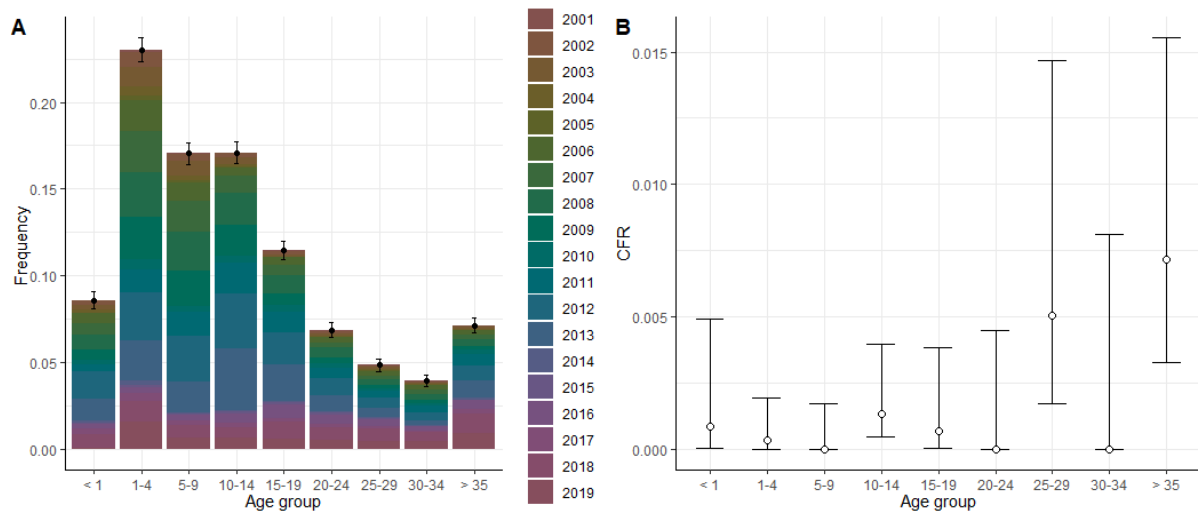
Figure 4. 3 Measles in the U.K. (A) *Measles age distribution for cases reported in the last 20 years.* **(B)** *Case fatality ratio per age group. Estimated from the U.K official reported cases and deaths (Public Health England, 2019, Public Health England, 2020).*

To determine the burden due to mortality, I first calculated deaths by age group, using model projections of measles incidence and the estimated case fatality ratio (CFR). CFR per age group was estimated from reported measles cases and deaths in the U.K. over the last 20 years (Public Health England, 2020, Public Health England, 2019) and uncertainty was captured with binomial confidence intervals (**Figure 4. 3**). This uncertainty was carried over to the economic analysis. I then quantified QALYs due to mortality based on the Quality-adjusted life expectancy (QALE) (**Table 4. 3**) and the estimated deaths per age group. QALE was determined using reported life expectancy parameters for England (Love-Koh et al., 2015) and the following equation, defined by (Sassi, 2006):

$$QALE = \sum_{t=a}^{a+L} \frac{Q_t}{(1+\delta)^{t-a}}$$

where L is the residual life expectancy at age a; δ is the discount rate, which was set at 3%; and Q_t is the health-related quality of life weight attached to a year of life. **Table 4. 3** shows discounted QALE estimated per age group.

Table 4. 3 QALE per age group estimated based on equation above and parameters in Table 4. 2

Age group	QALE
<1	26.99
1-4	26.83
5-9	26.40
10-14	25.91
15-19	25.33
20-24	24.66
25-29	23.89
30-34	22.99
>35	15.42

The overall economic impact of measles was estimated over a time horizon of 20 years. This impact represents the welfare (i.e., economic wellbeing) loss as a result of a reduction in consumption of vaccination. In order to estimate this welfare loss, health care costs, productivity costs and disease burden were totalled for each year. To translate disease burden into monetary terms, I assumed a value per QALY of GBP30 0000 as it this is the current upper threshold accepted by the U.K. healthcare system when assessing intervention technologies (McCabe et al., 2008). Given that this valuation of QALY has been contested before as being too high (Claxton et al., 2015), I also implemented a more conservative valuation of QALY. For this, I assumed a value per QALY of GBP 13,000 per QALY as this value has been suggested as an alternative national guidance for England (Claxton et al., 2015). Future costs took into account an inflation rate of 1% and the net present value (NPV) of the overall economic impact was calculated assuming a 3% discount rate.

4.3   Results

4.3.1 Model dynamics
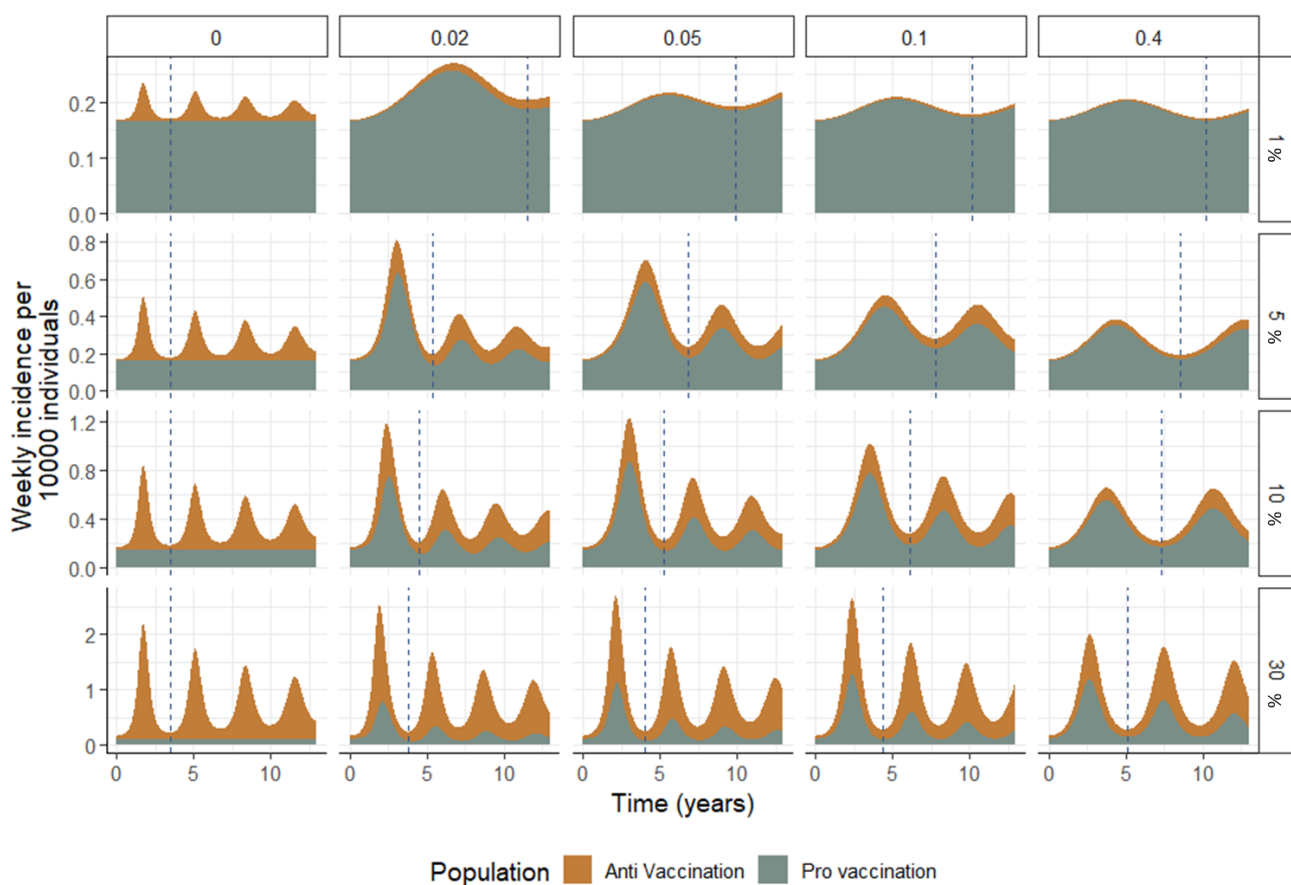
Figure 4. 4 Projected measles dynamics for different anti-vaccination population sizes, represented as a percentage within the overall population (rows), and different mixing between anti-vaccination and pro-vaccination populations (λ in columns). Incidence is presented weekly per 10 000 individuals. Dashed blue line represents the end of the first outbreak.

Measles trajectories under different mixing levels and anti-vaccinator population sizes are shown in **Figure 4. 4**. The first column shows how outbreaks are contained to the anti-vaccination population in the absence of mixing. When there is mixing between both populations a dilution effect is evidenced. While outbreaks include cases from both sub-populations when there is mixing, unvaccinated individuals from the anti-vaccination sub-population are also protected by those vaccinated in the pro-vaccination sub-population. As a consequence, outbreaks are longer and flatter. The number of outbreaks and their magnitude differ in each one of the scenarios modelled. In order to compare these scenarios, I evaluated disease trajectories from the first outbreak of each simulation and estimated their average yearly incidence. This incidence was then compared to the baseline scenario to estimate the number of additional cases.

The level of mixing between pro- and anti-vaccination populations, (λ) has a significant effect on the first outbreak size. For a scenario with 15% of anti-vaccination individuals, increasing the mixing coefficient λ by 0.03 can increase annual incidence by up to 10.65 cases per 10 000 individuals in the overall population (**Figure 4.5A**). However, the relationship between mixing and outbreak size is not monotonic. The largest changes in outbreak size are observed with changes in λ at low levels of mixing ($0 < \lambda < 0.1$); increasing mixing beyond 20% ($\lambda = 0.1$), does not have an additional significant impact on the total number of cases in the first outbreak (**Figure 4.5A**). The effect of low levels of mixing for the pro-vaccination population on the pro-vaccination population is shown as a steep increment for the cases per capita, which peaks before $\lambda = 0.05$ and then plateaus (**Figure 4.5B).** While, for the anti-vaccination population the effect is seen as a steep decrease in the outbreak size as mixing is incremented, after $\lambda = 0.1$ the decline slows down (**Figure 4.5C**).
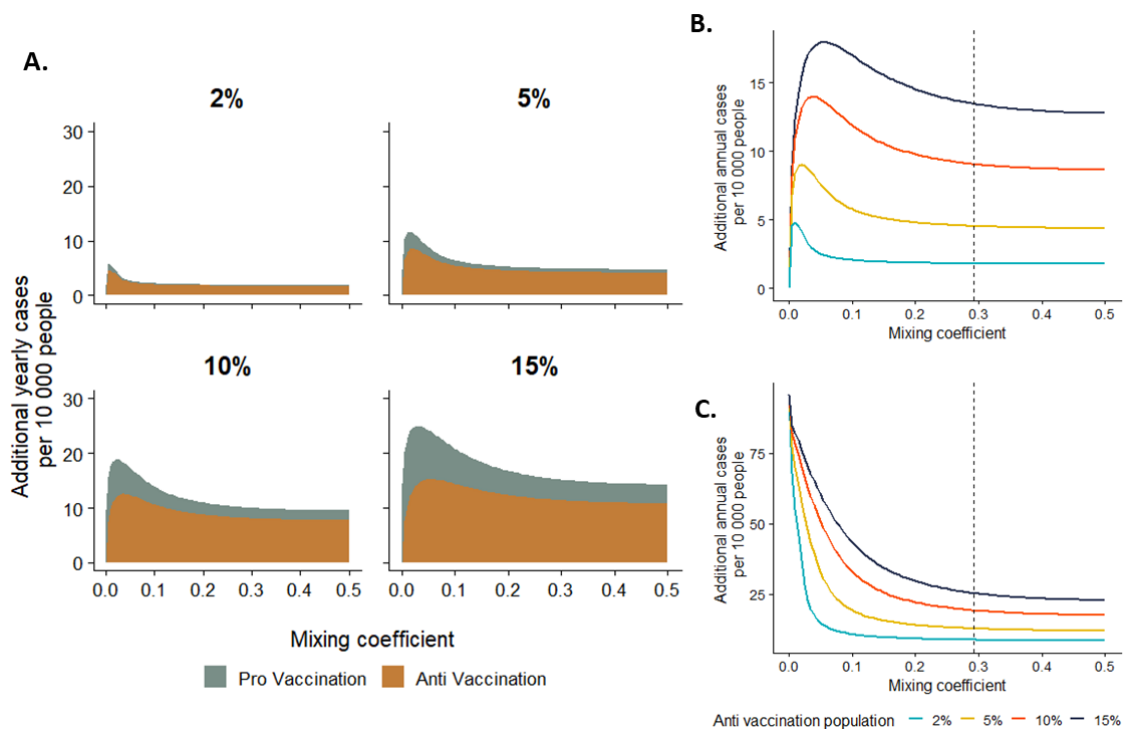
Figure 4.5 The modelled impact of population mixing and vaccine hesitancy on measles cases*. Additional yearly cases presented during the first outbreak compared to the number of cases in the same time frame for a steady state without anti-vaccinators. Results are shown for different anti-vaccination population percentages within the overall population: 2%, 5%, 10% and 15%. Additional yearly cases are presented per 10 000 individuals for the overall population **(A)** and individually for the pro-vaccination population **(B)** and the anti-vaccination population **(C)**. Dotted vertical line shows mixing coefficient used for an England-like scenario simulation*

On the other hand, as the anti-vaccination fraction in the overall population increases so does the additional yearly incidence for the first outbreak (**Figure 4.5A)** as a result of an increase in the susceptible population. However, this increase is not proportional to the anti-vaccination population increment. When incrementing the anti-vaccination population from 5% to 10% the peak number of cases increases by 62.4%. At 15% we see that this increment rises by 114%

4.3.2 Case scenario simulations

Disease trajectories for the case scenario projected two outbreaks during the 20 years analysed. During the first outbreak, incidence peaks at 36 070 cases per year (**Figure 4. 6A**). This translates to a cumulative impact of 340 857 additional cases and 416 deaths in the 20 years analysed compared to a situation in which 90% of the population are vaccinated. The majority (82%) of these are predicted to happen in the pro-vaccination population (**Figure 4. 6** B and **D**). However, the impact per capita in the anti-vaccinator population is significantly higher compared to the pro-vaccination population (**Figure 4.7**); during the peak of the first predicted outbreak, the incidence per million for the anti-vaccination population is 2.6 times that of the pro-vaccination population. Low estimates for deaths projections are consistent with a case scenario where the CFR is low. Due to the low reported number of deaths the projected deaths in **Figure 4. 6** have wide uncertainty intervals.
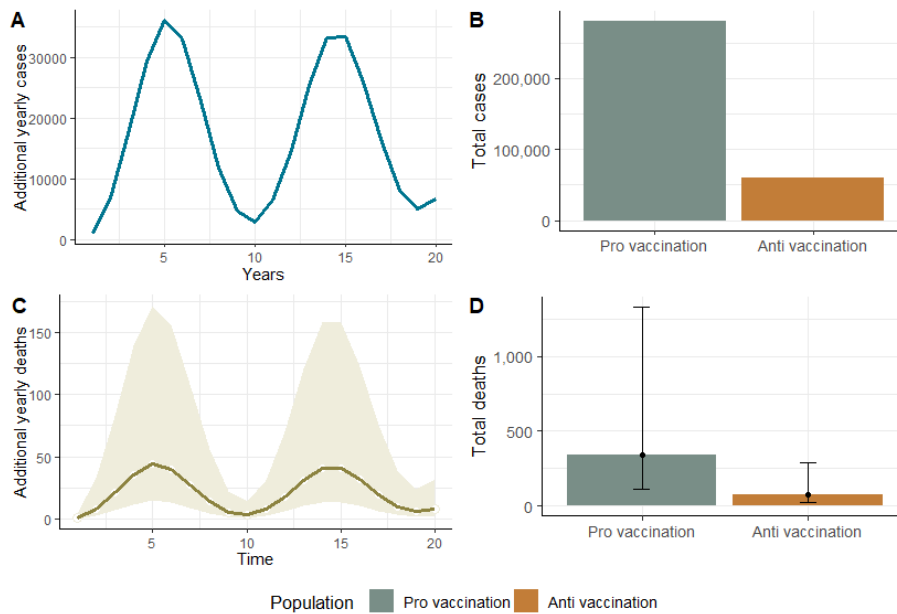
Figure 4. 6. Measles projections for the case scenario. *(A) Model trajectories for annual measles incidence. **(B)** Additional cases in each subpopulation for the 20 years analysed. **(C)** Measles deaths dynamics estimated using measles age distribution and CFR from Figure 4. 3. (D) Cumulative deaths for the 20 years analysed. Shaded area shows uncertainty in the number of deaths carried from the CFR estimates. Simulations were run for a 60 million population with a 3% anti- vaccination population and a λ= 0.292. Additional incidence and deaths were estimating comparing simulation's output with baseline scenario.*
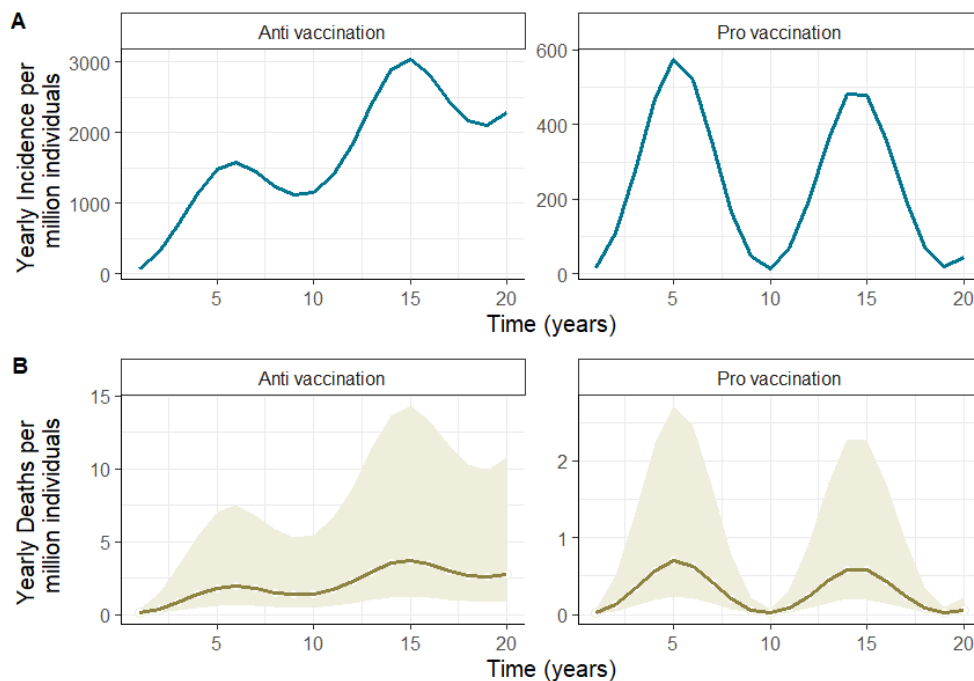
Figure 4.7 Measles trajectories per capita for each sub-population. *Results are shown for each population independently: Anti-vaccination (right) and pro vaccination (left). (A) Additional annual incidence per million individuals **(B)** Additional annual deaths per capita. Shaded area shows uncertainty in the number of deaths given confidence intervals of CFR. Simulations were run for 20 years in a 60 million population, with a 3% anti-vaccination population and λ= 0.292*

87

4.3.3 Cost of vaccine refusal

Total costs for the case scenario modelled are shown in *Figure 4. 8*. These costs represent the estimated cost of additional measles cases and deaths due to the presence of an anti-vaccination population. During the first outbreak projected by the model, the costs are estimated to peak at 99 (78-196) million GBP yearly. Over the 20 years analysed the total welfare loss was estimated at 536 (423- 1 059) million GBP at net present value assuming a 3% discount rate. Of these costs: 35.2% are attributed to productivity costs of non-fatal cases, which are borne by the employer for sickness absence and sick pay due to measles related issues; 30.3% are due to deaths and 22.3% due short-term morbidity, both of which are borne by the patient and the remaining 12.2% are attributed to the direct costs of healthcare, which are borne by taxpayers contributing to the healthcare system in a country with a national health service (*Figure 4. 8* A). When assuming a more conservative value for a QALY (*Figure 4. 8*B), total welfare loss over 20 years was estimated at 376 million GBP (327- 603) (NPV with 3% discount rate), with the majority of costs attributed to productivity costs (50.1%) followed by costs attributed to deaths (18.7%).
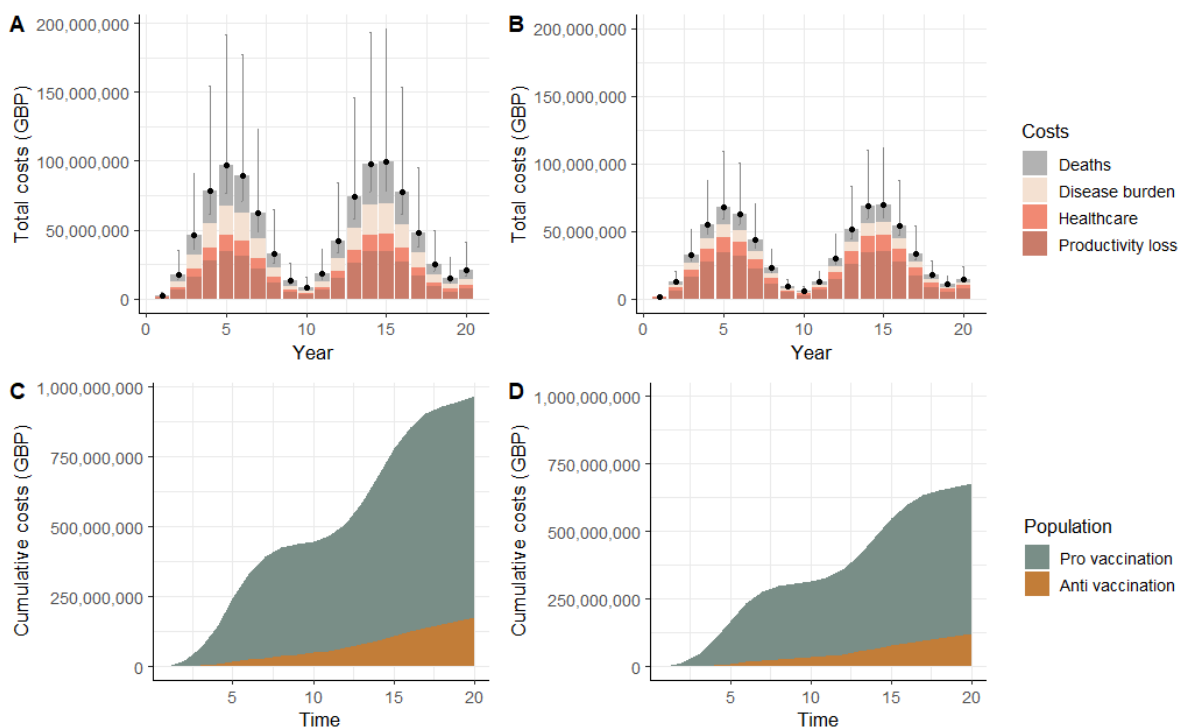
Figure 4. 8 Economic impact of an anti-vaccination population for the case scenario. Additional costs compared to a baseline scenario without anti-vaccinators in the population. (A) –(B) Total welfare loss per year discretised by cost type: direct healthcare costs, productivity costs, economic burden due to deaths, short term burden of the disease while sick. Confidence intervals show minimum and maximum costs per year given uncertainty in the number of deaths. (C) –(D) Mean cumulative welfare loss over the 20 years analysed, discretised by population. Results are shown for a 60 million population, with a 3% anti-vaccination population and a mixing parameter. λ= 0.292. Costs are estimated assuming a 1% inflation rate and a QALY value of GBP30 000 for (A) and (C) and a value of GBP13 000 for (B) and (D).

The cumulative costs over time (**Figure 4. 8 B, D)** emphasise how the pro-vaccination population accrued most of the costs, as the majority of cases are predicted in this sub-population and anti-vaccination individuals only constitute 3% of the overall population. Despite their low proportion in the population, the effects of anti-vaccination individuals are substantial. Welfare loss per anti-vaccination individual is projected to be 298 (235- 588) GBP for the case scenario modelled. Despite a proportional increase in the societal welfare losses as the size of the anti-vaccination population increases (**Table 4. 4**), this impact per anti-vaccinator remains relatively stable (**Figure 4. 9**), with the highest cost per antivaccination predicted to be 347 (274 − 686) GBP, when the anti-population is 10%.
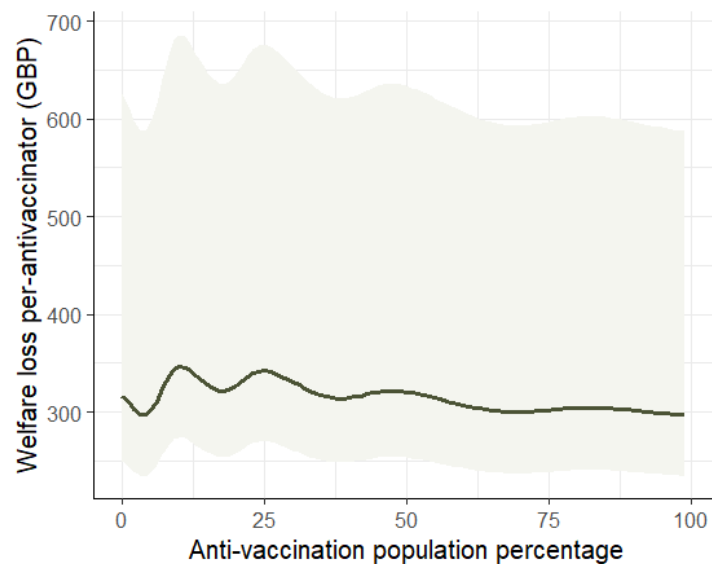
Figure 4. 9 Total welfare loss sustained by the overall population per individual in the anti-vaccination population.
Values were estimated based on simulation results with λ=0.292 projected for 20 years and assuming a cost per QALY of GBP 30 000. Net present values were estimated with a discount rate of 3%. Shaded area shows uncertainty in welfare loss which is determined by uncertainty in the number of deaths.

Table 4. 4 Estimated welfare loss sustained by the overall population due to an anti-vaccination population. *Total welfare loss is shown per capita and per anti- vaccination. Values were estimated based on simulation results with a λ=0.292 projected for 20 years and assuming a cost per QALY of GBP 30 000. Values were brought to 2020 GBP with a discount rate of 3%.*

Anti-vaccination population	Total Welfare Loss Million GBP	Welfare loss per capita GBP	Welfare loss per anti- vaccinator GBP
3%	536 (423 -1059)	9 (7 -8)	298 (235- 588)
5%	906 (715 - 1790)	15 (12 – 30)	302 (238 -596)
10%	2083 (1646 – 4119)	35 (27-69)	347 (274 – 686)
25%	5131 (4054 - 10144)	86 (68 -169)	342 (270 – 676)

4.4   Discussion

Vaccine use is an individual choice; however, this choice not only has an impact on the individual's health but has social welfare consequences as well. In this Chapter, I modified the metapopulation model developed in Chapter 2 to represent measles dynamics when sub-populations have different vaccine acceptance views. I used the measles metapopulation model combined with measles outbreak health burden estimates and estimates of economic costs to investigate the societal effects of an emerging anti-vaccination population in a HIC context. Results presented in this Chapter suggest that the presence of an anti-vaccination population is responsible for a substantial economic burden to society. For simulations projected for 20 years in an England-like scenario, the societal economic burden was estimated to be 536 (423 -1059) million GBP.

The economic consequences of sub-optimal vaccination coverage are greater than just the costs of treating the disease, as most of the welfare loss is attributed to indirect costs. Productivity costs to employers due to measles-related absenteeism account for the largest portion of the economic impact. This is followed by the monetised health loss costs owing to deaths. However, these costs usually tend to be overlooked when outbreak costs are analysed. Many of the studies in the literature focus on the health care cost of measles, underestimating the full societal impact of measles cases (Pike et al., 2020); my estimates show that these healthcare costs only comprise 12% of the total economic burden.

Overall, as the anti-vaccination population increases the welfare loss increases proportionally and the mean time between epidemics decreases. For the 20 years analysed, there is a maximum of six outbreaks once the anti-vaccination population is greater than 50% of the total population (not shown). More outbreaks entail a higher burden to the public health system given that besides the welfare loss due to the cases, outbreak response interventions will require more resources. Response interventions such as supplementary vaccination campaigns and contact tracing can represent up to 40% of outbreak costs (Ghebrehewet et al., 2016). However, model simulations did not consider outbreak response interventions and simulations illustrated measles trajectories of unmitigated outbreaks. Therefore, these results, therefore, need to be interpreted with caution.

In order to mitigate the economic consequences of vaccine hesitancy, countries have put into place mandates to incentivise vaccination among parents and health practitioners. In countries like Italy and France, children are restricted access to nurseries and schools if they do not have the mandatory vaccinations (Maltezou et al., 2019). This intervention has been shown to motivate parents to vaccinate their children and reduce the number of contacts between pro- and anti-vaccination populations. However, the partial isolation of anti-vaccination individuals may increase the number of measles cases as results presented here suggest that when mixing levels are low, the incidence in the anti-vaccination population increases. In the modelled scenario, I used a relatively high interaction parameter, resulting in the anti-vaccination population benefitting from the dilution effect. This parameter was obtained from a social network analysis (Johnson et al., 2020); however, this estimate was based on data from media platform interactions and it is likely that this number is different for in-person interactions. Further research is required to establish the interaction patterns between anti- and pro-vaccination populations.

Monetary incentives are another strategy established to promote vaccine uptake. These can take the form of monetary subsidies for each child vaccinated or sanctions to parents that do not vaccinate their children (Gostin et al., 2020, Attwell and M, 2019). These incentives have been shown to improve vaccination coverages when they are implemented (Li and Toll, 2021). The value of these incentives and sanctions varies between countries and represents the monetary compensation due to the anti-vaccination population free-riding on the benefits of vaccination-induced herd immunity and causing negative externalities to the population. The methods developed in this study allowed me to estimate

the economic burden of one anti-vaccination individual to society and can be used as a guide to help policymakers determine the extent to which these incentives would be justifiable.

Besides mandates and monetary incentives, understanding the underlying reasons behind vaccine refusal and addressing these reasons through appropriate health communication strategies has proven to increase vaccine acceptance (Goldstein et al., 2015, Dubé et al., 2018). However, these communication strategies require great financial and human resources given that optimal communication is case specific (Dubé et al., 2020, Larson, 2018).The findings of this Chapter can be used to justify the investing on communication strategies as these results can help to assess the societal value of reducing the anti-vaccination population.

It is important to note that the model described in this Chapter has several limitations. First, the model is a simplification of measles dynamics and does not account for spatial or age heterogeneity. I have assumed a uniform interaction between anti- and pro-vaccinators, which may have overestimated the role of herd immunity. Anti-vaccination groups are not evenly distributed in the territory and usually, outbreaks start off in small, insular communities with low vaccination rates (Gostin et al., 2020). A study assessing the effect of heterogenous uptake of MMR vaccine in California, USA, found that interactions between children are heterogenous, and this heterogeneity has a strong effect on the disease dynamics (Glasser et al., 2016). For the analysis presented here, I have assumed homogenous mixing for all age groups, and have ignored age-specific interactions, which may have led me to underestimate transmission. Furthermore, the scope of the analysis was limited to HIC countries given the parameters and costs assumed. However, vaccine hesitancy has also been reported in LMIC (Tomori, 2011, Njau et al., 2019, de Figueiredo et al., 2020). For these settings, mortality and morbidity are higher, and health care costs are different (Njau et al., 2019); in order to estimate the impact of anti-vaccination population in these settings the methods developed in this Chapter could be replicated using new parameters accordingly.

Moreover, there is uncertainty around cost estimates and findings may be somewhat limited by the cost types included in the cost estimation. I have considered productivity costs as part of the economic impact analysis. However, the inclusion of productivity costs in economic evaluations is an area of controversy in health economics (Drummond et al., 2015). Estimates of productivity cost are variable to the methods used to calculate them. Some authors argue that including these costs could lead to

the *double counting* of effects, given that disease burden measurements (QALY) could already include the value of productivity (Drummond et al., 2015, Turner et al., 2021). It is, therefore, possible that results presented here may have overestimated the societal costs of vaccine refusal for measles. Another reason my results do not necessarily provide a general representative estimate of measles costs is that these were estimated for a specific outbreak in England (Ghebrehewet et al., 2016, Thorrington et al., 2014). Furthermore, the value placed on a QALY has been the subject of intense debate within the economic community. Finding a single all-purpose monetary value of a QALY has shown to be theoretically unattainable and most authors agree that the willingness to pay per QALY is context specific (Gyrd-Hansen, 2005, Pinto-Prades et al., 2009). In this Chapter I have analysed two different monetary values per QALY, which have been suggested for economic analyses in the U.K. Yet, these values may be country specific and cost estimates presented here may be difficult to translate into other countries.

Despite these limitations, the metapopulation model was useful in understanding the impact of an emerging anti-vaccination population. The results of this Chapter provide a valuable and practical insight into the economic strains pro-vaccination populations undergo due to the growing anti-vaccination movement and demonstrate that the economic burden of anti-vaccination is greater than just the cost of treating cases. Vaccine hesitancy movements have put a burden on society, and a demand on countries' policymakers as the return of previously eliminated disease needs to be stopped. The findings of this study can be considered when assessing investments, monetary compensations and incentives to promote vaccination.

Chapter 5 The impact of vaccine hesitancy in the COVID-19 pandemic

During the development of this thesis, the COVID-19 pandemic started. When the first vaccines were approved, this Chapter was conceived to estimate the effects of vaccine hesitancy for the vaccine rollout being deployed at the time, implementing the tools developed in this thesis. Two versions of this work have been previously published as a paper in Communications Medicine with an earlier version released as a report for the MRC Centre for Global Infectious Disease Analysis

- Olivera Mesa, D., Hogan, A. B., Watson, O. J., Charles, G. D., Hauck, K., Ghani, A. C., & Winskill, P. (2022). Modelling the impact of vaccine hesitancy in prolonging the need for Non-Pharmaceutical Interventions to control the COVID-19 pandemic. Communications Medicine, 2(1), 14. doi:10.1038/s43856-022-00075-x
- D Olivera Mesa, AB Hogan, OJ Watson et al. Quantifying the impact of vaccine hesitancy in prolonging the need for Non-Pharmaceutical Interventions to control the COVID-19 pandemic. Imperial College London (24-03-2021), doi: https://doi.org/10.25561/87096.

5.1   Introduction

As described in Chapter 1, in March 2020, the World Health Organization declared the novel coronavirus (COVID-19) outbreak a pandemic and countries started implementing non-pharmaceutical interventions (NPIs) to stop the spread of the virus. These interventions were based on encouraging social distancing and imposed lockdowns. NPI strategies varied between countries, yet the economic consequences of these restrictions were observed worldwide (Lenzen et al., 2020, Wang et al., 2021). Governments were faced with the decision to trade-off between public health and economic impact (Anderson et al., 2021).

In December 2020, the first vaccine against SARS-CoV-2 was approved and a new road out of the pandemic was made possible. Vaccination rollout plans started being implemented in HIC and the world started working towards herd immunity. To achieve this goal by mass vaccination, 5 factors have been significant (Anderson et al., 2021). First, infectiousness of SARS-CoV-2, given by the basic

reproduction number, which was estimated to range between 3-4 for the wild type variant (Flaxman et al., 2020). Second, vaccine efficacy of available vaccines, which was reported to range from 50% to over 95% against symptomatic disease (Polack et al., 2020, Voysey et al., 2021, Baden et al., 2020, Logunov et al., 2021, Hitchings et al., 2021). Third, supply chain and logistics of mass production. Fourth, the rate at which population can be vaccinated, which could vary between urban and rural settings. Lastly, the public acceptance of the vaccines (Anderson et al., 2021). Given all these factors, high levels of vaccine uptake were required to achieve herd immunity (Hogan et al., 2021), particularly if children were not vaccinated during the first phase of roll-out.

One major concern that threatens the herd immunity goal has been vaccine hesitancy (Loomba et al., 2021). As explained in Chapter 4, vaccine hesitancy leads to lower vaccination uptake which hinders efforts to control the pandemic. Since vaccines were at the development stage vaccine hesitancy was acknowledged as a risk to the pandemic and multiple surveys were conducted to assess the problem. These surveys found that between 14% (Lazarus et al., 2021) and 27% (Jones et al., 2021) of adults would not accept a vaccine if available, whilst between 14% (Lazarus et al., 2021) and 19% (Jones et al., 2021) said that they were uncertain. A large variation in vaccine hesitancy between countries was also identified, with the proportion saying that they would get a SARS-Cov-2 vaccine if it became available, ranging from 40% for France (Jones et al., 2021) to 89% for China (Lazarus et al., 2021). As evidenced for other vaccines, vaccine hesitancy was found to be heterogenous across sub-populations depending on gender, age, ethnicity, religion, or socioeconomic status (Lazarus et al., 2021, Freeman et al., 2020, Jones et al., 2021). Furthermore, these surveys highlighted that the key drivers of SARS-CoV-2 vaccine hesitancy were related to concerns about the accelerated pace of vaccine development (Freeman et al., 2020), side-effects (Jones et al., 2021), and the spread of misinformation about the pandemic (Loomba et al., 2021).

The aim of this Chapter is to understand the likely impact of vaccine hesitancy on control of the pandemic, using a mathematical model of SARS-CoV-2 transmission (Hogan et al., 2021). For this, I capture the effect of reduced coverage using measured levels of vaccine hesitancy from behavioural survey data on self-reported intention to be vaccinated. Then, I implement a deterministic COVID-19 transmission model to project pandemic trajectories with low vaccination coverage due to vaccine hesitancy and compare them to an ideal counterfactual. I model each scenario with both a high and

a moderate vaccine efficacy profile that represents the range of efficacies of vaccines approved by March 2021.

5.2   Methods

5.2.1   Vaccine hesitancy data

Attitudes towards COVID-19 vaccination were obtained from the Imperial College London YouGov Covid 19 Behaviour Tracker Data (Jones et al., 2020). This data set includes weekly surveys about people's behaviours in response to COVID-19 (including vaccines) as well as standard demographic questions on age, gender, and household structure. Ethics approval and informed consent were not required given that all data was publicly available and de-identified.

I extracted the survey results from February 8th - February 15th, 2021 for 10 European countries. To assess vaccine hesitancy, I used data from one question pertaining to COVID-19 vaccine acceptance in which participants were asked to what extent they would definitely get a COVID-19 vaccine if it became available to them next week. Answers were obtained on a numeric scale ranging from "Strongly agree – 1" to "Strongly disagree – 5". To capture survey uncertainty, answers per age group were used to parameterise a multinomial distribution, from which 100 replicates were drawn. To capture further uncertainty associated with the translation of survey response to vaccine uptake, for each replicate, coverage per age group was estimated assuming the probability of vaccination as a beta distribution with means: 0.98, 0.75, 0.50, 0.25 and 0.02 for survey responses 1, 2, 3, 4 and 5, respectively. Coverage distributions per age group, median as well as the 10% and 90% quantiles are shown in **Figure 5. 1**.
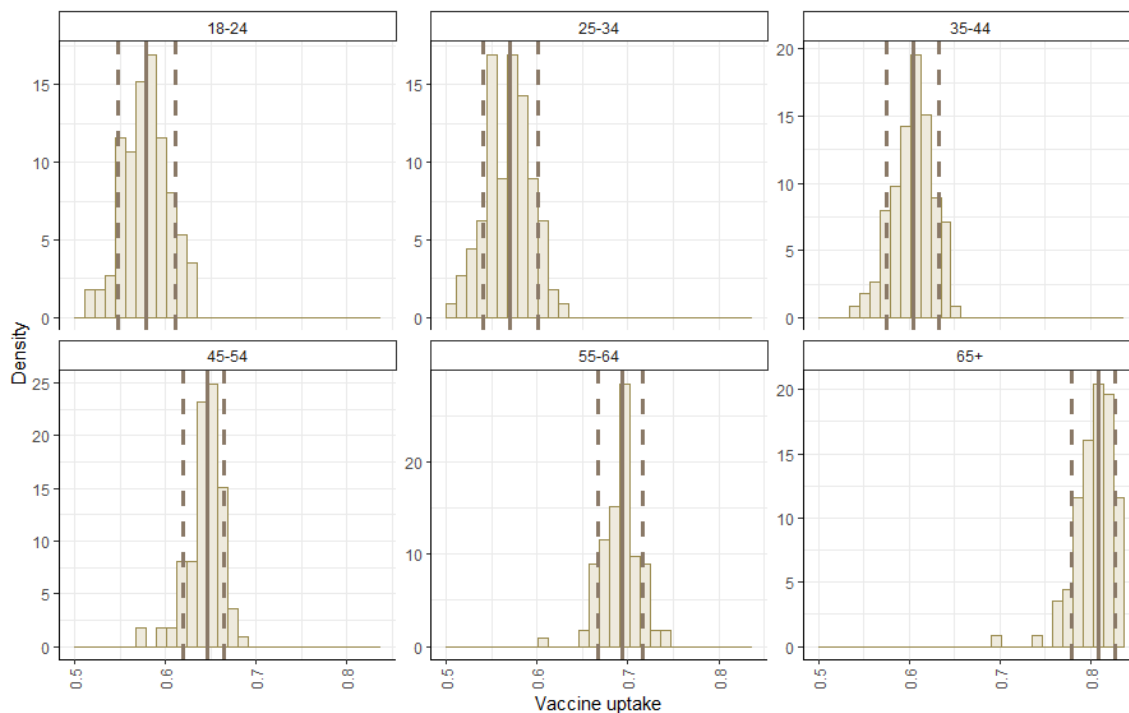
Figure 5. 1 Vaccine uptake distribution per age group. Based on vaccine acceptance reported by Jones et al (Jones et al., 2021) distribution of coverage per age group (panel in the plot) was estimated after translating survey results into multinomial distribution and drawing 100 replicates. Probability of vaccination was modelled as a beta distribution with mean 0.98, 0.75,0.50,0.25 and 0.02 for survey response 1,2,3,4,5, respectively.

5.2.2 Mathematical model

To predict the public health impact of vaccine hesitancy, I used a previously developed mathematical model for SARS-CoV-2 transmission and vaccination (Hogan et al., 2021). The model captures the disease dynamics among nine different infection states, stratified by age and vaccination status (

Figure 5. 2).

- S = uninfected and therefore **susceptible** to infection
- E = **exposed** to infection but not yet infectious
- I_{MILD} = **infected** and infectious with mild infection that does not require hospitalisation (this includes both symptomatic and asymptomatic infection)
- I_{CASE} = **infected** and infectious with disease that will require hospitalisation
- I_{HOSP} = cases that have been **hospitalised** in a general ward bed
- I_{ICU} = cases that have been admitted to **an intensive care unit (ICU)**
- I_{REC} = cases that have been stepped down from ICU into a general ward bed for **recovery**
- D = cases that have **died**

- R = infections and cases that have **recovered** and are immune to re-infection

Disease states E, I_{CASE}, $I_{HOSPITAL}$, I_{ICU} and R are split into two sequential states such that the durations of stay are Erlang-distributed. Individuals become infected at a rate that depends on the number of people in states I_{MILD} and I_{CASE} and the transmission probability. Following infection, individuals in the I_{CASE} state proceed to an ICU unit (I_{IICU}) or hospitalisation in general ward (I_{HOSP}) at rates based on age specific probabilities and country-specific hospital bed capacity. After infection, cases either died (D) or recover (R) following the path shown in

Figure 5. 2 (with the final outcome tracked by splitting both the I_{HOSP} and I_{ICU} states into two compartments reflecting those that die or recover respectively in order to capture the different durations of stay associated with these outcomes). Finally, recovered individuals can lose naturally acquired immunity and then return to the susceptible state. Additional constraints are included in the hospitalisation pathway to capture situations in which the need exceeds capacity; with those that do not receive appropriate care experiencing higher death rates(Walker et al., 2020). These constrains are country-dependent for the country-specific scenarios and are described in **Table 5. 1**.

Table 5. 1 Hospital capacity parameters per country

Parameter	Country	Value	Description
Maximum hospital beds per capita	U.K	4.63	Values taken from R package squire using methods described by Walker et al. (Walker et al., 2020). For the representative scenario U.K values were implemented
	France	6.5	
	Germany	7.4	
Maximum ICU beds per capita	U.K	0.15	Values taken from R package squire using methods described by Walker et al. (Walker et al., 2020) For the representative scenario U.K values were implemented
	France	0.21	
	Germany	0.24	

The level of transmission in the model is parameterised by the reproduction number, R_t, in the absence of vaccine or naturally induced immunity. This is equal to R_0 at the start of the simulation and may be modified forwards in time by the introduction of NPIs. The transmission probability is obtained as the ratio between the reproductive number and the leading eigen value of the next generation matrix, which depends on duration of infectiousness, the age-stratified mixing matrix and age-dependent probability of hospitalisation.
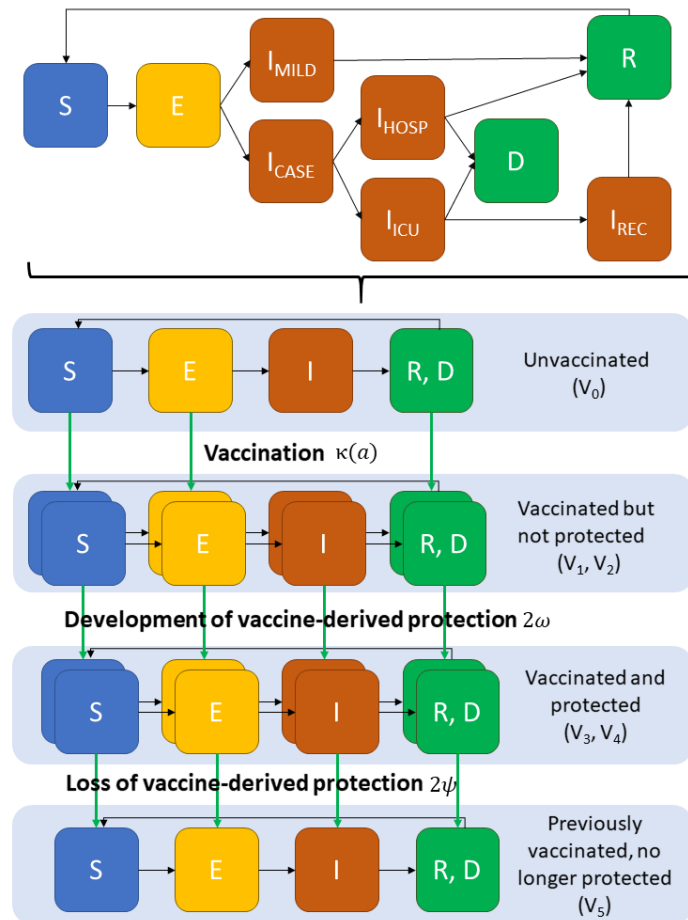
Figure 5. 2 Schematic of SARS-Cov-2 transmission model. **Reproduced from (Hogan et al., 2021)**. *The schematic Susceptible-Exposed- Infected-Recovered (SEIR) model representation is based on the model described by Hogan et al Hogan et al. (Hogan et al., 2021). Infected individuals are disaggregated into mild cases and the disease clinical cases, which include hospitalisation and intensive care. Vaccination status is included as a new dimension in the model. Only individuals in the susceptible (S), exposed (E) and recovered (R) compartments can be vaccinated.*

Vaccination is modelled as an additional dimension disaggregating the population into 6 vaccination classes, with the vaccinated states split into two compartments (v1/v2 and v3/v4) to generate Erlang-distributed waiting times:

- v_0 = unvaccinated
- v_1 and v_2 = vaccinated but not yet protected, reflecting the two-dose vaccine schedule and need to wait approximately 28 days from dose 1 for protection to develop
- v_3 and v_4 = vaccinated and protected
- v_5 = previously vaccinated but no longer protected, used to capture waning vaccine efficacy.

Only individuals who are susceptible, in the latent period, or recovered can be vaccinated. It is assumed that individuals receive a single two-dose schedule (with no drop-out) and that vaccine efficacy is generated after the second dose. This approximation, therefore, ignores the partial efficacy obtained from the first dose. It is assumed that the vaccine protects against infection – by reducing the transmission parameter by a constant factor; and against severe disease in breakthrough infections – by reducing the rate of hospitalisation by a constant factor.

Vaccines are distributed by age groups at a constant rate and a matrix of coverage targets that represents prioritisation strategies. In this matrix, rows represent ordered prioritisation steps and columns the age group. The target coverage per age group was changed according to the different scenarios modelled. In each prioritisation step (s), vaccines are given at a rate to all age groups that satisfy. Once all target coverages are met in the current prioritisation step, the step is incremented, and the process is repeated. When all coverage targets in the final prioritisation step are met, vaccination is ceased. This, therefore, means that if vaccine uptake is lower, vaccines will be distributed to younger age-groups rather than waiting for a set period of time for each age-group. This is consistent with a constant supply of vaccines and best matches the roll-out of vaccines in high-income countries.

5.2.3   Parameters

Parameters for SARS-CoV-2 infection, health care capacity, age-distribution and contact patterns are based on previous work (Walker et al., 2020, Hogan et al., 2021). With these parameters, the transmission probability is estimated based on the reproductive number (Rt), which is given as an input for each simulation as a function of time. Vaccine induced immunity is assumed lifelong, while natural immunity is assumed to last for an average of one year (Hall et al., 2021). To produce simulations representing the different vaccines approved by March 2021, scenarios are run for two vaccines: one with high efficacy (94% efficacy against infection (Polack et al., 2020)) and one with moderate efficacy (63% efficacy against infection (Voysey et al., 2021)). For both vaccines I assumed an additional 60% efficacy against hospitalisation for breakthrough infections, resulting in an overall vaccine efficacy against hospitalisation and death of 98% for the high efficacy vaccine and 85% for the moderate efficacy vaccine.

To mimic vaccine rollout plans, vaccination is introduced to the population at the beginning of January 2021. I assume a constant vaccination rate (κ), at which all individuals aged 15 years and

above (~78% of the population) will be vaccinated over a 10-month period. This rate is implemented for all scenarios modelled since I assume vaccination rate is constrained not by vaccine uptake but by the supply and delivery of vaccines. Therefore, lower levels of coverage, result in shorter vaccination campaigns; given that in the model, once coverage targets are met, vaccination is ceased. To illustrate the effect including children vaccination, vaccination rate is maintained constant and vaccination period was extended such that all individuals aged 5-15 years could be vaccinated.

Vaccines are targeted by age groups at the constant rate κ, prioritising older age groups: with 80+ years vaccinated first and then sequentially including additional age groups in 5-year age-bands down to 15-19 years for adults only vaccination simulations and down to 5-10 years for simulations including children vaccination.

Table 5. 2 *Vaccination parameters and values*

Parameter	Symbol	Value	Description
Vaccine efficacy against infection	$1 - v_{inf}(a)$	94%; 63%	It was assumed infection-blocking efficacy is the same as reported vaccine efficacy against clinical disease. Values were selected to cover the range of approved vaccines efficacies reported to March 2021 (Polack et al., 2020, Voysey et al., 2021)
Vaccine efficacy against disease	$1 - v_{dis}(a)$	60%	Estimate based on reported vaccine effectiveness data in the UK which suggests ~86% efficacy against hospitalisation/death compared to ~65% against mild disease for a single dose of the Pfizer vaccine (Public Health England, 2021, Bernal et al., 2021). The assumed value of 60% generates 98% efficacy against hospitalisation/death for the high efficacy vaccines and 85% for the moderate efficacy vaccine, with both representing two dose schedules.
Vaccine mean duration of protection	$1/\psi$	5000 days	Assumption generating durable immunity for 1 year simulations.
Rate of vaccination	$\kappa(a)$	135 399 per day (representative) 183 834 per day (U.K) 176 810 per day (France) 237 142 per day (Germany)	Population-dependent: set such that number of people vaccinated per day achieves vaccination of all individuals aged 15 years and above in a 10-month period. Representative scenario assumes a total population of 50 million individuals and U.K age demographics
Mean time to develop vaccine-acquired immunity following second dose	$1/\psi$	7 days	Based on immunogenicity data from Phase II trials in which antibody titres plateau ~7 days post dose 2 (Jackson et al., 2020, Zhu et al., 2020, Mulligan et al., 2020, Sahin et al., 2020, Folegatti et al., 2020)
Vaccine schedule	-	21 days	2 doses modelled 21 days apart(Voysey et al., 2021, Polack et al., 2020, Baden et al., 2020, Logunov et al., 2021). Efficacy follows 2nd dose (so only modelling final dose of any vaccine schedule)

5.2.4   Reproductive number profiles

To simulate a representative pre-vaccination scenario, a reproductive number profile was generated. In this profile, Rt was the same as R_0 ($R_0 = 3$ (Walker et al., 2020)) up to April 2020, subsequently decreased to 1 to represent the impact of NPIs against the first wave, and then rose to 1.5 during the latter half of 2020 to represent a second wave. Following the introduction of vaccination in January 2021, I set Rt to increase in 10 fixed steps. Each step representing the lifting of NPIs. The time for each step increase was determined by estimating when vaccination coverage had reached levels such that the herd immunity threshold due to vaccine immunity was reached. At the end of the vaccination period, R_t remained at a value such that the herd immunity threshold was maintained, given final vaccination coverage and vaccine efficacy against infection.

To estimate the coverage needed for each Rt step, the following herd immunity threshold equation was used:

$$Coverage = \left(1 - \frac{1}{R_t}\right)\frac{1}{efficacy}$$

When analysing the impact of lifting NPIs, the Rt profile following the introduction of vaccination was generated based on an ideal scenario for vaccination uptake. Conversely, when evaluating the degree to which NPIs would need to remain in place, the Rt profile after the introduction of vaccination was set up based on vaccine coverage due to vaccine hesitancy.

5.2.5   Scenarios

I consider two potential scenarios for vaccine coverage target per age group: An ideal scenario where final coverage was 95% for all age groups vaccinated, and a vaccine hesitancy scenario where final coverage per age group was given by the multinomial distribution from the survey. For the first scenario, it was assumed that a small proportion (5%) of the population cannot be reached for vaccination. This value is based on maximum vaccination uptake reported for England's COVID-19 vaccine rollout (NHS, 2021). For the latter scenario, it was assumed vaccine hesitancy remain the same within the age bins reported by the survey and I modelled the median coverage per age group as well as the 10% and 90% quantiles, to determine upper and lower bounds. Representative scenarios were simulated using U.K demographics and representative contact matrix (Funk et al., 2020) and epidemics were seeded at the end of February 2020 with 20 cases. A simulation was run for each vaccine coverage scenario for both adult-only vaccination campaign and vaccination campaign including children. As an output for each simulation, I estimated the number of deaths and

hospitalisations associated with COVID-19 over the two-year period from 1 January 2021 to 31 December 2022.

To generate country specific simulations, I parameterise the model with data on the population size and age distribution of the country and representative contact matrices obtained from a systematic review of social contact surveys through the socialmixR package in R (Funk et al., 2020). Rt trajectories up to December 31st, 2020, were extracted from the Global LMIC reports for each country. These trajectories are estimated, fitting the model, without vaccination, to reported daily cases and deaths (MRC Centre for Global Infectious Disease Analysis, 2020). After January 1st, 2021, Rt was set to increase by 10 fixed steps, up to the theoretical herd immunity threshold based on an ideal vaccination schedule (as described above). The pandemic trajectory was evaluated using country specific data on vaccine hesitancy and demography for the two coverage scenarios described above and assuming vaccination for individuals aged 15 years and above only.

5.3   Results

5.3.1   Vaccine hesitancy public health impact

I first sought to determine the public health impact of vaccination and vaccine hesitancy as NPIs are lifted. To do so, I allowed the time-varying reproductive number in the absence of immunity R$_t$, to be increased in steps such that the herd immunity threshold accounting for vaccine-induced immunity was maintained, under the assumption of ideal vaccination uptake (**Figure 5. 3a, c**). In this ideal scenario, NPIs can be fully lifted at the end of the vaccination period with a high efficacy vaccine (94% efficacy, **Figure 5. 3a**). However, with a moderate efficacy vaccine (63% efficacy), some NPIs or other population-level behavioural changes may need to remain to control the epidemic (**Figure 5. 3c**).
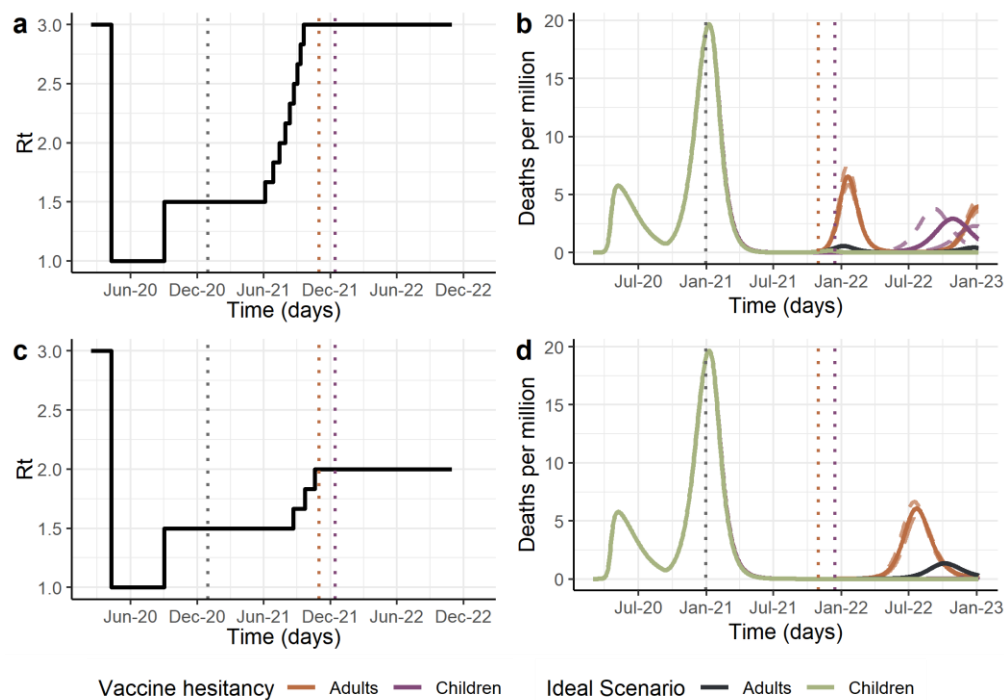
Figure 5. 3 Projected COVID-19 dynamics given vaccine hesitancy. Panels **a-b** show a high vaccine efficacy (94% against infection, 98% against hospitalisation and death), panels **c-d** moderate vaccine efficacy (63% against infection, 85% against hospitalisation and death). Panels **a** and **c** show the reproductive number Rt profile, which represents the level of NPI stringency, with lower numbers indicating higher stringency. In this illustrative example, I assume that a first wave of transmission occurred at the beginning of 2020 with the assumed value of Ro: 3. This was followed by NPIs leading to a reduction in Rt to 1, followed by an Rt of 1.5 as NPIs are lifted leading to a second wave of transmission in the latter half of 2020. After vaccination is introduced at the beginning of 2021, NPIs in all scenarios are lifted according to a schedule based on coverage under the ideal scenario (no vaccine hesitancy, 95% of individuals 15 years plus are vaccinated). Panels **b** and **d** show projected deaths per million under vaccine hesitancy scenarios: adults-only vaccination (orange), vaccination including children (purple). Continuous lines represent simulations of median vaccine coverage per age group, while dashed lines represent simulations of 10% and 90% quantiles. For the ideal scenario, black line represents adults-only vaccination and green line represents ideal scenario when children vaccination is considered. In each scenario, final vaccination coverage per age group and deaths vary according to vaccine hesitancy. Vertical dashed lines indicate the vaccination rollout period in the ideal scenario.

In the presence of vaccine hesitancy, lifting NPIs and relying on vaccine-induced immunity for control is predicted to lead to periodic outbreaks determined by the duration of naturally induced immunity (**Figure 5. 3b, d**). For a high efficacy vaccine, daily deaths per million at the peak of the first outbreak are projected to be 11.5 (10.1-13.2) times higher than under the ideal scenario (**Figure 5. 3b**). This translates to a cumulative impact of 532 (457-612) more deaths per million population in the two years after vaccination begins. Simulations project fewer deaths are projected for a vaccine of moderate efficacy compared to a higher efficacy vaccine. This is partly due to prolonged NPIs being

required to maintain herd immunity where efficacy is lower, resulting in an outbreak that is more spread out and resulting in a lower final Rt compared to the high vaccine efficacy simulations. For a moderate efficacy vaccine, the cumulative impact of vaccine hesitancy is projected to lead to 456 (416-504) extra deaths per million population.

These adverse impacts of vaccine hesitancy on transmission, symptomatic disease, hospitalisations, and deaths affect vaccinated as well as unvaccinated individuals because of imperfect vaccine efficacy (**Figure 5. 4**). Under the vaccine hesitancy scenario, the resulting lower vaccination coverage is projected to lead to a 16.7% and 30.4% increase in hospitalisations in the vaccinated population for the high and moderate vaccine efficacy profile, respectively, and a 9.4% and 27.2% increase in deaths in the vaccinated population, compared to an ideal vaccination scenario (**Figure 5. 4**).
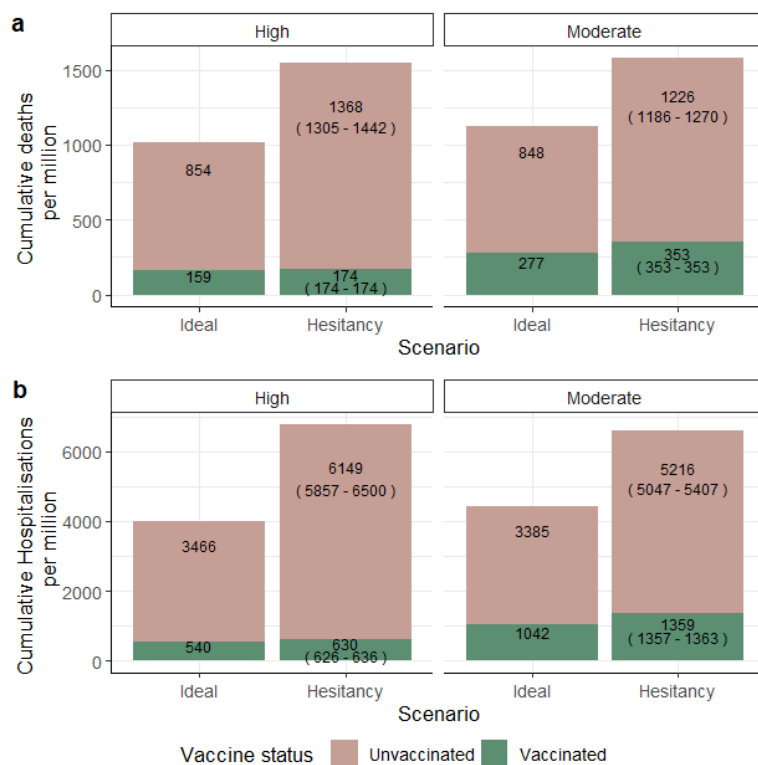
Figure 5. 4 Public health impact of vaccine hesitancy. *High vaccine efficacy is shown on the left and moderate vaccine efficacy on the right. The annotated numbers are the cumulative deaths **(a)** and hospitalisations **(b)** per million individuals for the vaccinated and unvaccinated populations at the end of the projection horizon (1 January 2021 - 31 December 2022). Vaccination coverage of individuals aged 15 years and older is highest in the ideal scenario at 95%. For the hesitancy scenario annotated number is for median vaccine coverage per age group, number in parenthesis are results for 10% and 90% quantiles coverage per age group.*

5.3.2 Relaxation of NPIs

As an alternative way to assess the impact of vaccine hesitancy on the pandemic, I evaluated the degree to which other NPIs would need to remain in place given the real-time achieved vaccine coverage in order to prevent further epidemics (i.e. maintain herd immunity threshold, **Figure 5. 5**). For the high efficacy vaccine, under the ideal scenario, simulations predict that NPIs could be fully lifted by the end of 2021 whilst keeping transmission under control (**Figure 5. 6**). However, under the vaccine hesitancy scenario, limited NPIs or other behavioural modifications might need to remain in place, with Rt having to stay below 2.05 (1.96-2.14) to prevent further epidemics, this represents a 32% reduction of the assumed R0 of 3. A difference of ~35% in the effective reproductive number could represent the closure of educational institutions or limiting interaction between households to achieve control of the epidemic (Brauner et al., 2021); both of which are not sustainable or desirable.
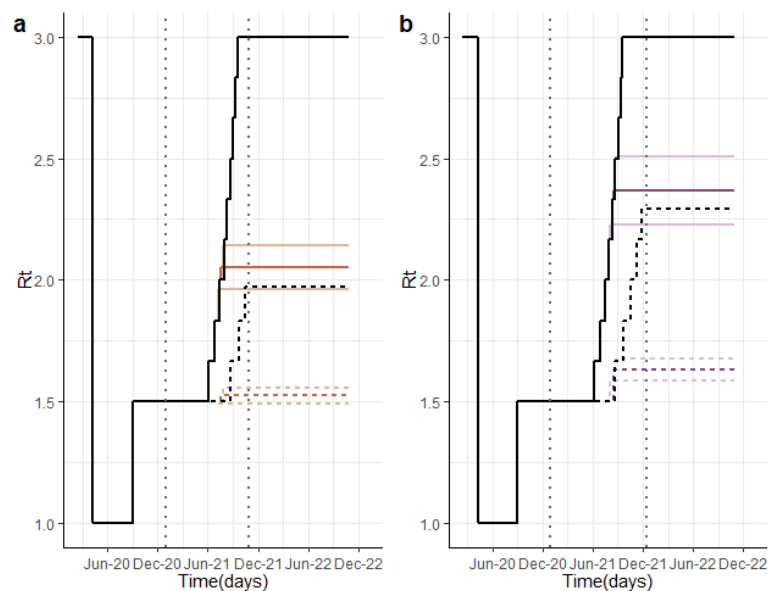
Figure 5. 5 Stringency of NPIs required to control the epidemic under different vaccine hesitancy scenarios. Panel a shows Rt profiles for an adults-only vaccination campaign. Panel b shows Rt profiles for a vaccination campaign including children. Reproductive number profiles are estimated to keep the herd immunity threshold such that epidemic impact is the same for each scenario as in the ideal scenario. A lower reproductive number corresponds to more stringent NPIs. Continuous lines represent profiles for a high efficacy vaccine and dashed lines represent profiles for a moderate efficacy vaccine. Vertical dotted lines show the period of vaccination in the ideal scenario.
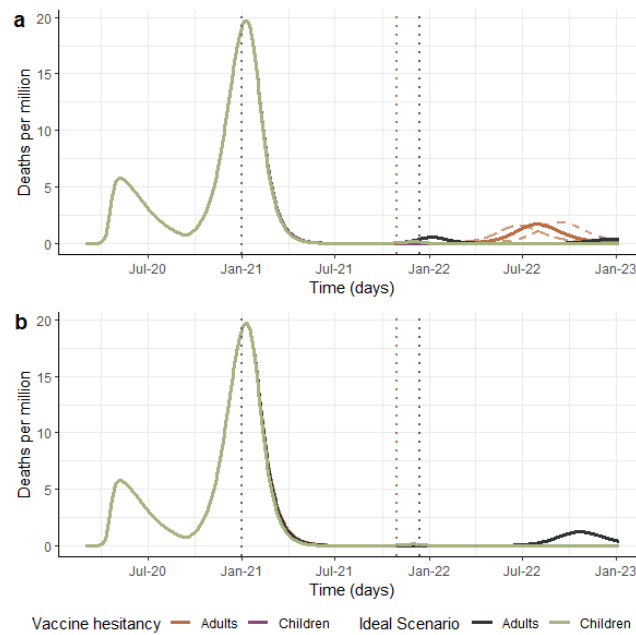
Figure 5. 6 COVID-19 dynamics for different reproductive number profiles. *Profiles were estimated for each vaccine hesitancy scenario in order to achieve herd immunity and control the pandemic. **a)** Daily projected deaths per million for a high vaccine efficacy. **b)** Daily projected deaths per million for a moderate vaccine efficacy. Orange shows a scenario with vaccine hesitancy and adults-only vaccination. Purple shows scenario with vaccine hesitancy and vaccination including children Ideal scenario. Ideal scenario for adults-only vaccination is shown with a black line shows and for a vaccination including children is shown with a green line. Continuous lines show results for median vaccine coverage per age group and dashed lines show results for 10% and 90% quantiles.*

5.3.3 Vaccination of children

During the development of this Chapter, vaccination rollout plan of adults was going swiftly in most high-income countries and public health authorities were looking to include children into their vaccination campaigns while results of COVID-19 vaccine efficacy in children became available (Mahase, 2021). To evaluate the impact of including children in vaccination rollouts, I model all scenarios with a longer vaccination campaign, which allowed individuals above 5 years old to get vaccinated, assuming vaccine hesitancy for 5-17 years old the same levels reported for 18-24 years old. If children are included in vaccine rollout, results illustrate that in a scenario with vaccine hesitancy daily deaths per million at the peak of the first outbreak could be reduced by 56% (51%-60%) for a vaccine with high efficacy (**Figure 5. 3b**). Which implies a total reduction of 272 (242-346) deaths per million in the two years after vaccination begins (**Figure 5. 7**). For a moderate vaccine efficacy, higher NPIs stringency at the end of vaccine rollout entails later outbreaks, which do not take place during the two years after vaccination begins, resulting in similar results for the ideal and vaccine hesitancy

scenario when including the vaccination of children (**Figure 5. 3d**). Including children in vaccine rollout leads to higher vaccine coverage that compensates for vaccine hesitancy levels in adults. This is evident when evaluating the degree to which other NPIs would need to remain in place in order to maintain the herd immunity threshold based on vaccine-acquired immunity levels. For a high efficacy vaccine, in a vaccine hesitancy scenario, Rt levels can increase up to 2.5 (**Figure 5. 5b**), ~20% more than for adult-only vaccination rollout. This increase entails milder NPIs at the end of the vaccination campaign.
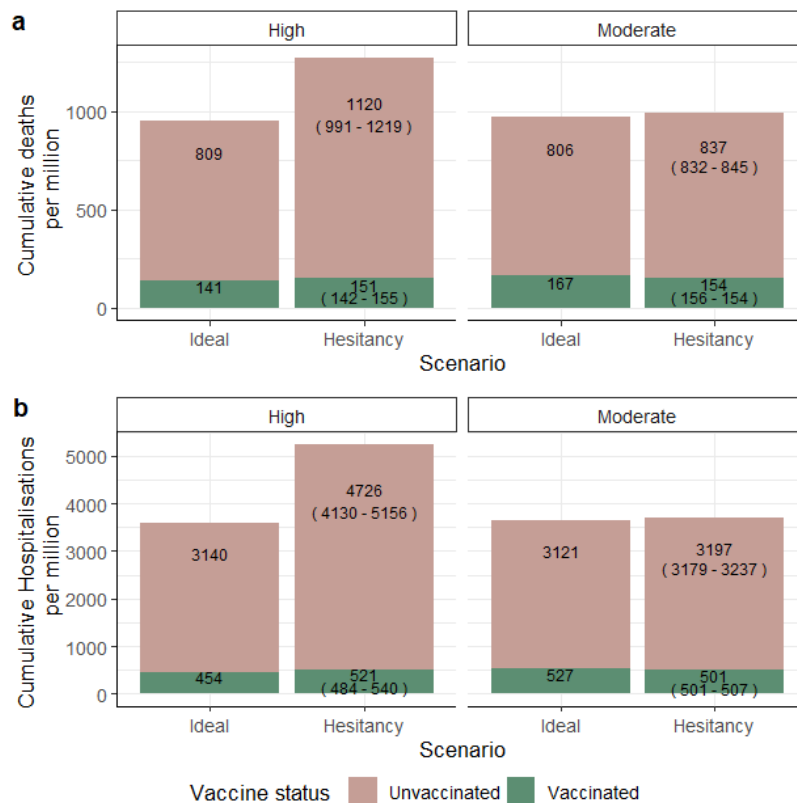
Figure 5. 7 Public health impact of vaccine hesitancy for a vaccine roll out including children. *High vaccine efficacy is shown on the left and moderate vaccine efficacy on the right.* *The annotated numbers are the cumulative deaths* *(a)* *and hospitalisations* *(b)* *per million individuals for the vaccinated and unvaccinated populations at the end of the projection horizon (1 January 2021 - 31 December 2022). Vaccination coverage of individuals aged 5 years and older is highest in the ideal scenario at 95%. For the hesitancy scenario annotated number is for median vaccine coverage per age group, number in parenthesis are results for 10% and 90% quantiles coverage per age group.*

5.3.4   Country specific simulations

The representative scenarios described above are comparable to the waves of COVID-19 outbreaks in Europe. However, as explained in Chapter 4 vaccine hesitancy varies between countries. To evaluate the impact of these variations, I chose three European countries with different vaccine acceptance views: France, Germany, and the United Kingdom (UK) (**Figure 5. 8b**). For each country, I extracted Rt

trajectories up to December 31sr 2020 and I modelled the trajectory of the pandemic under an ideal vaccination and a vaccine hesitancy scenario for each country independently. Rt profiles for each country are shown in **Figure 5. 8c**.
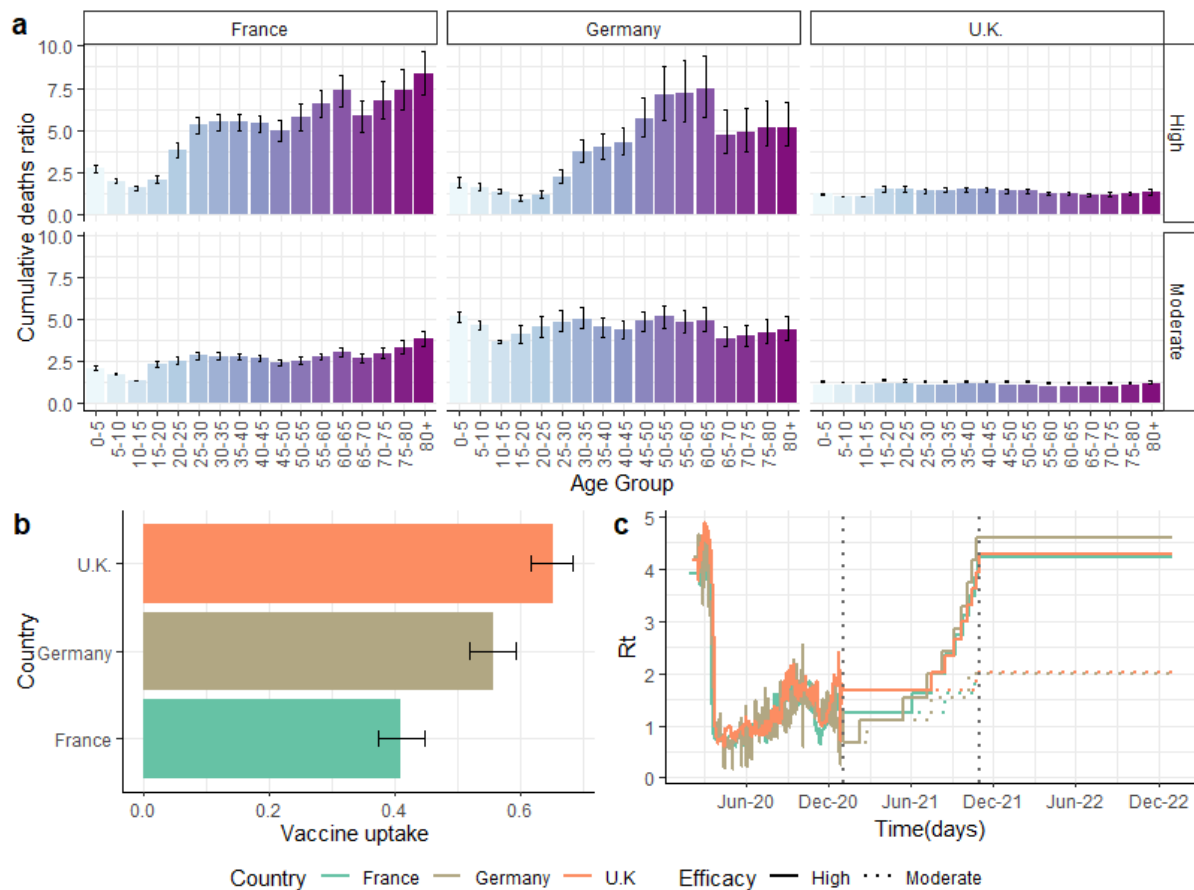
Figure 5. 8 Impact of vaccine hesitancy for three European countries. a) Cumulative death ratios per age group compared to the ideal vaccine uptake scenario, by country and vaccine efficacy profile. The ratio compares cumulative deaths projected over a two-year period after vaccination starts for two scenarios: An ideal scenario, where 95% of the population older than 15 years gets vaccinated and a vaccine hesitancy scenario, where coverage for people over 15 years old is based on vaccine acceptance from *b)* Reported vaccine acceptance per age group in France, Germany and the United Kingdom reproduced from Jones et al.(Jones et al., 2021) Values show median vaccine coverage and bars show 10-90% quantiles obtained by running the model at the quantiles from the data.. *c)* Reproductive number profile for country specific simulations. Profiles, before vaccination begins, are taken from model fittings to country-specific data (MRC Centre for Global Infectious Disease Analysis, 2020). After vaccination starts, NPIs are lifted based on an ideal vaccination coverage over time. Reproductive number is set to increase in ten steps from the value at the beginning of vaccination to an average initial reproductive number. Continuous lines show profiles for a high efficacy vaccine. Dotted lines show profiles for a moderate efficacy vaccine.

For a vaccine with high efficacy, I project 1.2 (1.1-1.3), 5.0 (4.0- 6.3)- and 6.6 (5.7-7.6) times more deaths in 2021/2022 in a scenario with hesitancy compared to an ideal scenario in the UK, Germany and France respectively (**Figure 5. 8a**). Death ratios vary between age groups, vaccine efficacy and countries depending on deaths predicted in their corresponding ideal scenarios. Nonetheless, for both high and moderate vaccine efficacy, the highest impact on total deaths is for the oldest age groups and it increases in countries with higher vaccine hesitancy (**Figure 5. 9** and **Figure 5. 10**).

Figure 5. 9 Predicted COVID-19 dynamics for each country for a high efficacy vaccine. a) *Daily projected deaths per million. Black line shows an ideal scenario without vaccine hesitancy and 95% of individuals above 15 years old, are vaccinated. Purple shows scenario with vaccine hesitancy. Continuous lines show results for median vaccine coverage per age group and shadowed area show upper and lower bounds for 10% and 90% quantile for vaccination coverage.* ***b)*** *Total deaths per age group for median vaccination coverage. Total deaths are estimated over a two-year period since vaccination starts. Vertical dotted lines show vaccination period for an ideal scenario.*
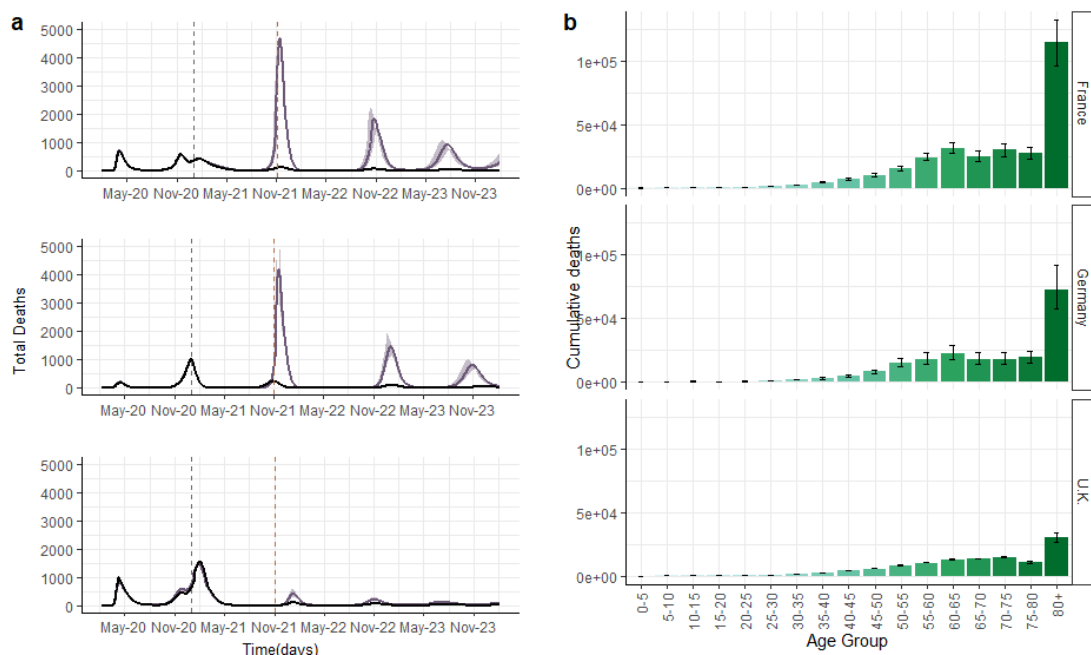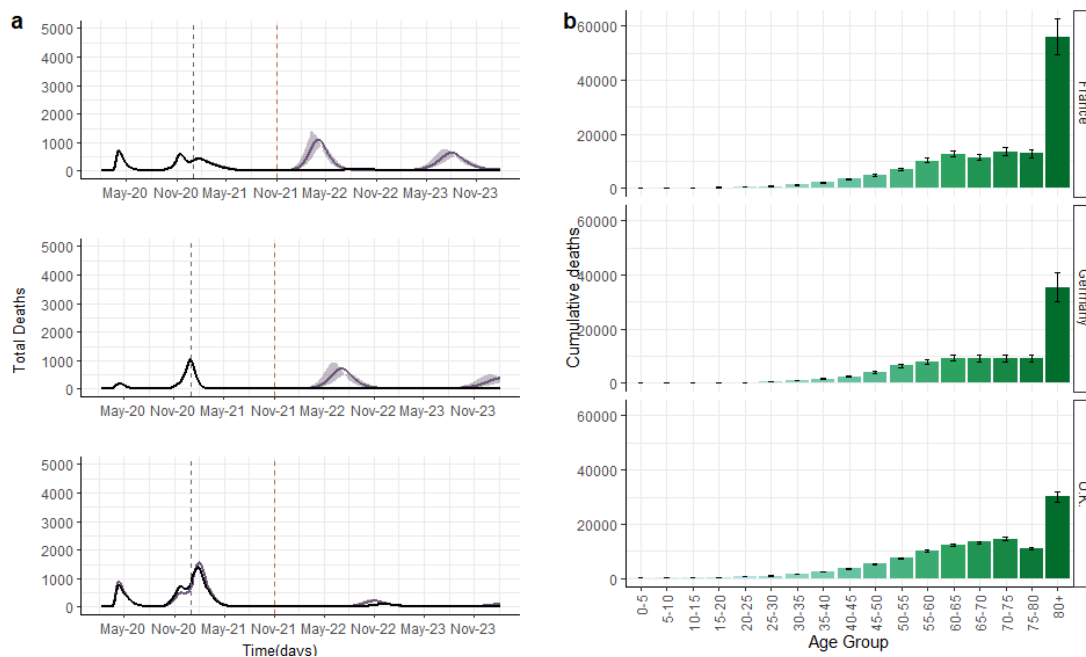
Figure 5. 10 Predicted COVID-19 dynamics for each country for a moderate efficacy vaccine. a) *Daily projected deaths per million. Black line shows an ideal scenario without vaccine hesitancy and 95% of individuals above 15 years old, are vaccinated. Purple shows scenario with vaccine hesitancy. Continuous lines show results for median vaccine coverage per age group and shadowed area show upper and lower bounds for 10% and 90% quantile vaccination coverage.* **b)** *Total deaths per age group for median vaccination coverage. Total deaths are estimated over a two-year period since vaccination starts. Vertical dotted lines show the period of vaccination in the ideal scenario.*

5.4 Discussion

In this Chapter, I have examined the effects of low vaccine uptake due to vaccine hesitancy for the current COVID-19 pandemic and have shown the substantial impact of vaccine hesitancy, detailing the considerable mortality that could be averted with increased vaccine coverage. Results presented here have demonstrated that including less vulnerable groups, like children, can reduce the impact of vaccine hesitancy for current vaccination campaigns. These results further support the idea of the indirect benefits of vaccination, which are necessary to achieve herd immunity (Bonsall et al., 2021, Hogan et al., 2021). However, the control of the pandemic as a reduction of severe cases (i.e., hospitalisations) and mortality, does not only depend on vaccine uptake but on vaccine efficacy and stringency levels of NPIs (Hogan et al., 2021, Bubar et al., 2021, Moore et al., 2021), which I have represented as underlying transmissibility (Rt). Simulation outputs confirm that vaccination alone is unlikely to control the current pandemic and NPIs still have a large impact on the epidemic trajectories until sufficient coverage is reached (Giordano et al., 2021). In a scenario with lower vaccine efficacy and vaccine hesitancy, longer and more stringent NPIs would be required to compensate lower efficacy as higher coverage levels are required to achieve herd immunity (Bonsall et al., 2021).

The model structure presented here was able to capture vaccine hesitancy heterogeneity between age groups (Jones et al., 2020, Lazarus et al., 2021, Freeman et al., 2020) and analyse its effect in current vaccine rollout plans, which are prioritising older individuals. I have shown that even though older age groups have higher vaccine acceptance levels, these groups have higher mortality in a vaccine hesitancy scenario. As the model does not capture differential risk within sub-populations, it was not possible to assess the effect of vaccine hesitancy in other prioritised populations like health care workers. In which high levels of vaccine hesitancy have been reported despite having higher risk of infection (Biswas et al., 2021).

Country specific Rt profiles are higher compared to the illustrative example. These values are consistent with those estimated for other European countries, where initial Rt values have been estimated as high as ~4.5, which may be due to possible under-ascertainment in deaths in early periods of the pandemics (Flaxman et al., 2020). It is still unknown how transmission levels will develop in the long term as more transmissible variants have emerged and NPIs behaviour may persist after the pandemic. Here I have assumed a staged release of NPIs with a step-wise increase of Rt, representing governments' easing of restrictions. This step function is a simplification to illustrate the process of balancing the relaxation of NPIs whilst continuing to suppress transmission. Nonetheless, the evaluation approaches introduced in this study can be adjusted to include complex Rt dynamics as more information on COVID-19 transmissibility evolution become available.

The analysis in this Chapter necessarily makes many simplifying assumptions, and it is important to note that the future trajectory of the epidemic will depend on the complex interactions between vaccination uptake, behaviour, and government interventions. First, I have assumed homogenous mixing between vaccine hesitant individuals. However, as has been seen for other diseases, COVID-19 vaccine hesitancy is heterogeneous and clustered within population subgroups (de Figueiredo, 2020). Transmission is more likely to be sustained within clusters with low vaccine coverage (Truelove et al., 2019, Salathé and Bonhoeffer, 2008). In Chapter 4 I demonstrated that when modelling vaccine hesitancy in a heterogeneous population, mixing between pro and anti-vaccination individuals can have a significant impact on disease dynamics. If vaccine hesitant individuals are mostly isolated, therefore future outbreaks may be limited to these sub-populations. Secondly, I have modelled

hesitancy levels constant over the time frame analysed; yet, self-reported attitudes to COVID-19 vaccines are changing over time (Jones et al., 2020, Lazarus et al., 2021) as the perceived risk for both disease and vaccines keeps varying (Moore et al., 2021, Larson and Broniatowski, 2021). Thirdly, I have assumed vaccination rate remains constant over the vaccination period. However, vaccination logistics depend on multidisciplinary factors (Wouters et al., 2021) and both vaccine availably and uptake can be dynamic. Finally, the model assumes vaccine induced life-long immunity and does not account for immune escape from the vaccine due to new variants arising. Current vaccines seem to protect against severe disease for most variants, yet the higher infectiousness reported for these new variants has accelerated booster programmes and raised herd immunity threshold goals (Anderson et al., 2021, Krause et al., 2021). Whilst second generation vaccines will likely become available to address these issues, it is currently unclear whether some of the high levels of vaccine uptake observed in early vaccine rollouts would be sustained in subsequent booster programmes.

Getting vaccinated is an individual choice, but these individual choices have population wide effects that are likely to challenge current efforts to control COVID-19. Findings from this Chapter suggest that vaccine hesitancy may have a substantial impact on the pandemic trajectory, deaths, and hospitalization. To prevent such adverse outcomes, NPIs would need to stay in place longer, or possibly indefinitely, resulting in high economic and social costs (Nicola et al., 2020, Mandel and Veetil, 2020). Reducing vaccine hesitancy is, therefore, an important public health priority. Interventions that aim to build trust, for example with community-based public education or via positive role models, are proven efficacious approaches to address hesitancy (Vergara et al., 2021). There is an ongoing debate about vaccine passports as a condition to travel, or a vaccination requirement for employees (Brown et al., 2021). Such interventions may be effective because they incentivize individuals to get vaccinated, but they are controversial in libertarian democracies because they curtail personal freedom and individual choice about medical treatments. The alternative will be to accept some level of disease, hospitalisation and deaths given the level of vaccine coverage achieved whilst allowing NPIs to be lifted, given that NPIs are not a sustainable long-term method for control.

Chapter 6 Discussion

6.1 Key findings and implications

The aim of this thesis was to investigate the trade-offs and economic optimisations of infectious disease control strategies in a heterogeneous population, integrating economic analysis and epidemiological tools. After developing a metapopulation framework to analyse heterogeneities and evaluate the health and economic impact of different control strategies, results from this thesis highlighted how the optimal approach for disease control varies between stakeholders. The approach that benefits a stakeholder the most and affects their decision to contribute to an intervention (e.g., invest in a prevention strategy, share resources, vaccinate), may generate positive or negative externalities to other involved parties and might interfere with public health goals. Estimating benefits for different actors can help to inform policymakers on how far to extend interventions or to find incentives for individuals/countries to take up an intervention.

Regional and global resource allocation are compared in Chapters 2 and 3. In Chapter 2, the concept of aligning goals is introduced after comparing three different vaccine allocation strategies. Results from both the SIS and SIR models illustrated that while keeping resources in low transmission patches improves welfare locally and might achieve elimination of the disease in those patches, it also increases disease burden globally. This concept is further explored in Chapter 3 for the malaria context. Optimisation results showed that current international funding allocations for malaria are aligned with the global optimal allocation strategy. Yet, this allocation may not be beneficial for low transmission settings, particularly if these are not well mixed with neighbouring populations. However, when there are high levels of mixing between populations, allocating resources to high transmission settings reduces the burden of malaria both locally and globally.

Elimination of malaria is a regional and global public good. Once a country eliminates malaria, the risk of importation to neighbouring countries is reduced facilitating the elimination path in those countries (Newby et al., 2016). The findings reported in Chapter 3 suggest that cooperation between countries would prevent importation of cases to near elimination country settings while reducing the burden of the disease in high transmission neighbouring countries. Currently, 68% of funding towards malaria comes from international donors like the Global Fund (World Health Organization, 2021d), which gives

most grant support to individual countries (although there are a few regional initiatives). However, the insights gained from this study support the need for cross-border funding to support a regional approach where countries are well connected and at different stages of the malaria elimination path.

Cooperation between different actors is important to achieve optimal disease control. In Chapters 4 and 5 I have evaluated the need for cooperation at the individual level, using vaccination as an intervention example. I demonstrated how decisions based on individual benefits could change considerably the course of transmission and hence the overall health burden. From the traditional economics perspective, an individual's demand for vaccination is associated with the marginal private benefits (MPB) of the intervention. In Chapter 2, my results illustrated how these MPB can differ significantly from marginal societal benefits (MSB), particularly at high vaccination coverages near the herd immunity threshold. As explained in Chapters 4 and 5, vaccine demand is also determined by social factors like trust in health authorities and perception of risks associated with the disease and vaccine risk perception of the disease and vaccine. These social factors amplify the difference between private and social benefits as more individuals decide not to vaccinate and rely on indirect protection from vaccinated individuals. Results from Chapters 4 and 5 demonstrated how this decision generates negative externalities, represented as substantial health and economic burden to society.

To reduce the negative externalities generated by vaccine hesitant individuals, policy interventions need to increase vaccine uptake using appropriate incentives to individuals. Currently, restrictions that limit access to places for the unvaccinated and monetary compensation have been implemented to encourage vaccination uptake in some places (Maltezou et al., 2019, Attwell and M, 2019). However, there remains a paucity of evidence on how these policies increase and sustain vaccination coverage (Salisbury, 2012). Theoretical analysis suggests that subsidising vaccination costs will counter vaccine hesitancy more efficiently than penalising anti-vaccination individuals through restrictions or fines (Gans, 2021). Additionally, understanding and addressing the reasons underlying vaccine hesitancy instead of implementing vaccine mandates has been suggested as an efficient long-term strategy to increase vaccine uptake (Dubé et al., 2018). Ensuring the appropriate response should be a priority to reduce the gap between individual and global goals. Otherwise, without appropriate incentives, considerable negative externalities are expected.

This thesis has provided a comprehensive assessment of the differences between actors' perspectives. Results from the individual and local perspectives are in accord with economic analyses that assess private perspectives, which may be narrow and underestimate the effects of interventions (Meltzer and Smith, 2011). I also evaluated the effects of interventions from the societal perspective. Results from these analyses account for all benefits regardless of to whom they accrue. However, they ignore the distribution of effects between the affected parties. Including multiple perspectives when analysing disease interventions can help increase engagement from all parties as decision makers can identify suitable incentives to align private and social net benefits (Meltzer and Smith, 2011).

In order to include a multi perspective analysis, I combined different epidemiological and economic methods. In Chapter 2, I integrated analyses of externalities and an epidemiological framework that represented heterogeneous transmission dynamics, which contributed towards the understanding of the role of externalities in vaccination policies. In Chapter 3, I used constrained optimisation to analyse real-world allocation challenges for the malaria context. Results from this Chapter provided a deeper insight into how to maximise health gain with limited health care resources. In Chapter 4, I conducted a cost analysis including both private and societal perspectives to estimate the burden of an emerging anti-vaccination population. This analysis established a quantitative framework for assessing the impact of individual free-riding on disease control programs, which was then explored in the context of the COVID-19 pandemic in Chapter 5.

Throughout this thesis, I was able to represent heterogeneous disease dynamics by adapting the metapopulation framework developed in Chapter 2. This framework was flexible enough to incorporate complex infection dynamics like malaria transmission and its structure was generalisable for different heterogeneity contexts such as various transmission intensities or intervention uptake levels. Additionally, simulation outputs from this framework were easily integrated into further analyses including constrained optimisations and economic analyses. The framework developed in this thesis was designed to be general, flexible, and adaptable to any disease and heterogeneity context. The methods used for this thesis may be applied to support public policy makers' analyses in order to improve infectious disease control planning.

6.2   Limitations and future work

There are several limitations to the approaches taken in this thesis. Even with the inclusion of heterogeneity with the metapopulation model, the mathematical models implemented in this work were a simplification of complex disease dynamics. As discussed in more depth in previous chapters, within each patch, transmission was assumed homogenous, and most parameters were assumed the same between patches. I have ignored model complications such as age heterogeneity in measles, transmission heterogeneity due to new SARS-CoV-2 variants or seasonal transmission in malaria given by climate patterns. The ability to make recommendations based on the results presented here is limited by these simplifications. Further modelling work can incorporate these complexities into the metapopulation framework in order to model more specific and realistic contexts.

Moreover, results from sensitivity analysis in Chapters 3 and 4 demonstrated disease trajectories are highly sensitive to the mixing parameters. In the metapopulation framework, the mixing matrix represents the coupling strength between sub-populations, which is a simplification of human movement patterns. Previous studies have shown that this simplification can overestimate the transmission rate of infection (Keeling et al., 2010). Therefore, great care is needed when interpreting the magnitude of results presented here. In order to model more realistic scenarios, and provide a useful tool for policymakers, further research is required to match the coupling strength matrix with complex human movement patterns.

In addition, the time horizon varied between the diseases and intervention analysed. When assessing future costs, implementing discount rates and optimising resource allocation, the time horizon of analyses becomes relevant, and results can change significantly if this horizon changes (Klepac et al., 2012, Meltzer and Smith, 2011). For instance, it has been demonstrated that the allocation of interventions that eradicate a disease may not be the same as the allocation that maximises health in the next couple of years (Brandeau, 2004). I evaluated the effect of malaria interventions at steady state, assessed costs of measles for 20 years and estimated the effect of vaccine hesitancy after two years for COVID-19. I selected each of these time windows, based on the natural history of infection, such that time impact of interventions could be evaluated by balancing out against future uncertainties, particularly for COVID-19, where the research landscape is evolving quickly. Additionally, when analysing future costs in Chapter 4, I evaluated different discount rates to estimate the effect of different discounting methods. Yet, results from this thesis must be interpreted with caution as they may be specific for the time window analysed.

Finally, an issue that was not addressed in depth in this study was whether the intervention strategies analysed were equitable. I have assumed constant and equal access to all interventions. However, policymakers face political and social challenges, which may invalidate this assumption and make allocation of interventions harder. Targeting resources to underserved populations like marginalised groups or hard to reach populations sometimes is not the most cost-effective solution or does not account for the greatest reduction in disease burden. Yet, governments still need to protect these populations (Dieleman and Haakenstad, 2015, Brandeau, 2004). The disparity in access is currently one of the main challenges in the policy response to the COVID-19 pandemic. While only 1.9% of individuals in LMIC have received at least one dose of vaccine, HIC have bought more doses than needed (Pilkington et al., 2022, Usher, 2021). Further work could extend the methodology proposed in this thesis to develop models to reflect inequity issues and understand their effect on control intervention plans.

6.3   Conclusions

In spite of the limitations mentioned above, this thesis provides a comprehensive assessment of epidemiological and economic aspects of disease preventive interventions. Results from this study highlighted the importance of considering different perspectives when assessing disease intervention strategies. For this, I developed a metapopulation framework that allows the estimation of the effects of interventions for different transmission strata. I was also able to adapt this framework to various disease dynamics and analyse specific challenges for the control of each disease. Although much of this work is theoretical, it may be used to guide future research questions and to provide an initial framework for analysing the trade-offs between different infectious disease control strategies.

References

ALTHOUSE, B. M., BERGSTROM, T. C. & BERGSTROM, C. T. 2010. A public choice framework for controlling transmissible and evolving diseases. *Proceedings of the National Academy of Sciences,* 107**,** 1696-1701.

ANDERSON, R. M., ANDERSON, B. & MAY, R. M. 1992. *Infectious diseases of humans: dynamics and control*, Oxford university press.

ANDERSON, R. M., VEGVARI, C., HOLLINGSWORTH, T. D., PI, L., MADDREN, R., NG, C. W. & BAGGALEY, R. F. 2021. The SARS-CoV-2 pandemic: remaining uncertainties in our understanding of the epidemiology and transmission dynamics of the virus, and challenges to be overcome. *Interface Focus,* 11**,** 20210008.

ATTWELL, K. & M, C. N. 2019. Childhood Vaccination Mandates: Scope, Sanctions, Severity, Selectivity, and Salience. *Milbank Q,* 97**,** 978-1014.

BADEN, L. R., EL SAHLY, H. M., ESSINK, B., KOTLOFF, K., FREY, S., NOVAK, R., DIEMERT, D., SPECTOR, S. A., ROUPHAEL, N., CREECH, C. B., MCGETTIGAN, J., KHETAN, S., SEGALL, N., SOLIS, J., BROSZ, A., FIERRO, C., SCHWARTZ, H., NEUZIL, K., COREY, L., GILBERT, P., JANES, H., FOLLMANN, D., MAROVICH, M., MASCOLA, J., POLAKOWSKI, L., LEDGERWOOD, J., GRAHAM, B. S., BENNETT, H., PAJON, R., KNIGHTLY, C., LEAV, B., DENG, W., ZHOU, H., HAN, S., IVARSSON, M., MILLER, J. & ZAKS, T. 2020. Efficacy and Safety of the mRNA-1273 SARS-CoV-2 Vaccine. *New England Journal of Medicine,* 384**,** 403-416.

BAKER, R. E., MAHMUD, A. S., MILLER, I. F., RAJEEV, M., RASAMBAINARIVO, F., RICE, B. L., TAKAHASHI, S., TATEM, A. J., WAGNER, C. E., WANG, L.-F., WESOLOWSKI, A. & METCALF, C. J. E. 2022. Infectious disease in an era of global change. *Nature Reviews Microbiology,* 20**,** 193-205.

BALL, F., BRITTON, T., HOUSE, T., ISHAM, V., MOLLISON, D., PELLIS, L. & SCALIA TOMBA, G. 2015. Seven challenges for metapopulation models of epidemics, including households models. *Epidemics,* 10**,** 63-67.

BAMBER, F., BURKE, M., CHAMBERS, M., JOBLING, S., TAYLOR, A. & MCDOUGALL, A. 2019. Investigation into pre-school vaccinations. *In:* OFFICE, N. A. (ed.). London.

BANHOLZER, N., VAN WEENEN, E., LISON, A., CENEDESE, A., SEELIGER, A., KRATZWALD, B., TSCHERNUTTER, D., SALLES, J. P., BOTTRIGHI, P., LEHTINEN, S., FEUERRIEGEL, S. & VACH, W. 2021. Estimating the effects of non-pharmaceutical interventions on the number of new infections with COVID-19 during the first epidemic wave. *PLOS ONE,* 16**,** e0252827.

BARRETT, S. 2004. Eradication versus control: the economics of global infectious disease policies. *Bulletin of the World Health Organization,* 82**,** 683-688.

BARRETT, S. 2006. The Smallpox Eradication Game. *Public Choice,* 130**,** 179-207.

BARRETT, S. 2013a. Economic considerations for the eradication endgame. *Philosophical Transactions of the Royal Society B: Biological Sciences,* 368**,** 20120149.

BARRETT, S. 2013b. Economic considerations for the eradication endgame. *Philosophical Transactions of the Royal Society B: Biological Sciences,* 368.

BATISTA, C., HOTEZ, P., AMOR, Y. B., KIM, J. H., KASLOW, D., LALL, B., ERGONUL, O., FIGUEROA, J. P., GURSEL, M., HASSANAIN, M., KANG, G., LARSON, H., NANICHE, D., SHEAHAN, T., WILDER-SMITH, A., SHOHAM, S., SOW, S. O., YADAV, P., STRUB-WOURGAFT, N., LOVEDAY, S.-J., HANNAY, E. & BOTTAZZI, M. E. 2022. The silent and dangerous inequity around access to COVID-19 testing: A call to action. *eClinicalMedicine,* 43.

BAUCH, C. T., BHATTACHARYYA, S. & BALL, R. F. 2010. Rapid Emergence of Free-Riding Behavior in New Pediatric Immunization Programs. *PLOS ONE,* 5**,** e12594.

BERNAL, J. L., ANDREWS, N., GOWER, C., STOWE, J., ROBERTSON, C., TESSIER, E., SIMMONS, R., COTTRELL, S., ROBERTS, R., O'DOHERTY, M., BROWN, K., CAMERON, C., STOCKTON, D., MCMENAMIN, J. & RAMSAY, M. 2021. Early effectiveness of COVID-19 vaccination with BNT162b2 mRNA vaccine and ChAdOx1 adenovirus vector vaccine on symptomatic disease, hospitalisations and mortality in older adults in England. *medRxiv***,** 2021.03.01.21252652.

BISWAS, N., MUSTAPHA, T., KHUBCHANDANI, J. & PRICE, J. H. 2021. The Nature and Extent of COVID-19 Vaccination Hesitancy in Healthcare Workers. *Journal of Community Health*.

BLOOM, D. E. & CADARETTE, D. 2019. Infectious Disease Threats in the Twenty-First Century: Strengthening the Global Response. *Frontiers in immunology,* 10**,** 549-549.

BONSALL, M. B., HUNTINGFORD, C. & RAWSON, T. 2021. Optimal time to return to normality: parallel use of COVID-19 vaccines and circuit breakers. *medRxiv***,** 2021.02.01.21250877.

BOULIER BRYAN, L., DATTA TEJWANT, S. & GOLDFARB ROBERT, S. 2007. Vaccination Externalities. *The B.E. Journal of Economic Analysis & Policy.*

BOUSEMA, T., STRESMAN, G., BAIDJOE, A. Y., BRADLEY, J., KNIGHT, P., STONE, W., OSOTI, V., MAKORI, E., OWAGA, C., ODONGO, W., CHINA, P., SHAGARI, S., DOUMBO, O. K., SAUERWEIN, R. W., KARIUKI, S., DRAKELEY, C., STEVENSON, J. & COX, J. 2016. The Impact of Hotspot-Targeted Interventions on Malaria Transmission in Rachuonyo South District in the Western Kenyan Highlands: A Cluster-Randomized Controlled Trial. *PLOS Medicine,* 13**,** e1001993.

BRANDEAU, M. L. 2004. Allocating Resources to Control Infectious Diseases. *In:* BRANDEAU, M. L., SAINFORT, F. & PIERSKALLA, W. P. (eds.) *Operations Research and Health Care: A Handbook of Methods and Applications.* Boston, MA: Springer US.

BRANDEAU, M. L., ZARIC, G. S. & RICHTER, A. 2003. Resource allocation for control of infectious diseases in multiple independent populations: beyond cost-effectiveness analysis. *Journal of Health Economics,* 22**,** 575-598.

BRAUNER, J. M., MINDERMANN, S., SHARMA, M., JOHNSTON, D., SALVATIER, J., GAVENČIAK, T., STEPHENSON, A. B., LEECH, G., ALTMAN, G., MIKULIK, V., NORMAN, A. J., MONRAD, J. T., BESIROGLU, T., GE, H., HARTWICK, M. A., TEH, Y. W., CHINDELEVITCH, L., GAL, Y. & KULVEIT, J. 2021. Inferring the effectiveness of government interventions against COVID-19. *Science,* 371**,** eabd9338.

BROWN, R. C. H., KELLY, D., WILKINSON, D. & SAVULESCU, J. 2021. The scientific and ethical feasibility of immunity passports. *The Lancet Infectious Diseases,* 21**,** e58-e63.

BUBAR, K. M., REINHOLT, K., KISSLER, S. M., LIPSITCH, M., COBEY, S., GRAD, Y. H. & LARREMORE, D. B. 2021. Model-informed COVID-19 vaccine prioritization strategies by age and serostatus. *Science,* 371**,** 916-921.

BURKI, T. K. 2022. Omicron variant and booster COVID-19 vaccines. *The Lancet Respiratory Medicine,* 10**,** e17.

CARANDE-KULIS, V. G., GETZEN, T. E. & THACKER, S. B. 2007. Public goods and externalities: a research agenda for public health economics. *J Public Health Manag Pract,* 13**,** 227-32.

CDC. 2020. *Measles Cases and Outbreaks* [Online]. Available: https://www.cdc.gov/measles/cases-outbreaks.html [Accessed September 01 2020].

CHANG, H.-H., CHANG, M.-C., KIANG, M., MAHMUD, A. S., EKAPIRAT, N., ENGØ-MONSEN, K., SUDATHIP, P., BUCKEE, C. O. & MAUDE, R. J. 2021. Low parasite connectivity among three malaria hotspots in Thailand. *Scientific Reports,* 11**,** 23348.

CHAUDHURI, S., KUMAR DWIBEDI, J. & BISWAS, A. 2017. Subsidizing healthcare in the presence of market distortions. *Economic Modelling,* 64**,** 539-552.

CHEN, X. & FU, F. 2019. Imperfect vaccine and hysteresis. *Proceedings of the Royal Society B: Biological Sciences,* 286**,** 20182406.

CITRON, D. T., GUERRA, C. A., DOLGERT, A. J., WU, S. L., HENRY, J. M., SÁNCHEZ, C. H. & SMITH, D. L. 2021. Comparing metapopulation dynamics of infectious diseases under different models of human movement. *Proc Natl Acad Sci U S A,* 118.

CLAXTON, K., MARTIN, S., SOARES, M., RICE, N., SPACKMAN, E., HINDE, S., DEVLIN, N., SMITH, P. C. & SCULPHER, M. 2015. Methods for the estimation of the National Institute for Health and Care Excellence cost-effectiveness threshold. *Health Technol Assess,* 19**,** 1-503, v-vi.

COLDIRON, M. E., VON SEIDLEIN, L. & GRAIS, R. F. 2017. Seasonal malaria chemoprevention: successes and missed opportunities. *Malaria Journal,* 16**,** 481.

COLIZZA, V. & VESPIGNANI, A. 2008. Epidemic modeling in metapopulation systems with heterogeneous coupling pattern: Theory and simulations. *Journal of Theoretical Biology,* 251**,** 450-467.

COOK, J., JEULAND, M., MASKERY, B., LAURIA, D., SUR, D., CLEMENS, J. & WHITTINGTON, D. 2009. Using private demand studies to calculate socially optimal vaccine subsidies in developing countries. *J Policy Anal Manage,* 28**,** 6-28.

COTTER, C., STURROCK, H. J. W., HSIANG, M. S., LIU, J., PHILLIPS, A. A., HWANG, J., GUEYE, C. S., FULLMAN, N., GOSLING, R. D. & FEACHEM, R. G. A. 2013. The changing epidemiology of malaria elimination: new strategies for new challenges. *The Lancet,* 382**,** 900-911.

DE FIGUEIREDO, A. 2020. Sub-national forecasts of COVID-19 vaccine acceptance across the UK: a large-scale cross-sectional spatial modelling study. *medRxiv.*

DE FIGUEIREDO, A., SIMAS, C., KARAFILLAKIS, E., PATERSON, P. & LARSON, H. J. 2020. Mapping global trends in vaccine confidence and investigating barriers to vaccine uptake: a large-scale retrospective temporal modelling study. *The Lancet,* 396**,** 898-908.

DEKA, A. & BHATTACHARYYA, S. 2019. Game dynamic model of optimal budget allocation under individual vaccination choice. *J Theor Biol,* 470**,** 108-118.

DIEKMANN, O., HEESTERBEEK, J. A. & ROBERTS, M. G. 2010. The construction of next-generation matrices for compartmental epidemic models. *J R Soc Interface,* 7**,** 873-85.

DIELEMAN, J. L. & HAAKENSTAD, A. 2015. The complexity of resource allocation for health. *The Lancet Global Health,* 3**,** e8-e9.

DIXON, M. G., FERRARI, M., ANTONI, S., XI LI, M., PORTNOY, A., LAMBERT, B., HAURYSKI, S., HATCHER, C., NEDELEC, Y., PATEL, M., ALEXANDER, J. P., STEULET, C., GACIC-DOBO, M., ROTA, P. A., MULDERS, M. N., BOSE, A. S., ROSEWELL, A., KRETSINGER, K. & CROWCROFT, N. S. 2021. Progress Toward Regional Measles Elimination — Worldwide, 2000–2020. *In:* REP, M. M. M. W. (ed.) *MMWR Morb Mortal Wkly Rep* Centers for Disease Control and Prevention.

DRAKE, T. L., LUBELL, Y., KYAW, S. S., DEVINE, A., KYAW, M. P., DAY, N. P. J., SMITHUIS, F. M. & WHITE, L. J. 2017. Geographic Resource Allocation Based on Cost Effectiveness: An Application to Malaria Policy. *Appl Health Econ Health Policy,* 15**,** 299-306.

DRUMMOND, M. F., SCULPHER, M. J., CLAXTON, K., STODDART, G. L. & TORRANCE, G. W. 2015. *Methods for the Economic Evaluation of Health Care Programmes,* Oxford, Oxford: Oxford University Press.

DUBÉ, E., GAGNON, D., MACDONALD, N., BOCQUIER, A., PERETTI-WATEL, P. & VERGER, P. 2018. Underlying factors impacting vaccine hesitancy in high income countries: a review of qualitative studies. *Expert Review of Vaccines,* 17**,** 989-1004.

DUBÉ, E., GAGNON, D. & VIVION, M. 2020. Optimizing communication material to address vaccine hesitancy. *Can Commun Dis Rep,* 46**,** 48-52.

DUBÉ, E. & MACDONALD, N. E. 2020. How can a global pandemic affect vaccine hesitancy? *Expert Review of Vaccines,* 19**,** 899-901.

DUINTJER TEBBENS, R. J., PALLANSCH, M. A., COCHI, S. L., WASSILAK, S. G., LINKINS, J., SUTTER, R. W., AYLWARD, R. B. & THOMPSON, K. M. 2010. Economic analysis of the global polio eradication initiative. *Vaccine,* 29**,** 334-43.

DUINTJER TEBBENS, R. J., PALLANSCH, M. A., COCHI, S. L., WASSILAK, S. G. & THOMPSON, K. M. 2015. An economic analysis of poliovirus risk management policy options for 2013-2052. *BMC Infect Dis,* 15**,** 389.

EDMUNDS, W. J. & VAN HOEK, A. J. 2009. The impact of increasing vaccine coverage on the distribution of disease: measles in the UK. *Reducing differences in the uptake of immunisations: Economic analysis 1.* National Institute for Health Care Excellence

EUROPEAN MEDICINES AGENCY. 2022. *COVID-19 treatments: authorised* [Online]. Netherlands. Available: https://www.ema.europa.eu/en/human-regulatory/overview/public-health-threats/coronavirus-disease-covid-19/treatments-vaccines/treatments-covid-19/covid-19-treatments-authorised [Accessed 04 May 2022].

FARINE, D. 2016. assortnet: Calculate the Assortativity Coefficient of Weighted and Binary Networks. 0.12 ed.

FEACHEM, R., PHILLIPS, A. & TARGETT, G. 2009. *Shrinking the Malaria Map: A Prospectus on Malaria Elimination,* United States of America, The Global Health Group, Global Health Sciences, University of California.

FERRARI, M. J., GRAIS, R. F., BHARTI, N., CONLAN, A. J. K., BJØRNSTAD, O. N., WOLFSON, L. J., GUERIN, P. J., DJIBO, A. & GRENFELL, B. T. 2008. The dynamics of measles in sub-Saharan Africa. *Nature,* 451**,** 679.

FITZJOHN, R. & FISCHER, T. 2022. odin: ODE Generation and Integration. 1.3.3 ed.

FITZPATRICK, T. & BAUCH, C. T. 2011. The potential impact of immunization campaign budget re-allocation on global eradication of paediatric infectious diseases. *BMC Public Health,* 11**,** 739.

FLAXMAN, S., MISHRA, S., GANDY, A., UNWIN, H. J. T., MELLAN, T. A., COUPLAND, H., WHITTAKER, C., ZHU, H., BERAH, T., EATON, J. W., MONOD, M., PEREZ-GUZMAN, P. N., SCHMIT, N., CILLONI, L., AINSLIE, K. E. C., BAGUELIN, M., BOONYASIRI, A., BOYD, O., CATTARINO, L., COOPER, L. V., CUCUNUBÁ, Z., CUOMO-DANNENBURG, G., DIGHE, A., DJAAFARA, B., DORIGATTI, I., VAN ELSLAND, S. L., FITZJOHN, R. G., GAYTHORPE, K. A. M., GEIDELBERG, L., GRASSLY, N. C., GREEN, W. D., HALLETT, T., HAMLET, A., HINSLEY, W., JEFFREY, B., KNOCK, E., LAYDON, D. J., NEDJATI-GILANI, G., NOUVELLET, P., PARAG, K. V., SIVERONI, I., THOMPSON, H. A., VERITY, R., VOLZ, E., WALTERS, C. E., WANG, H., WANG, Y., WATSON, O. J., WINSKILL, P., XI, X., WALKER, P. G. T., GHANI, A. C., DONNELLY, C. A., RILEY, S., VOLLMER, M. A. C., FERGUSON, N. M., OKELL, L. C., BHATT, S. & IMPERIAL COLLEGE, C.-R. T. 2020. Estimating the effects of non-pharmaceutical interventions on COVID-19 in Europe. *Nature,* 584**,** 257-261.

FOLEGATTI, P. M., BITTAYE, M., FLAXMAN, A., LOPEZ, F. R., BELLAMY, D., KUPKE, A., MAIR, C., MAKINSON, R., SHERIDAN, J., ROHDE, C., HALWE, S., JEONG, Y., PARK, Y.-S., KIM, J.-O., SONG, M., BOYD, A., TRAN, N., SILMAN, D., POULTON, I., DATOO, M., MARSHALL, J., THEMISTOCLEOUS, Y., LAWRIE, A., ROBERTS, R., BERRIE, E., BECKER, S., LAMBE, T., HILL, A., EWER, K. & GILBERT, S. 2020. Safety and immunogenicity of a candidate Middle East respiratory syndrome coronavirus viral-vectored vaccine: a dose-escalation, open-label, non-randomised, uncontrolled, phase 1 trial. *The Lancet Infectious Diseases,* 20**,** 816-826.

FONKWO, P. N. 2008. Pricing infectious disease. The economic and health implications of infectious diseases. *EMBO reports,* 9 Suppl 1**,** S13-S17.

FREEMAN, D., LOE, B. S., CHADWICK, A., VACCARI, C., WAITE, F., ROSEBROCK, L., JENNER, L., PETIT, A., LEWANDOWSKY, S., VANDERSLOTT, S., INNOCENTI, S., LARKIN, M., GIUBILINI, A., YU, L.-M., MCSHANE, H., POLLARD, A. J. & LAMBE, S. 2020. COVID-19 vaccine hesitancy in the UK: the Oxford coronavirus explanations, attitudes, and narratives survey (Oceans) II. *Psychological Medicine***,** 1-15.

FUNK, S., DUNBAR, M. B.-N., PEARSON, C. A. B., CLIFFORD, S., JARVIS, C. & ROBERT, A. 2020. socialmixr: Social Mixing Matrices for Infectious Disease Modelling. 0.1.8 ed.

GANS, J. S. 2021. Vaccine Hesitancy, Passports and the Demand for Vaccination. *NBER Working Paper* National Bureau of Economic Research: National Bureau of Economic Research.

GARBER, A. M. & SCULPHER, M. J. 2011. Chapter Eight - Cost Effectiveness and Payment Policy. *In:* PAULY, M. V., MCGUIRE, T. G. & BARROS, P. P. (eds.) *Handbook of Health Economics.* Elsevier.

GERSOVITZ, M. 2011. The Economics of Infection Control. *Annual Review of Resource Economics,* 3**,** 277-296.

GERSOVITZ, M. & HAMMER, J. S. 2003. The Economical Control of Infectious Diseases. *The Economic Journal,* 114**,** 1-27.

GHEBREHEWET, S., THORRINGTON, D., FARMER, S., KEARNEY, J., BLISSETT, D., MCLEOD, H. & KEENAN, A. 2016. The economic cost of measles: Healthcare, public health and societal costs of the 2012-13 outbreak in Merseyside, UK. *Vaccine,* 34**,** 1823-31.

GIAMBI, C., FABIANI, M., D'ANCONA, F., FERRARA, L., FIACCHINI, D., GALLO, T., MARTINELLI, D., PASCUCCI, M. G., PRATO, R., FILIA, A., BELLA, A., DEL MANSO, M., RIZZO, C. & ROTA, M. C. 2018. Parental vaccine hesitancy in Italy - Results from a national survey. *Vaccine,* 36**,** 779-787.

GIORDANO, G., COLANERI, M., DI FILIPPO, A., BLANCHINI, F., BOLZERN, P., DE NICOLAO, G., SACCHI, P., COLANERI, P. & BRUNO, R. 2021. Modeling vaccination rollouts, SARS-CoV-2 variants and the requirement for non-pharmaceutical interventions in Italy. *Nature Medicine,* 27**,** 993-998.

GLASSER, J. W., FENG, Z., OMER, S. B., SMITH, P. J. & RODEWALD, L. E. 2016. The effect of heterogeneity in uptake of the measles, mumps, and rubella vaccine on the potential for outbreaks of measles: a modelling study. *The Lancet Infectious Diseases,* 16**,** 599-605.

GOLDSTEIN, S., MACDONALD, N. E. & GUIRGUIS, S. 2015. Health communication and vaccine hesitancy. *Vaccine,* 33**,** 4212-4214.

GOODKIN-GOLD, M., KREMER, M., SNYDER, C. & WILLIAMS, H. 2020. Optimal Subsidies for Prevention of Infectious Disease. Centre for Economic Policy Research.: London.

GOSTIN, L. O., HODGE, J. G., BLOOM, B. R., EL-MOHANDES, A., FIELDING, J., HOTEZ, P., KURTH, A., LARSON, H. J., ORENSTEIN, W. A., RABIN, K., RATZAN, S. C. & SALMON, D. 2020. The public health crisis of underimmunisation: a global plan of action. *The Lancet Infectious Diseases,* 20**,** e11-e16.

GRENFELL, B. & HARWOOD, J. 1997. (Meta)population dynamics of infectious diseases. *Trends Ecol Evol,* 12**,** 395-9.

GRENFELL, B. T., BJØRNSTAD, O. N. & FINKENSTÄDT, B. F. 2002. DYNAMICS OF MEASLES EPIDEMICS: SCALING NOISE, DETERMINISM, AND PREDICTABILITY WITH THE TSIR MODEL. *Ecological Monographs,* 72**,** 185-202.

GRIFFIN, J. T., FERGUSON, N. M. & GHANI, A. C. 2014. Estimates of the changing age-burden of Plasmodium falciparum malaria disease in sub-Saharan Africa. *Nature Communications,* 5**,** 3136.

GRIFFIN, J. T., HOLLINGSWORTH, T. D., OKELL, L. C., CHURCHER, T. S., WHITE, M., HINSLEY, W., BOUSEMA, T., DRAKELEY, C. J., FERGUSON, N. M., BASÁÑEZ, M.-G. & GHANI, A. C. 2010a. Reducing Plasmodium falciparum Malaria Transmission in Africa: A Model-Based Evaluation of Intervention Strategies. *PLOS Medicine,* 7**,** e1000324.

GRIFFIN, J. T., HOLLINGSWORTH, T. D., OKELL, L. C., CHURCHER, T. S., WHITE, M., HINSLEY, W., BOUSEMA, T., DRAKELEY, C. J., FERGUSON, N. M., BASANEZ, M. G. & GHANI, A. C. 2010b. Reducing Plasmodium falciparum malaria transmission in Africa: a model-based evaluation of intervention strategies. *PLoS Med,* 7.

GUEYE, C. S., TENG, A., KINYUA, K., WAFULA, F., GOSLING, R. & MCCOY, D. 2012. Parasites and vectors carry no passport: how to fund cross-border and regional efforts to achieve malaria elimination. *Malaria Journal,* 11**,** 344.

GYRD-HANSEN, D. 2005. Willingness to pay for a QALY. *PharmacoEconomics,* 23**,** 423-432.

HALL, V., FOULKES, S., CHARLETT, A., ATTI, A., MONK, E., SIMMONS, R., WELLINGTON, E., COLE, M., SAEI, A., OGUTI, B., MUNRO, K., WALLACE, S., KIRWAN, P., SHROTRI, M., VUSIRIKALA, A., ROKADIYA, S., KALL, M., ZAMBON, M., RAMSAY, M., BROOKS, T., BROWN, C., CHAND, M. & HOPKINS, S. 2021. Do antibody positive healthcare workers have lower SARS-CoV-2 infection

rates than antibody negative healthcare workers? Large multi-centre prospective cohort study (the SIREN study), England: June to November 2020. *medRxiv***,** 2021.01.13.21249642.

HANSKI, I. & GAGGIOTTI, O. E. 2004. *Ecology, genetics and evolution of metapopulations,* Amsterdam

London, Academic.

HAUCK, K. 2018. The Economics of Infectious Diseases. Oxford University Press.

HELLEWELL, J., SLATER, H., UNWIN, J. & WATSON, O. 2022. ICDMM: Deterministic malaria odin model. 0.1.1 ed.

HICKSON, R. I. & ROBERTS, M. G. 2014. How population heterogeneity in susceptibility and infectivity influences epidemic dynamics. *Journal of Theoretical Biology,* 350**,** 70-80.

HITCHINGS, M. D. T., RANZANI, O. T., SCARAMUZZINI TORRES, M. S., DE OLIVEIRA, S. B., ALMIRON, M., SAID, R., BORG, R., SCHULZ, W. L., DE OLIVEIRA, R. D., DA SILVA, P. V., DE CASTRO, D. B., DE SOUZA SAMPAIO, V., CLÁUDIO DE ALBUQUERQUE, B., AMORIM RAMOS, T. C., HAUACHE FRAXE, S. H., DA COSTA, C. F., NAVECA, F. G., SIQUEIRA, A. M., DE ARAÚJO, W. N., ANDREWS, J. R., CUMMINGS, D. A. T., KO, A. I. & CRODA, J. 2021. Effectiveness of CoronaVac in the setting of high SARS-CoV-2 P.1 variant transmission in Brazil: A test-negative case-control study. *medRxiv***,** 2021.04.07.21255081.

HOFFER, A. J., SHUGHART, W. F. & THOMAS, M. D. 2014. Sin Taxes and Sindustry: Revenue, Paternalism, and Political Interest. *The Independent Review,* 19**,** 47-64.

HOGAN, A. B., WINSKILL, P., WATSON, O. J., WALKER, P. G. T., WHITTAKER, C., BAGUELIN, M., BRAZEAU, N. F., CHARLES, G. D., GAYTHORPE, K. A. M., HAMLET, A., KNOCK, E., LAYDON, D. J., LEES, J. A., LØCHEN, A., VERITY, R., WHITTLES, L. K., MUHIB, F., HAUCK, K., FERGUSON, N. M. & GHANI, A. C. 2021. Within-country age-based prioritisation, global allocation, and public health impact of a vaccine against SARS-CoV-2: A mathematical modelling analysis. *Vaccine*.

HOLZMANN, H., HENGEL, H., TENBUSCH, M. & DOERR, H. W. 2016. Eradication of measles: remaining challenges. *Med Microbiol Immunol,* 205**,** 201-8.

HOTEZ, P. J., NUZHATH, T. & COLWELL, B. 2020. Combating vaccine hesitancy and other 21st century social determinants in the global fight against measles. *Current Opinion in Virology,* 41**,** 1-7.

HUANG, F., LI, S.-G., TIAN, P., GUO, X.-R., XIA, Z.-G., ZHOU, S.-S., ZHOU, H.-N. & ZHOU, X.-N. 2021. A retrospective analysis of malaria epidemiological characteristics in Yingjiang County on the China–Myanmar border. *Scientific Reports,* 11**,** 14129.

JACKSON, L. A., ANDERSON, E. J., ROUPHAEL, N. G., ROBERTS, P. C., MAKHENE, M., COLER, R. N., MCCULLOUGH, M. P., CHAPPELL, J. D., DENISON, M. R., STEVENS, L. J., PRUIJSSERS, A. J., MCDERMOTT, A., FLACH, B., DORIA-ROSE, N. A., CORBETT, K. S., MORABITO, K. M., O'DELL, S., SCHMIDT, S. D., SWANSON, P. A., 2ND, PADILLA, M., MASCOLA, J. R., NEUZIL, K. M., BENNETT, H., SUN, W., PETERS, E., MAKOWSKI, M., ALBERT, J., CROSS, K., BUCHANAN, W., PIKAART-TAUTGES, R., LEDGERWOOD, J. E., GRAHAM, B. S. & BEIGEL, J. H. 2020. An mRNA Vaccine against SARS-CoV-2 - Preliminary Report. *N Engl J Med,* 383**,** 1920-1931.

JOHNSON, N. F., VELÁSQUEZ, N., RESTREPO, N. J., LEAHY, R., GABRIEL, N., EL OUD, S., ZHENG, M., MANRIQUE, P., WUCHTY, S. & LUPU, Y. 2020. The online competition between pro- and anti-vaccination views. *Nature,* 582**,** 230-233.

JOHNSON, S. G. 2022. The NLopt nonlinear-optimization package.

JONES, S. P., IMPERIAL COLLEGE LONDON & YOUGOV PLC 2020. Imperial College London YouGov Covid Data Hub. YouGov Plc.

JONES, S. P., IMPERIAL COLLEGE LONDON BIG DATA ANALYTICAL UNIT & YOUGOV PLC 2021. Imperial College London YouGov Covid Data Hub. 1.0 ed.: YouGov Plc.

KEELING, M. J., BJØRNSTAD, O. N. & GRENFELL, B. T. 2004. 17 - Metapopulation Dynamics of Infectious Diseases. *In:* HANSKI, I. & GAGGIOTTI, O. E. (eds.) *Ecology, Genetics and Evolution of Metapopulations.* Burlington: Academic Press.

KEELING, M. J., DANON, L., VERNON, M. C. & HOUSE, T. A. 2010. Individual identity and movement networks for disease metapopulations. *Proceedings of the National Academy of Sciences,* 107**,** 8866-8870.

KEELING, M. J. & ROHANI, P. 2008. *Modeling infectious diseases in humans and animals,* Princeton, N.J.

Woodstock, Princeton University Press.

KHADKA, A., PERALES, N. A., WEI, D. J., GAGE, A. D., HABER, N., VERGUET, S., PATENAUDE, B. & FINK, G. 2018. Malaria control across borders: quasi-experimental evidence from the Trans-Kunene malaria initiative (TKMI). *Malaria Journal,* 17**,** 224.

KIRBY, T. 2022. MMR vaccination in England falls below critical threshold. *The Lancet Infectious Diseases,* 22**,** 453.

KLEIN, E., LAXMINARAYAN, R., SMITH, D. L. & GILLIGAN, C. A. 2007. Economic incentives and mathematical models of disease. *Environment and Development Economics,* 12**,** 707-732.

KLEPAC, P., BJØRNSTAD, O. N., METCALF, C. J. E. & GRENFELL, B. T. 2012. Optimizing Reactive Responses to Outbreaks of Immunizing Infections: Balancing Case Management and Vaccination. *PLOS ONE,* 7**,** e41428.

KLEPAC, P., LAXMINARAYAN, R. & GRENFELL, B. T. 2011. Synthesizing epidemiological and economic optima for control of immunizing infections. *Proceedings of the National Academy of Sciences of the United States of America,* 108**,** 14366-14370.

KNERER, G., CURRIE, C. S. M. & BRAILSFORD, S. C. 2021. Reducing dengue fever cases at the lowest budget: a constrained optimization approach applied to Thailand. *BMC Public Health,* 21**,** 807.

KNIPL, D. 2016. A new approach for designing disease intervention strategies in metapopulation models. *J Biol Dyn,* 10**,** 71-94.

KRAUSE, P. R., FLEMING, T. R., PETO, R., LONGINI, I. M., FIGUEROA, J. P., STERNE, J. A. C., CRAVIOTO, A., REES, H., HIGGINS, J. P. T., BOUTRON, I., PAN, H., GRUBER, M. F., ARORA, N., KAZI, F., GASPAR, R., SWAMINATHAN, S., RYAN, M. J. & HENAO-RESTREPO, A.-M. 2021. Considerations in boosting COVID-19 vaccine immune responses. *The Lancet,* 398**,** 1377-1380.

LAI, S., SUN, J., RUKTANONCHAI, N. W., ZHOU, S., YU, J., ROUTLEDGE, I., WANG, L., ZHENG, Y., TATEM, A. J. & LI, Z. 2019. Changing epidemiology and challenges of malaria in China towards elimination. *Malaria Journal,* 18**,** 107.

LARSON, H. J. 2018. The state of vaccine confidence. *The Lancet,* 392**,** 2244-2246.

LARSON, H. J. & BRONIATOWSKI, D. A. 2021. Volatility of vaccine confidence. *Science,* 371**,** 1289-1289.

LAZARUS, J. V., RATZAN, S. C., PALAYEW, A., GOSTIN, L. O., LARSON, H. J., RABIN, K., KIMBALL, S. & EL-MOHANDES, A. 2021. A global survey of potential acceptance of a COVID-19 vaccine. *Nature Medicine,* 27**,** 225-228.

LEE, B. Y., BROWN, S. T., HAIDARI, L. A., CLARK, S., ABIMBOLA, T., PALLAS, S. E., WALLACE, A. S., MITGANG, E. A., LEONARD, J., BARTSCH, S. M., YEMEKE, T. T., ZENKOV, E. & OZAWA, S. 2019. Economic value of vaccinating geographically hard-to-reach populations with measles vaccine: A modeling application in Kenya. *Vaccine,* 37**,** 2377-2386.

LENZEN, M., LI, M., MALIK, A., POMPONI, F., SUN, Y.-Y., WIEDMANN, T., FATURAY, F., FRY, J., GALLEGO, B., GESCHKE, A., GÓMEZ-PAREDES, J., KANEMOTO, K., KENWAY, S., NANSAI, K., PROKOPENKO, M., WAKIYAMA, T., WANG, Y. & YOUSEFZADEH, M. 2020. Global socio-economic losses and environmental gains from the Coronavirus pandemic. *PLOS ONE,* 15**,** e0235654.

LI, A. & TOLL, M. 2021. Removing conscientious objection: The impact of 'No Jab No Pay' and 'No Jab No Play' vaccine policies in Australia. *Preventive Medicine,* 145**,** 106406.

LIU, Y. & ROCKLÖV, J. 2021. The reproductive number of the Delta variant of SARS-CoV-2 is far higher compared to the ancestral SARS-CoV-2 virus. *Journal of Travel Medicine,* 28.

LO, N. C. & HOTEZ, P. J. 2017. Public Health and Economic Consequences of Vaccine Hesitancy for Measles in the United States. *JAMA Pediatr,* 171**,** 887-892.

LOGUNOV, D. Y., DOLZHIKOVA, I. V., SHCHEBLYAKOV, D. V., TUKHVATULIN, A. I., ZUBKOVA, O. V., DZHARULLAEVA, A. S., KOVYRSHINA, A. V., LUBENETS, N. L., GROUSOVA, D. M., EROKHOVA, A. S., BOTIKOV, A. G., IZHAEVA, F. M., POPOVA, O., OZHAROVSKAYA, T. A., ESMAGAMBETOV, I. B., FAVORSKAYA, I. A., ZRELKIN, D. I., VORONINA, D. V., SHCHERBININ, D. N., SEMIKHIN, A. S., SIMAKOVA, Y. V., TOKARSKAYA, E. A., EGOROVA, D. A., SHMAROV, M. M., NIKITENKO, N. A., GUSHCHIN, V. A., SMOLYARCHUK, E. A., ZYRYANOV, S. K., BORISEVICH, S. V., NARODITSKY, B. S. & GINTSBURG, A. L. 2021. Safety and efficacy of an rAd26 and rAd5 vector-based heterologous prime-boost COVID-19 vaccine: an interim analysis of a randomised controlled phase 3 trial in Russia. *The Lancet*.

LOOMBA, S., DE FIGUEIREDO, A., PIATEK, S. J., DE GRAAF, K. & LARSON, H. J. 2021. Measuring the impact of COVID-19 vaccine misinformation on vaccination intent in the UK and USA. *Nature Human Behaviour*.

LOVE-KOH, J., ASARIA, M., COOKSON, R. & GRIFFIN, S. 2015. The Social Distribution of Health: Estimating Quality-Adjusted Life Expectancy in England. *Value in Health,* 18**,** 655-662.

LOVER, A. A., HARVARD, K. E., LINDAWSON, A. E., SMITH GUEYE, C., SHRETTA, R., GOSLING, R. & FEACHEM, R. 2017. Regional initiatives for malaria elimination: Building and maintaining partnerships. *PLoS Med,* 14**,** e1002401.

LSHTM VACCINE CENTRE. 2021. *COVID-19 vaccine tracker* [Online]. Available: https://vac-lshtm.shinyapps.io/ncov_vaccine_landscape/# [Accessed 18 February 2021].

MACDONALD, G. 1956. Epidemiological basis of malaria control. *Bulletin of the World Health Organization,* 15**,** 613-626.

MACDONALD, N. E. 2015. Vaccine hesitancy: Definition, scope and determinants. *Vaccine,* 33**,** 4161-4.

MAHARAJ, R., KISSOON, S., LAKAN, V. & KHESWA, N. 2019. Rolling back malaria in Africa - challenges and opportunities to winning the elimination battle. *S Afr Med J,* 109**,** 53-56.

MAHASE, E. 2021. Covid vaccine could be rolled out to children by autumn. *BMJ,* 372**,** n723.

MALTEZOU, H. C., LEDDA, C. & RAPISARDA, V. 2019. Mandatory vaccinations for children in Italy: The need for a stable frame. *Vaccine,* 37**,** 4419-4420.

MANDEL, A. & VEETIL, V. 2020. The Economic Cost of COVID Lockdowns: An Out-of-Equilibrium Analysis. *Economics of Disasters and Climate Change,* 4**,** 431-451.

MCCABE, C., CLAXTON, K. & CULYER, A. J. 2008. The NICE cost-effectiveness threshold: what it is and what that means. *Pharmacoeconomics,* 26**,** 733-44.

MELTZER, D. O. & SMITH, P. C. 2011. Chapter Seven - Theoretical Issues Relevant to the Economic Evaluation of Health Technologies. *In:* PAULY, M. V., MCGUIRE, T. G. & BARROS, P. P. (eds.) *Handbook of Health Economics.* Elsevier.

MIDEGA, J. T., MBOGO, C. M., MWNAMBI, H., WILSON, M. D., OJWANG, G., MWANGANGI, J. M., NZOVU, J. G., GITHURE, J. I., YAN, G. & BEIER, J. C. 2007. Estimating dispersal and survival of Anopheles gambiae and Anopheles funestus along the Kenyan coast by using mark-release-recapture methods. *J Med Entomol,* 44**,** 923-9.

MILLWARD, G. 2019. *Vaccinating Britain*, Manchester University Press.

MOONASAR, D., MAHARAJ, R., KUNENE, S., CANDRINHO, B., SAUTE, F., NTSHALINTSHALI, N. & MORRIS, N. 2016. Towards malaria elimination in the MOSASWA (Mozambique, South Africa and Swaziland) region. *Malaria Journal,* 15**,** 419.

MOORE, S., HILL, E. M., TILDESLEY, M. J., DYSON, L. & KEELING, M. J. 2021. Vaccination and non-pharmaceutical interventions for COVID-19: a mathematical modelling study. *The Lancet Infectious Diseases*.

MRC CENTRE FOR GLOBAL INFECTIOUS DISEASE ANALYSIS. 2020. *Global LMIC COVID-19 reports* [Online]. Available: https://mrc-ide.github.io/global-lmic-reports/ [Accessed].

MULLIGAN, M. J., LYKE, K. E., KITCHIN, N., ABSALON, J., GURTMAN, A., LOCKHART, S., NEUZIL, K., RAABE, V., BAILEY, R., SWANSON, K. A., LI, P., KOURY, K., KALINA, W., COOPER, D., FONTES-GARFIAS, C., SHI, P.-Y., TÜRECI, Ö., TOMPKINS, K. R., WALSH, E. E., FRENCK, R., FALSEY, A. R., DORMITZER, P. R., GRUBER, W. C., ŞAHIN, U. & JANSEN, K. U. 2020. Phase I/II study of COVID-19 RNA vaccine BNT162b1 in adults. *Nature,* 586**,** 589-593.

NATIONAL INSTITUTES OF HEALTH. 2022. *Antiviral Drugs That Are Approved, Authorized, or Under Evaluation for the Treatment of COVID-19* [Online]. Available: https://www.covid19treatmentguidelines.nih.gov/therapies/antiviral-therapy/summary-recommendations/ [Accessed 04/05/2022].

NDEFFO MBAH, M. L. & GILLIGAN, C. A. 2011. Resource Allocation for Epidemic Control in Metapopulations. *PLOS ONE,* 6**,** e24577.

NEWBY, G., BENNETT, A., LARSON, E., COTTER, C., SHRETTA, R., PHILLIPS, A. A. & FEACHEM, R. G. A. 2016. The path to eradication: a progress report on the malaria-eliminating countries. *The Lancet,* 387**,** 1775-1784.

NEWMAN, M. E. J. 2003. Mixing patterns in networks. *Physical Review E,* 67**,** 026126.

NHS 2019. Childhood Vaccination Coverage Statistics - England 2018-19. 26 September ed.

NHS. 2021. *COVID-19 Vaccinations* [Online]. Available: COVID-19 Vaccinations [Accessed March 2021].

NICOLA, M., ALSAFI, Z., SOHRABI, C., KERWAN, A., AL-JABIR, A., IOSIFIDIS, C., AGHA, M. & AGHA, R. 2020. The socio-economic implications of the coronavirus pandemic (COVID-19): A review. *International journal of surgery (London, England),* 78**,** 185-193.

NJAU, J., JANTA, D., STANESCU, A., PALLAS, S., PISTOL, A., KHETSURIANI, N., REEF, S., CIUREA, D., BUTU, C., WALLACE, A. & ZIMMERMAN, L. 2019. Assessment of Economic Burden of Concurrent Measles and Rubella Outbreaks, Romania, 2011–2012. *Emerging Infectious Disease journal,* 25**,** 1101.

NYBERG, T., FERGUSON, N. M., NASH, S. G., WEBSTER, H. H., FLAXMAN, S., ANDREWS, N., HINSLEY, W., BERNAL, J. L., KALL, M., BHATT, S., BLOMQUIST, P., ZAIDI, A., VOLZ, E., AZIZ, N. A., HARMAN, K., FUNK, S., ABBOTT, S., NYBERG, T., FERGUSON, N. M., NASH, S. G., WEBSTER, H. H., FLAXMAN, S., ANDREWS, N., HINSLEY, W., LOPEZ BERNAL, J., KALL, M., BHATT, S., BLOMQUIST, P., ZAIDI, A., VOLZ, E., ABDUL AZIZ, N., HARMAN, K., FUNK, S., ABBOTT, S., HOPE, R., CHARLETT, A., CHAND, M., GHANI, A. C., SEAMAN, S. R., DABRERA, G., DE ANGELIS, D., PRESANIS, A. M., THELWALL, S., HOPE, R., CHARLETT, A., CHAND, M., GHANI, A. C., SEAMAN, S. R., DABRERA, G., DE ANGELIS, D., PRESANIS, A. M. & THELWALL, S. 2022. Comparative analysis of the risks of hospitalisation and death associated with SARS-CoV-2 omicron (B.1.1.529) and delta (B.1.617.2) variants in England: a cohort study. *The Lancet,* 399**,** 1303-1312.

OECD 2022. Consumer Price Index of All Items in the United Kingdom [GBRCPIALLMINMEI]. FRED, Federal Reserve Bank of St. Louis.

ONS, O. O. N. S. 2019. *Births in England and Wales: 2018* [Online]. Available: https://www.ons.gov.uk/peoplepopulationandcommunity/birthsdeathsandmarriages/livebirths/bulletins/birthsummarytablesenglandandwales/2018 [Accessed February 13 2020].

ORABY, T. & BAUCH, C. T. 2015. Bounded rationality alters the dynamics of paediatric immunization acceptance. *Sci Rep,* 5**,** 10724.

OUR WORLD IN DATA. 2022. *COVID-19 Data Explorer* [Online]. Available: https://ourworldindata.org/explorers/coronavirus-data-explorer?zoomToSelection=true&facet=none&hideControls=true&Metric=Confirmed+cases&Interval=Cumulative&Relative+to+Population=false&Color+by+test+positivity=false&country=~OWID_WRL [Accessed 04 May 2022].

PAULES, C. I., MARSTON, H. D. & FAUCI, A. S. 2019a. Measles in 2019 — Going Backward. *New England Journal of Medicine,* 380**,** 2185-2187.

PAULES, C. I., MARSTON, H. D. & FAUCI, A. S. 2019b. Measles in 2019 — Going Backward. *New England Journal of Medicine,* 0**,** null.

PERRINGS, C., CASTILLO-CHAVEZ, C., CHOWELL, G., DASZAK, P., FENICHEL, E. P., FINNOFF, D., HORAN, R. D., KILPATRICK, A. M., KINZIG, A. P., KUMINOFF, N. V., LEVIN, S., MORIN, B., SMITH, K. F. & SPRINGBORN, M. 2014. Merging Economics and Epidemiology to Improve the Prediction and Management of Infectious Disease. *EcoHealth,* 11**,** 464-475.

PERTWEE, E., SIMAS, C. & LARSON, H. J. 2022. An epidemic of uncertainty: rumors, conspiracy theories and vaccine hesitancy. *Nature Medicine,* 28**,** 456-459.

PIKE, J., LEIDNER, A. J. & GASTAÑADUY, P. A. 2020. A Review of Measles Outbreak Cost Estimates From the United States in the Postelimination Era (2004–2017): Estimates by Perspective and Cost Type. *Clinical Infectious Diseases*.

PILKINGTON, V., KEESTRA, S. M. & HILL, A. 2022. Global COVID-19 Vaccine Inequity: Failures in the First Year of Distribution and Potential Solutions for the Future. *Frontiers in Public Health,* 10.

PINTO-PRADES, J. L., LOOMES, G. & BREY, R. 2009. Trying to estimate a monetary value for the QALY. *Journal of Health Economics,* 28**,** 553-562.

POLACK, F. P., THOMAS, S. J., KITCHIN, N., ABSALON, J., GURTMAN, A., LOCKHART, S., PEREZ, J. L., PÉREZ MARC, G., MOREIRA, E. D., ZERBINI, C., BAILEY, R., SWANSON, K. A., ROYCHOUDHURY, S., KOURY, K., LI, P., KALINA, W. V., COOPER, D., FRENCK, R. W., HAMMITT, L. L., TÜRECI, Ö., NELL, H., SCHAEFER, A., ÜNAL, S., TRESNAN, D. B., MATHER, S., DORMITZER, P. R., ŞAHIN, U., JANSEN, K. U. & GRUBER, W. C. 2020. Safety and Efficacy of the BNT162b2 mRNA Covid-19 Vaccine. *New England Journal of Medicine,* 383**,** 2603-2615.

POWELL, M. J. D. 1994. A Direct Search Optimization Method That Models the Objective and Constraint Functions by Linear Interpolation. *In:* GOMEZ, S. & HENNART, J.-P. (eds.) *Advances in Optimization and Numerical Analysis.* Dordrecht: Springer Netherlands.

PUBLIC HEALTH ENGLAND. 2019. *Measles deaths by age group: 1980 to 2017 (ONS data)* [Online]. Available: https://www.gov.uk/government/publications/measles-deaths-by-age-group-from-1980-to-2013-ons-data/measles-deaths-by-age-group-from-1980-to-2013-ons-data [Accessed 20 August 2020].

PUBLIC HEALTH ENGLAND. 2020. *Confirmed cases of measles in England and Wales by region and age: 2012 to 2019* [Online]. Available: https://www.gov.uk/government/publications/measles-confirmed-cases/confirmed-cases-of-measles-in-england-and-wales-by-region-and-age-2012-to-2014 [Accessed 20 August 2020].

PUBLIC HEALTH ENGLAND 2021. PHE monitoring of the early impact and effectiveness of COVID-19 vaccination in England. Public Health England

REY, D., FRESSARD, L., CORTAREDONA, S., BOCQUIER, A., GAUTIER, A., PERETTI-WATEL, P., VERGER, P. & GROUP, O. B. O. T. B. S. 2018. Vaccine hesitancy in the French population in 2016, and its association with vaccine uptake and perceived vaccine risk–benefit balance. *Eurosurveillance,* 23**,** 17-00816.

ROBERTS, M. G. & HEESTERBEEK, J. A. 2003. A new method for estimating the effort required to control an infectious disease. *Proc Biol Sci,* 270**,** 1359-64.

ROCK, K., BRAND, S., MOIR, J. & KEELING, M. J. 2014. Dynamics of infectious diseases. *Rep Prog Phys,* 77**,** 026602.

ROTA, P. A., MOSS, W. J., TAKEDA, M., DE SWART, R. L., THOMPSON, K. M. & GOODSON, J. L. 2016. Measles. *Nature Reviews Disease Primers,* 2**,** 16049.

RYAN, J. A., ULRICH, J. M., THIELEN, W., TEETOR, P. & BRONDER, S. 2020. quantmod: Quantitative Financial Modelling Framework. 0.4.18 ed.

SAHIN, U., MUIK, A., DERHOVANESSIAN, E., VOGLER, I., KRANZ, L. M., VORMEHR, M., BAUM, A., PASCAL, K., QUANDT, J., MAURUS, D., BRACHTENDORF, S., LÖRKS, V., SIKORSKI, J., HILKER, R., BECKER, D., ELLER, A.-K., GRÜTZNER, J., BOESLER, C., ROSENBAUM, C., KÜHNLE, M.-C.,

LUXEMBURGER, U., KEMMER-BRÜCK, A., LANGER, D., BEXON, M., BOLTE, S., KARIKÓ, K., PALANCHE, T., FISCHER, B., SCHULTZ, A., SHI, P.-Y., FONTES-GARFIAS, C., PEREZ, J. L., SWANSON, K. A., LOSCHKO, J., SCULLY, I. L., CUTLER, M., KALINA, W., KYRATSOUS, C. A., COOPER, D., DORMITZER, P. R., JANSEN, K. U. & TÜRECI, Ö. 2020. COVID-19 vaccine BNT162b1 elicits human antibody and TH1 T cell responses. *Nature,* 586**,** 594-599.

SALATHÉ, M. & BONHOEFFER, S. 2008. The effect of opinion clustering on disease outbreaks. *Journal of the Royal Society, Interface,* 5**,** 1505-1508.

SALISBURY, D. M. 2012. Should childhood vaccination be mandatory? No. *BMJ : British Medical Journal,* 344**,** e2435.

SASSI, F. 2006. Calculating QALYs, comparing QALY and DALY calculations. *Health Policy Plan,* 21**,** 402-8.

SCOTT, N., HUSSAIN, S. A., MARTIN-HUGHES, R., FOWKES, F. J. I., KERR, C. C., PEARSON, R., KEDZIORA, D. J., KILLEDAR, M., STUART, R. M. & WILSON, D. P. 2017. Maximizing the impact of malaria funding through allocative efficiency: using the right interventions in the right locations. *Malar J,* 16**,** 368.

SICURI, E., EVANS, D. B. & TEDIOSI, F. 2015. Can Economic Analysis Contribute to Disease Elimination and Eradication? A Systematic Review. *PLOS ONE,* 10**,** e0130603.

SILAL, S. P., LITTLE, F., BARNES, K. I. & WHITE, L. J. 2015. Hitting a Moving Target: A Model for Malaria Elimination in the Presence of Population Movement. *PLOS ONE,* 10**,** e0144990.

SIMAS, C. & LARSON, H. J. 2021. Overcoming vaccine hesitancy in low-income and middle-income regions. *Nature Reviews Disease Primers,* 7**,** 41.

THE GLOBAL FUND 2019. Description of the 2020-2022 Allocation Methodology.

THORRINGTON, D., RAMSAY, M., VAN HOEK, A. J., EDMUNDS, W. J., VIVANCOS, R., BUKASA, A. & EAMES, K. 2014. The effect of measles on health-related quality of life: a patient-based survey. *PLoS One,* 9**,** e105153.

TIZIFA, T. A., KABAGHE, A. N., MCCANN, R. S., VAN DEN BERG, H., VAN VUGT, M. & PHIRI, K. S. 2018. Prevention Efforts for Malaria. *Current Tropical Medicine Reports,* 5**,** 41-50.

TOMORI, O. 2011. From smallpox eradication to the future of global health: innovations, application and lessons for future eradication and control initiatives. *Vaccine,* 29 Suppl 4**,** D145-8.

TRUELOVE, S. A., GRAHAM, M., MOSS, W. J., METCALF, C. J. E., FERRARI, M. J. & LESSLER, J. 2019. Characterizing the impact of spatial clustering of susceptibility for measles elimination. *Vaccine,* 37**,** 732-741.

TURNER, H. C., ARCHER, R. A., DOWNEY, L. E., ISARANUWATCHAI, W., CHALKIDOU, K., JIT, M. & TEERAWATTANANON, Y. 2021. An Introduction to the Main Types of Economic Evaluations Used for Informing Priority Setting and Resource Allocation in Healthcare: Key Features, Uses, and Limitations. *Frontiers in Public Health,* 9.

TUTEJA, R. 2007. Malaria – an overview. *The FEBS Journal,* 274**,** 4670-4679.

USHER, A. D. 2021. A beautiful idea: how COVAX has fallen short. *The Lancet,* 397**,** 2322-2325.

VERGARA, R. J. D., SARMIENTO, P. J. D. & LAGMAN, J. D. N. 2021. Building public trust: a response to COVID-19 vaccine hesitancy predicament. *Journal of Public Health*.

VERGUET, S., JOHRI, M., MORRIS, S. K., GAUVREAU, C. L., JHA, P. & JIT, M. 2015. Controlling measles using supplemental immunization activities: a mathematical model to inform optimal policy. *Vaccine,* 33**,** 1291-6.

VOYSEY, M., CLEMENS, S. A. C., MADHI, S. A., WECKX, L. Y., FOLEGATTI, P. M., ALEY, P. K., ANGUS, B., BAILLIE, V. L., BARNABAS, S. L., BHORAT, Q. E., BIBI, S., BRINER, C., CICCONI, P., COLLINS, A. M., COLIN-JONES, R., CUTLAND, C. L., DARTON, T. C., DHEDA, K., DUNCAN, C. J. A., EMARY, K. R. W., EWER, K. J., FAIRLIE, L., FAUST, S. N., FENG, S., FERREIRA, D. M., FINN, A., GOODMAN, A. L., GREEN, C. M., GREEN, C. A., HEATH, P. T., HILL, C., HILL, H., HIRSCH, I., HODGSON, S. H. C., IZU, A., JACKSON, S., JENKIN, D., JOE, C. C. D., KERRIDGE, S., KOEN, A., KWATRA, G., LAZARUS, R., LAWRIE, A. M., LELLIOTT, A., LIBRI, V., LILLIE, P. J., MALLORY, R., MENDES, A. V. A., MILAN, E. P., MINASSIAN, A. M., MCGREGOR, A., MORRISON, H., MUJADIDI, Y. F., NANA,

A., O'REILLY, P. J., PADAYACHEE, S. D., PITTELLA, A., PLESTED, E., POLLOCK, K. M., RAMASAMY, M. N., RHEAD, S., SCHWARZBOLD, A. V., SINGH, N., SMITH, A., SONG, R., SNAPE, M. D., SPRINZ, E., SUTHERLAND, R. K., TARRANT, R., THOMSON, E. C., TÖRÖK, M. E., TOSHNER, M., TURNER, D. P. J., VEKEMANS, J., VILLAFANA, T. L., WATSON, M. E. E., WILLIAMS, C. J., DOUGLAS, A. D., HILL, A. V. S., LAMBE, T., GILBERT, S. C., POLLARD, A. J., ABAN, M., ABAYOMI, F., ABEYSKERA, K., ABOAGYE, J., ADAM, M., ADAMS, K., ADAMSON, J., ADELAJA, Y. A., ADEWETAN, G., ADLOU, S., AHMED, K., AKHALWAYA, Y., AKHALWAYA, S., ALCOCK, A., ALI, A., ALLEN, E. R., ALLEN, L., ALMEIDA, T. C. D. S. C., et al. 2021. Safety and efficacy of the ChAdOx1 nCoV-19 vaccine (AZD1222) against SARS-CoV-2: an interim analysis of four randomised controlled trials in Brazil, South Africa, and the UK. *The Lancet,* 397**,** 99-111.

WALKER, P. G., GRIFFIN, J. T., FERGUSON, N. M. & GHANI, A. C. 2016. Estimating the most efficient allocation of interventions to achieve reductions in Plasmodium falciparum malaria burden and transmission in Africa: a modelling study. *Lancet Glob Health*

4**,** e474-84.

WALKER, P. G. T., WHITTAKER, C., WATSON, O. J., BAGUELIN, M., WINSKILL, P., HAMLET, A., DJAFAARA, B. A., CUCUNUBÁ, Z., OLIVERA MESA, D., GREEN, W., THOMPSON, H., NAYAGAM, S., AINSLIE, K. E. C., BHATIA, S., BHATT, S., BOONYASIRI, A., BOYD, O., BRAZEAU, N. F., CATTARINO, L., CUOMO-DANNENBURG, G., DIGHE, A., DONNELLY, C. A., DORIGATTI, I., VAN ELSLAND, S. L., FITZJOHN, R., FU, H., GAYTHORPE, K. A. M., GEIDELBERG, L., GRASSLY, N., HAW, D., HAYES, S., HINSLEY, W., IMAI, N., JORGENSEN, D., KNOCK, E., LAYDON, D., MISHRA, S., NEDJATI-GILANI, G., OKELL, L. C., UNWIN, H. J., VERITY, R., VOLLMER, M., WALTERS, C. E., WANG, H., WANG, Y., XI, X., LALLOO, D. G., FERGUSON, N. M. & GHANI, A. C. 2020. The impact of COVID-19 and strategies for mitigation and suppression in low- and middle-income countries. *Science,* 369**,** 413-422.

WANG, C., WANG, D., ABBAS, J., DUAN, K. & MUBEEN, R. 2021. Global Financial Crisis, Smart Lockdown Strategies, and the COVID-19 Spillover Impacts: A Global Perspective Implications From Southeast Asia. *Front Psychiatry,* 12**,** 643783.

WANG, H., PAULSON, K. R., PEASE, S. A., WATSON, S., COMFORT, H., ZHENG, P., ARAVKIN, A. Y., BISIGNANO, C., BARBER, R. M., ALAM, T., FULLER, J. E., MAY, E. A., JONES, D. P., FRISCH, M. E., ABBAFATI, C., ADOLPH, C., ALLORANT, A., AMLAG, J. O., BANG-JENSEN, B., BERTOLACCI, G. J., BLOOM, S. S., CARTER, A., CASTRO, E., CHAKRABARTI, S., CHATTOPADHYAY, J., COGEN, R. M., COLLINS, J. K., COOPERRIDER, K., DAI, X., DANGEL, W. J., DAOUD, F., DAPPER, C., DEEN, A., DUNCAN, B. B., ERICKSON, M., EWALD, S. B., FEDOSSEEVA, T., FERRARI, A. J., FROSTAD, J. J., FULLMAN, N., GALLAGHER, J., GAMKRELIDZE, A., GUO, G., HE, J., HELAK, M., HENRY, N. J., HULLAND, E. N., HUNTLEY, B. M., KERESELIDZE, M., LAZZAR-ATWOOD, A., LEGRAND, K. E., LINDSTROM, A., LINEBARGER, E., LOTUFO, P. A., LOZANO, R., MAGISTRO, B., MALTA, D. C., MÅNSSON, J., MANTILLA HERRERA, A. M., MARINHO, F., MIRKUZIE, A. H., MISGANAW, A. T., MONASTA, L., NAIK, P., NOMURA, S., O'BRIEN, E. G., O'HALLORAN, J. K., OLANA, L. T., OSTROFF, S. M., PENBERTHY, L., REINER JR, R. C., REINKE, G., RIBEIRO, A. L. P., SANTOMAURO, D. F., SCHMIDT, M. I., SHAW, D. H., SHEENA, B. S., SHOLOKHOV, A., SKHVITARIDZE, N., SORENSEN, R. J. D., SPURLOCK, E. E., SYAILENDRAWATI, R., TOPOR-MADRY, R., TROEGER, C. E., WALCOTT, R., WALKER, A., WIYSONGE, C. S., WORKU, N. A., ZIGLER, B., PIGOTT, D. M., NAGHAVI, M., MOKDAD, A. H., LIM, S. S., HAY, S. I., GAKIDOU, E. & MURRAY, C. J. L. 2022. Estimating excess mortality due to the COVID-19 pandemic: a systematic analysis of COVID-19-related mortality, 2020–21. *The Lancet,* 399**,** 1513-1536.

WHITE, C. 2021. Measuring Social and Externality Benefits of Influenza Vaccination. *The Journal of human resources,* 56**,** 749-785.

WHITE, M. T., GRIFFIN, J. T., CHURCHER, T. S., FERGUSON, N. M., BASÁÑEZ, M.-G. & GHANI, A. C. 2011. Modelling the impact of vector control interventions on Anopheles gambiae population dynamics. *Parasites & Vectors,* 4**,** 153.

WHO 2012. Global measles and rubella strategic plan : 2012-2020.**,** 44.

WHO. 2018. *The top 10 causes of death* [Online]. Available: http://www.who.int/news-room/fact-sheets/detail/the-top-10-causes-of-death [Accessed 13/Sep/2018 2018].

WINSKILL, P., WALKER, P. G., CIBULSKIS, R. E. & GHANI, A. C. 2019. Prioritizing the scale-up of interventions for malaria control and elimination. *Malar J,* 18**,** 122.

WORLD HEALTH ORGANIZATION. 2022a. *14.9 million excess deaths associated with the COVID-19 pandemic in 2020 and 2021* [Online]. Available: https://www.who.int/news/item/05-05-2022-14.9-million-excess-deaths-were-associated-with-the-covid-19-pandemic-in-2020-and-2021 [Accessed 10 May 2022 2022].

WORLD HEALTH ORGANIZATION, W. 2015. Global technical strategy for malaria 2016-2030. Geneva.

WORLD HEALTH ORGANIZATION, W. 2019a. *Measles* [Online]. Available: https://www.who.int/news-room/fact-sheets/detail/measles [Accessed].

WORLD HEALTH ORGANIZATION, W. 2019b. *More than 140,000 die from measles as cases surge worldwide* [Online]. Available: https://www.who.int/news/item/05-12-2019-more-than-140-000-die-from-measles-as-cases-surge-worldwide [Accessed].

WORLD HEALTH ORGANIZATION, W. 2020. Measles and rubella strategic framework 2021–2030. Geneva.

WORLD HEALTH ORGANIZATION, W. 2021a. *Global progress against measles threatened amidst COVID-19 pandemic* [Online]. Available: https://www.who.int/news/item/10-11-2021-global-progress-against-measles-threatened-amidst-covid-19-pandemic [Accessed].

WORLD HEALTH ORGANIZATION, W. 2021b. Global technical strategy for malaria 2016–2030, 2021 update. Geneva.

WORLD HEALTH ORGANIZATION, W. 2021c. *Malaria* [Online]. Available: https://www.who.int/news-room/fact-sheets/detail/malaria [Accessed 27 January 2022].

WORLD HEALTH ORGANIZATION, W. 2021d. World malaria report 2021. *World Malaria Report.* World Health Organization.

WORLD HEALTH ORGANIZATION, W. 2022b. *WHO Coronavirus (COVID-19) Dashboard* [Online]. Available: https://covid19.who.int/ [Accessed 03 May 2022].

WOUTERS, O. J., SHADLEN, K. C., SALCHER-KONRAD, M., POLLARD, A. J., LARSON, H. J., TEERAWATTANANON, Y. & JIT, M. 2021. Challenges in ensuring global access to COVID-19 vaccines: production, affordability, allocation, and deployment. *The Lancet,* 397**,** 1023-1034.

YAN, A. W. C., BLACK, A. J., MCCAW, J. M., REBULI, N., ROSS, J. V., SWAN, A. J. & HICKSON, R. I. 2018. The distribution of the time taken for an epidemic to spread between two communities. *Math Biosci,* 303**,** 139-147.

YUREKLI, A. & BEYER, J. D. 2001. Tobacco Toolkit: Design and administer tobacco taxes. World Bank of Economics.

ZHU, F. C., LI, Y. H., GUAN, X. H., HOU, L. H., WANG, W. J., LI, J. X., WU, S. P., WANG, B. S., WANG, Z., WANG, L., JIA, S. Y., JIANG, H. D., WANG, L., JIANG, T., HU, Y., GOU, J. B., XU, S. B., XU, J. J., WANG, X. W., WANG, W. & CHEN, W. 2020. Safety, tolerability, and immunogenicity of a recombinant adenovirus type-5 vectored COVID-19 vaccine: a dose-escalation, open-label, non-randomised, first-in-human trial. *Lancet,* 395**,** 1845-1854.

communications
medicine

ARTICLE

OPEN

Check for updates

Modelling the impact of vaccine hesitancy in prolonging the need for Non-Pharmaceutical Interventions to control the COVID-19 pandemic

Daniela Olivera Mesa [1 ✉], Alexandra B. Hogan [1], Oliver J. Watson [1], Giovanni D. Charles[1], Katharina Hauck[1], Azra C. Ghani[1] & Peter Winskill [1]

Abstract

Background Vaccine hesitancy – a delay in acceptance or refusal of vaccines despite availability – has the potential to threaten the successful roll-out of SARS-CoV-2 vaccines globally. In this study, we aim to understand the likely impact of vaccine hesitancy on the control of the COVID-19 pandemic.

Methods We modelled the potential impact of vaccine hesitancy on the control of the pandemic and the relaxation of non-pharmaceutical interventions (NPIs) by combining an epidemiological model of SARS-CoV-2 transmission with data on vaccine hesitancy from population surveys.

Results Our simulations suggest that the mortality over a 2-year period could be up to 7.6 times higher in countries with high vaccine hesitancy compared to an ideal vaccination uptake if NPIs are relaxed. Alternatively, high vaccine hesitancy could prolong the need for NPIs to remain in place.

Conclusions While vaccination is an individual choice, vaccine-hesitant individuals have a substantial impact on the pandemic trajectory, which may challenge current efforts to control COVID-19. In order to prevent such outcomes, addressing vaccine hesitancy with behavioural interventions is an important priority in the control of the COVID-19 pandemic.

Plain language summary

People refusing or delaying COVID-19 vaccination might impact current efforts to control the pandemic caused by SARS-CoV-2. Here, we have examined the effects of low vaccine uptake due to vaccine hesitancy on the need to prolong other public health measures to control the pandemic. We used mathematical modelling and data on vaccine hesitancy from population surveys across different countries. Our results suggest that when there is vaccine hesitancy and relaxation of other public health measures, mortality could increase by up to seven times compared with ideal vaccination coverage of the population. Furthermore, for some scenarios analysed, longer and more stringent public health measures would be required to compensate for lower vaccine uptake. Our work demonstrates that vaccine hesitancy might have a substantial health impact on the population, and therefore, it is a public health priority to increase trust in vaccines.

[1] MRC Centre for Global Infectious Disease Analysis; and the Jameel Institute, School of Public Health, Imperial College London, London, UK. ✉email: d.olivera-mesa17@imperial.ac.uk